Synthesis and evaluation of novel modular fluorescent diboronic acid sensors

Frimat, Karine

Award date:
2002

Awarding institution:
University of Bath

SYNTHESIS AND EVALUATION OF NOVEL MODULAR FLUORESCENT DIBORONIC ACID SENSORS

submitted by Karine Frimat

for the degree of PhD

of the University of Bath

2002

Signed:

ProQuest LLC
789 East Eisenhower Parkway
P.O. Box 1346
Ann Arbor, MI 48106-1346

Abstract

The importance of the monitoring of saccharides is best illustrated by the case of diabetes. A high proportion of the population is affected by this disease and, to date, the only way of avoiding further complications is to frequently monitor the blood glucose level. Consequently, the past decade has seen an explosion in the development of a variety of saccharides sensors, and particularly glucose sensors.

Boronic acid sensors are, to date, the only receptors which bind saccharides covalently. Previous work proved that diboronic acid sensors could be glucose selective, where the relative position of the two boronic acid moieties is perfectly suited for the binding of a molecule of glucose.

The work developed in this thesis is an extension of work undertaken in the area of diboronic acid PET (Photoinduced Electron Transfer) sensors for saccharides. The systems developed use the electron transfer of a tertiary amine to a fluorophore unit. On formation of a cyclic ester with saccharides, the Lewis acidity of the boron is enhanced, and therefore the Lewis-base interaction between the boron and the amine is stronger. Saccharide binding then results in the suppression of the PET process and consequently, in the recovery of the fluorescence.

The exceptional feature of the systems developed in this thesis is their modular nature. The modularity of the sensors comes from their ingenious design, which allows single variation of the distance between the two boronic acids and the nature of the fluorophore. A novel and simple 3 step synthesis was developed to give 2 series of sensors (*para* series **43-45** and *meta* series **46-48**). Each series contains 3 different sensors varying only by the nature of the fluorophore. The interactions of the 6 sensors **43-48** with saccharides were then evaluated. All sensors **43-48** showed increasing fluorescence intensity upon the addition of saccharides with selectivity for glucose over galactose, fructose and mannose. Higher stability constants *K* were also observed for the *meta* series comparing to the *para* series. Two sensors belonging to the *meta* series (**46** and **47**) showed particular affinity for galactose with a high stability constant *K*. CD (Circular Dichroism) experiments gave information on the structure of the complex. It was shown that the two sensors **46** and **47** form a cyclic 1:1 complex with galactose. A 1:1 complex was also formed between the 6 sensors **43-48** and glucose.

Résumé

Le cas du diabète est un des exemples cruciaux témoignant de l'importance du suivi des sucres. Une grande proportion de la population est touchée par cette maladie et, jusqu'à présent, l'unique méthode pour éviter des complications est de contrôler fréquemment le niveau de glucose dans le sang. Le développement de capteurs de sucres a par conséquent explosé ces dix dernières années, surtout dans le domaine de capteurs de glucose.

Les capteurs composés d'acides boroniques sont, jusqu'à ce jour, les seuls à pouvoir se lier de manière covalente avec les saccharides. Des études antérieures ont montré que les capteurs composés d'acides boroniques peuvent être sélectifs pour le glucose lorsque la position relative des deux acides boroniques est astucieusement choisie afin qu'une molécule de glucose puisse s'y insérer. Le travail décrit dans cette thèse est une prolongation de l'étude sur les capteurs pour saccharides, ces capteurs étant composés d'acides boroniques et utilisant le principe de PET (Photoinduced Electron Transfer). Les systèmes décrits dans cette thèse utilisent le transfert d'électrons d'une amine tertiaire vers un fluorophore. Lorsque le capteur est lié au sucre, l'acidité de Lewis du bore augmente et, par conséquent, l'interaction acide-base entre le bore et l'amine est plus forte. De cela découle une diminution du transfert d'électron et donc, une augmentation de la fluorescence.

La particularité exceptionnelle des systèmes décrits dans cette thèse est leur modularité. Cette modularité provient de leur structure qui est particulièrement bien choisie pour permettre le changement de la distance entre les deux groupes acides boroniques et la nature du fluorophore. Une procédure nouvelle et facile de 3 étapes a été développée pour synthétiser 2 séries de capteurs (séries *para* **43-45** et séries *méta* **46-48**). Chaque série est composée de 3 capteurs qui diffèrent uniquement par la nature de leur fluorophore. Les interactions de ces 6 capteurs ont ensuite été étudiées. Ils ont tous montré une augmentation de leur fluorescence sous addition de saccharides ainsi qu'une sélectivité pour le glucose. Nous avons également observé des valeurs de constante de stabilité K beaucoup plus forte pour la série *méta* que pour la série *para*. Deux capteurs appartenant à la série *méta* (**46** and **47**) ont également montré une affinité particulière pour le galactose avec des valeurs de K élevées. Des analyses CD (Circular Dichroism) ont révélé que ces 2 capteurs formaient un complexe cyclique 1:1 avec le galactose.

Acknowledgements

I would like to start by thanking my supervisor Tony D. James who supervised me during the 3 years of my PhD. I would like to thank him for giving me the opportunity of studying in England and Japan and also for guidance along way and for being so approachable.

My second thanks would go to the fantastic team providing analytical services at Birmingham: Neil Spencer and Malcom Tolley for the NMR, Nick May and Peter Ashton for the mass spectrometry and Lianne for the Elemental Analysis. Their accurate analysis and friendly personalities were precious during the research work, especially for the more temperamental compounds.

This PhD has also allowed me to meet a number of great people. I would like to thank Coops, Skippy, Stalker and Mike-e for the weekly (daily?) memorable parties (known as "Staff-House" and "Club 99"), the girls: Suzi, Kate, Gitte and Fabienne for the same but especially the PRE-parties (more Mirabelle?), Sam, Sarah and Taryn (for making me play football), Thierry (for the usual 5 hours meal sessions), Mikey (for all our trips: whenever you want for the South Coast) and Catharine and Lucile (for the coffee breaks and long chats).

In Bath, thanks especially go to the group of runners: Selma, Christelle, Koko, Marie, Arash, J-P, Aliki and Leo for...making me run (and also

being there especially when the atmosphere in the lab wasn't that great!). By the way, I must also thank Koko and Fred for storing my stuff!

Thanks must also go to the members of BART , past and present: Chris (C and W), Jim, Yu Bai, Suvi, Arimori and Laurence for their team spirit.

Finally, I would like to extend my thanks to my family, my parents and Lysiane for their support. A very special thank you should go Mark for supporting me through my PhD (especially the stressful end) and for putting up with my varying moods.

Table of Contents

Abbreviations

AIBN	Azo-iso-butyronitrile
Anth	Anthracene
Boc	*tert*-Butoxycarbonyl
δ	Chemical shift
CI	Chemical ionisation
d	Doublet
D-	Dextrorotary
DCC	1,3-Dicyclohexylcarbodiimide
DCM	Dichloromethane
DCU	1,3-Dicyclohexyl-urea
DMF	*N*,*N*-dimethylformamide
DMSO	Dimethylsulphoxide
DIBAL-H	Diisobutylaluminium hydride
ē	Electron
EI	Electron Impact
EtOAc	Ethyl Acetate
EtOH	Ethanol
FAB	Fast Atom Bombardment
FAD	Flavin adenine dinucleotide
GOD	Glucose oxidase
HOMO	Highest occupied molecular orbital
HOOBt	3-Hydroxy-1,2,3-benzotriazin-4(3*H*)-one
hν	Electromagnetic radiation

IR	Infra-red
J	Coupling constant
K	Stability constant
L-	Leuvorotatory
LUMO	Lowest unoccupied molecular orbital
m	Multiplet
MHz	Megahertz
mp	Melting point
m/z	Mass to charge ratio
Naph	Naphthalene
NMR	Nuclear magnetic resonance
PET	Photoinduced electron transfer
ppm	Parts per million
PPTS	Pyridinium *p*-toluene sulfonate
Py	Pyrene
rt	Room temperature
s	Singlet
θ	Ellipticity
t	Triplet
TsOH	*p*-Toluenesulfonic acid
TFA	Trifluoroacetic acid
THF	Tetrahydrofuran
TLC	Thin layer chromatography
v/v	Volume for volume
w/w	Weight for weight

I Introduction

I-1 General Introduction

"A *sensor* is a device that interacts with matter or energy and yields a measurable signal in response".[1] This definition given by Czarnik bears witness to the extremely wide range of applications for sensors. We can distinguish *biosensors*, which utilise a biological element for analyte recognition, from *synthetic receptors*, in which the analyte interacts with a synthetically prepared entity. For example, the centuries old use of live birds or fish to detect the presence of toxins in air or water respectively can be interpreted as one of the first biosensors. Today, the contemporary technology has also permitted an impressive development of more 'sophisticated' biosensors and synthetic receptors able to detect increasingly specific analytes with greater selectivity. Many challenges have been conquered in this field of research but many still remain. For example, we can imagine a day when the glucose blood concentration could be continuously monitored through the use of a fibre optic filament inserted into an artery or vein.

The first part of this chapter will introduce different systems used for the detection of glucose (biosensors and synthetic receptors). The second part will describe different photophysical processes occurring in a sensor when fluorescence is used as a signal transducing the presence of the analyte. The final section will discuss the area of research I have undertaken over the last 3 years (boronic acid PET fluorescent sensors for saccharides).

I-2 Glucose Sensors

Saccharides play several crucial roles in living organisms. They can, for instance, be involved in a variety of biological functions such as cellular recognition or hormonal activities. However the most fundamental role attributed to saccharides, especially glucose, is one of an energy supplier. The breakdown of glucose transport leads to the development of diseases (i.e. diabetes,[2,3]cystic fibrosis,[4] renal glycosuria,[5,6] and cancer[7]). Diabetes is particularly topical because the number of people affected by this disease is constantly increasing (1.5 million people in the UK are diabetic and another estimated 1 million have undiagnosed diabetes) and its development can cause serious complications (blindness, kidney failure, heart attack and gangrene). Quick diagnosis and early prevention are critical for the control of the disease status. Therefore, glucose sensors have become an essential indicator tool for long-term management of the disease and have been the focus of a great deal of interest in different research groups.[8-12] An overview of the explosion in the development of biosensors and synthetic receptors for glucose detection will be discussed below.

I-2.1 Biosensors

A biosensor is an analytical device incorporating a deliberate and intimate combination of a specific biological element (that creates a recognition event) and a physical element (that transmits the recognition event). The bioelement is usually an enzyme or an antibody (Figure I-1).[13]

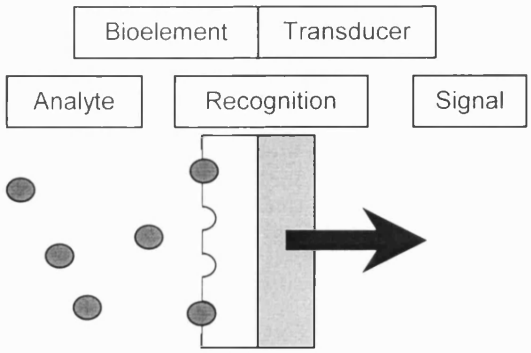

Figure I-1. The Biosensor Principle.

The nature of the transducer and the transduced parameter will depend on the type of analyte investigated. The recognition of the analyte can lead to a variety of different modifications of the environment, which can be physically measured in different ways. The five principal transducer classes are electrochemical, optical, thermometric, piezoelectric and magnetic.[14,15] Electrochemical sensors may be subdivided into potentiometric, amperometric, or conductiometric. Potentiometric devices measure the change in charge density at the surface of an electrode. Amperometric sensors monitor currents generated when electrons are exchanged either directly or indirectly between a biological system and an electrode, such as many new blood-glucose monitors. Conductiometric sensors measure changes in ionic conductance. Optical biosensors correlate changes in concentration, mass, or number to direct changes in the characteristics of light. For example D'Auria and co-workers use the fluorescence of a glucose sensitive protein (labelled with a fluorophore) as an analytical tool.[8] Other physiochemical sensors, such as thermometric, piezoelectric, and magnetic sensors, monitor biological interactions through changes in enthalpy, mass, or magnetic labels. Shih *et al.*, for example, utilise the surface pressure sensitivity of piezoelectric (PZ) crystals.[9] The adsorption of gluconic acid (the product of glucose oxidation) on PZ

crystals decreases the vibrational frequency of the PZ crystals and the decrease is proportional to the amount of gluconic acid adsorbed. Although the list of the physical process of the recognition event is varied, the first biosensors, and those mainly used for glucose, were based on an amperometric principle.

I-2.1.1 Amperometric Glucose Biosensors

Commercial home-tests glucose sensors everyday help millions of diabetics in the world to check their blood glucose level. These tests are based on amperometric biosensors. The signal measured is an electrical current produced by a redox reaction, which occurs between glucose and an enzyme chosen for its sensitivity to glucose. This concept was first introduced by Clark & Lyons who described the system as an "enzyme electrode".[16] The enzyme commonly used for the glucose recognition is glucose oxidase (GOD). GOD catalyses the oxidation of β-D-glucose to gluconolactone (reaction 1), which is then hydrolysed in aqueous medium to gluconic acid (reaction 2).[17] The result of these two reactions is summarized in reaction 3. As a consequence of the glucose oxidation occurring in reaction 1, the co-factor flavin-adenine dinucleotide (FAD) is reduced to $FADH_2$. The regeneration of the enzyme implies an oxido-reduction in which $FADH_2$ is oxidised to FAD by O_2, which is reduced to hydrogen peroxide (H_2O_2) (reaction 4). The overall reaction is usually expressed as in reaction 5.

β-D-glucose + GOD(FAD) $\longrightarrow$ glucono-δ-lactone + GOD($FADH_2$) (1)

glucono-δ-lactone + H_2O $\longrightarrow$ gluconic acid (2)

β-D-glucose + H_2O + GOD(FAD) $\longrightarrow$ gluconic acid + GOD($FADH_2$) (3)

GOD($FADH_2$) + O_2 $\longrightarrow$ GOD(FAD) + H_2O_2 (4)

$$\beta\text{-D-glucose} + O_2 + H_2O \longrightarrow \text{gluconic acid} + H_2O_2 \quad (5)$$

The principle of amperometric glucose biosensors is based on the oxidation or reduction of electrochemically active substances involved or produced in the reaction 4. We can categorise amperometric glucose biosensors into three generations differing from the electrochemical reaction involved. The first generation of biosensors is based on glucose oxidation by GOD in natural conditions (reaction 5). In this case the increase in hydrogen peroxide concentration or the decrease in oxygen concentration are detected electrochemically, both being proportional to the glucose concentration. An amperometric biosensor consists of a platinium (Pt) and a silver/ silver chloride (Ag/ AgCl) electrode. When a potential of – 0.6 V is applied to the platinium cathode, a current proportional to the oxygen concentration is produced. The following oxido-reduction reactions occur:

Ag anode $$4Ag^0 + 4Cl^- \longrightarrow 4AgCl + 4\bar{e} \quad (6)$$

Pt cathode $$O_2 + 4H^+ + 4\bar{e} \longrightarrow 2H_2O \quad (7)$$

The consumption of oxygen in reaction 5 (proportional to the concentration of glucose) can therefore be measured by the drop in the electric current. Figure I-2 gives a schematic representation of a simple amperometric biosensor. This biosensor is normally about 1 cm in diameter but has been scaled down to 0.25 mm diameter.

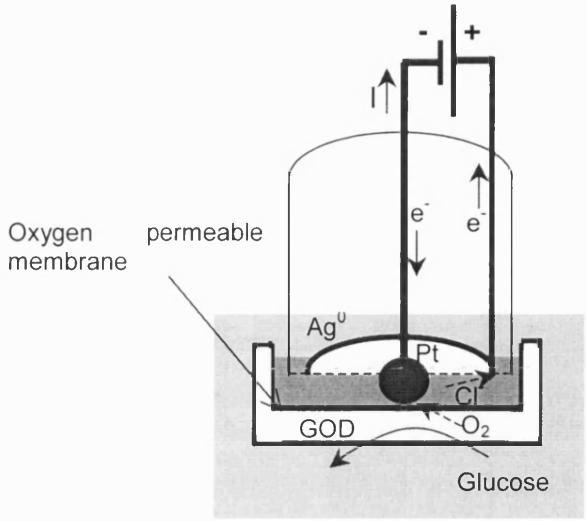

Figure I-2. Schematic Representation of a Simple Amperometric Biosensor.

A potential is applied between the central platinum cathode and the annular silver anode. This generates a current (I) which is carried between the electrodes by means of a saturated solution of KCl. This electrode compartment is separated from GOD by a thin plastic membrane, permeable only to oxygen. The analyte solution is separated from the biocatalyst by another membrane, permeable to the substrate and product.

Another alternative for determining the concentration of glucose is to detect the production of hydrogen peroxide. With the same platinium electrode, at a potential from + 0.6 V to + 0.8 V the following reactions occur:

Pt anode $H_2O_2 \longrightarrow O_2 + 2H^+ + 2\bar{e}$ (8)

Ag cathode $2AgCl + 2\bar{e} \longrightarrow 2Cl^- + 2Ag^0$ (9)

The electrical current measured is now proportional to the hydrogen peroxide produced by the oxidation of glucose by GOD (reaction 5).

This first generation of biosensors marked the first step towards commercial exploitation of home-care testing for diabetics. The principle of the first test for diabetics was based on the detection of H_2O_2 where subsequent chemical reactions

produced a colour change on a dry strip or in solution. The next generation of home-test glucose sensors were tested in the early 1980's.[18,19] The oxygen was substituted by a synthetic molecule called a mediator. The ferrocenes **1** represent a commonly used family of mediators.

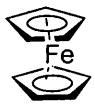

1

Instead of the oxygen reacting with reduced GOD($FADH_2$) as in reaction 4 page 6, it is an oxidised form of the mediator that does so (reaction 10 below). Thus, reduced mediator is formed instead of hydrogen peroxide. The reduced mediator is then reoxidised at the electrode, giving a current signal and regenerating the oxidised form of the mediator (reaction 11).

$$GOD(FADH_2) + Fe^{3+} \longrightarrow GOD(FAD) + Fe^{2+} \quad (10)$$

$$\text{Anode} \quad Fe^{2+} \longrightarrow Fe^{3+} + \bar{e} \quad (11)$$

The principle of the second generation of amperometric biosensors is represented in Scheme 1.1.

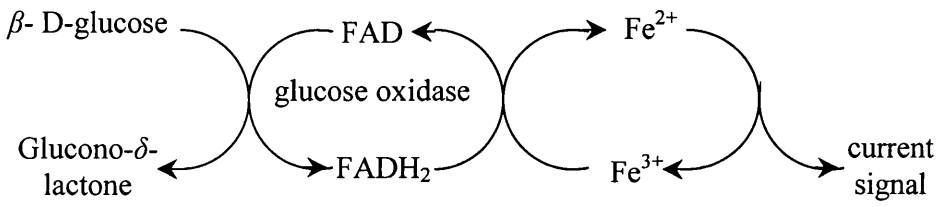

Scheme 1.1 - Mediator Glucose Biosensor Principle.

The development of the electrodes prompted the design of the most recent generation of amperometric biosensors. They allow for the direct electron transfer with the enzyme utilising a coating of electrically conducting organic salts. Many flavo-enzymes are strongly adsorbed by such organic conductors, which make the enzyme electrode very easy to prepare (simply by dipping the electrode into a solution of enzyme). Glucose biosensors are being investigated very intensively and new electrically conducting and porous materials used for immobilization of the enzyme/electron mediator system such as conducting polymer,[20,21] black platinium,[22] carbon paste[23,24] and carbon fiber[25] are still in development. The goal of such research is the development of an *in vivo* glucose sensor allowing continuous monitoring. Home-tests for diabetics represent such a big commercial market for glucose sensors that it also fuels the development of new approaches using artificial sensors.

I-2.2 Synthetic Receptors

During the last two decades, an alternative approach has emerged. In this approach natural biomolecules are replaced by synthetic receptors. The idea of using artificial receptors instead of natural enzymes in a glucose sensor has been driven by the practical needs for stable, sterilisable and nonimmunogenic materials. The synthetic receptors can be separated into two different categories, differing in the nature of their interactions with glucose (covalent or non-covalent).

I-2.2.1 Synthetic Sensors using Non-Covalent Interactions

As revealed by the X-ray crystal structures of protein-carbohydrate complexes, hydrogen bonding represents the main interaction used in nature by proteins for saccharide recognition (Figure I-3).[12]

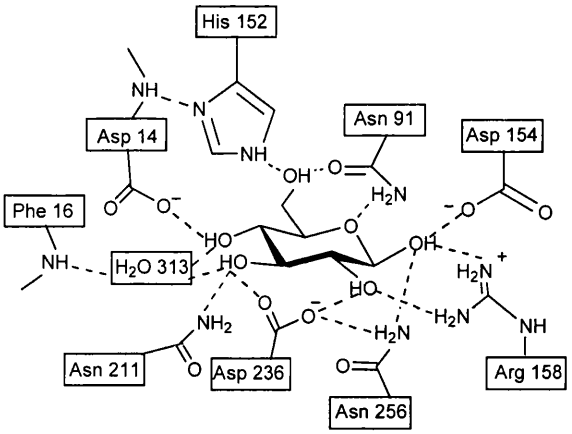

Figure I-3. Intermolecular Hydrogen Bonds in the Complex between D-glucose and "D-galactose-binding" Bacterial Periplasmic Protein.

The synthetic receptors described in this section utilise a similar approach. The strategy used for the recognition of a carbohydrate is to surround the latter with a complementary arrangement of H-bond donor and/or acceptor functionalities. The structure of the host molecule usually consists of a rigid core with two or more functional groups able to form electrostatic interactions with a saccharide. This section presents an overview of important synthetic receptors developed by different research groups. A more complete list is provided in the review by Davis *et al.*.[12] It is important to note that hydrogen bonds are especially effective in nonpolar media, where the solvent does not compete significantly for binding sites. In consequence, most of sensors described below are only efficient in organic media. The best results to date of significant noncovalent binding of common hexoses in water were obtained with a *β*-cyclodextrin system **2**.

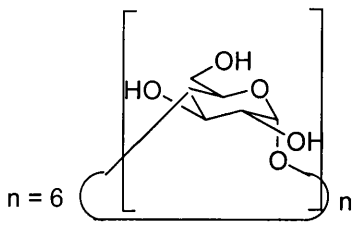

2

The size of the cavity of β-cyclodextrins **2** can only partially accept a pyranose nucleus. However, the calorimetric study performed by Danil de Namor and co-workers revealed encouraging results for hexoses (D-glucose K = 36 M^{-1}, D-fructose K = 52 M^{-1}, D-mannose K = 59 M^{-1} and D-galactose K = 15 M^{-1} in aqueous solution).[26] Among saccharides receptors acting in organic media, the first one to be successful employed a "face-to-face" binding geometry and was developed by Aoyama *et al* (compound **3**).[27] As represented below, the octahydroxy calix[4]arene **3** forms a bowl-shaped framework.

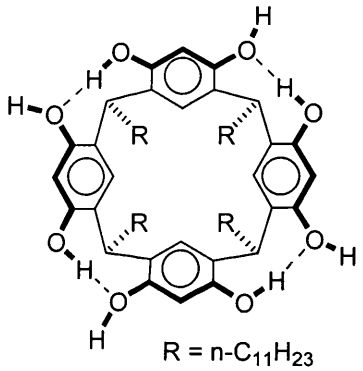

3

System **3** contains 4 different O-H....OH sites able to interact with 4 other hydroxy groups from an external molecule (Figure I-4)

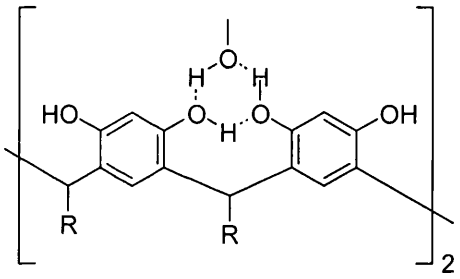

Figure I-4. One of the Four Binding Sites Present in Receptor **3**.

Receptor **3** was tested with different carbohydrates and showed the ability to extract a number of pentoses from water into carbon tetrachloride. Because of the solubility problem of saccharides in non-polar organic solvent, derivatives of glucose (glucosides **4**, **5** and **6**) were synthesized and used as guests.

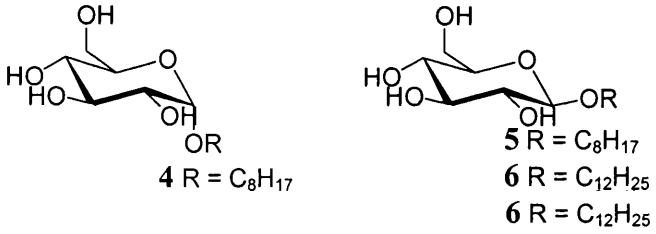

Figure I-5. Glucose Derivatives (α-L-octyl glucoside **4**, β-D-octyl glucoside **5**, β-D-dodecyl glucoside **6**)

Measurements in $CDCl_3$ revealed that **4** and **5** form the expected 1:4 complex with calix[4]arene **3**. The next interesting receptor to be presented utilises a different strategy for the recognition of the saccharide. Cholaplanes **7** and **8** are built with a rigid framework permitting the complete encapsulation of the carbohydrate and forming a 1:1 complex. The carbohydrate is thus surrounded by amide and hydroxyl groups suitable for the formation of H bonds. Receptors **7** and **8** were developed by Davis *et al.*[28,29] and were successfully tested with dodecyl β-D-glucopyranoside **6** in $CDCl_3$. The formation of a 1:1 complex was confirmed by ^1H NMR (K = 1740 and 700 M^{-1} for **7** and **8** respectively).

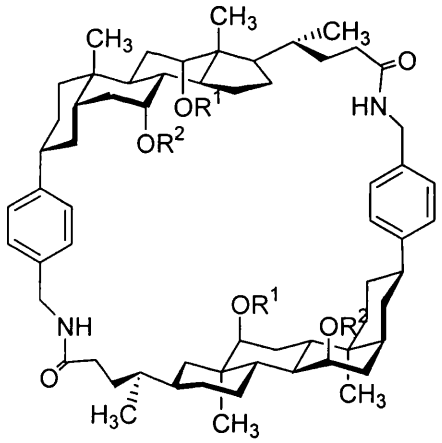

7 R^1, R^2 = H
8 R^1 = Bn, R^2 = H

Porphyrins have also been used for the design of new synthetic receptors for saccharides. Ogoshi and co-workers utilise a porphyrin unit as the solid base for U-shaped receptors **9**, **10** and **11**.[30,31]

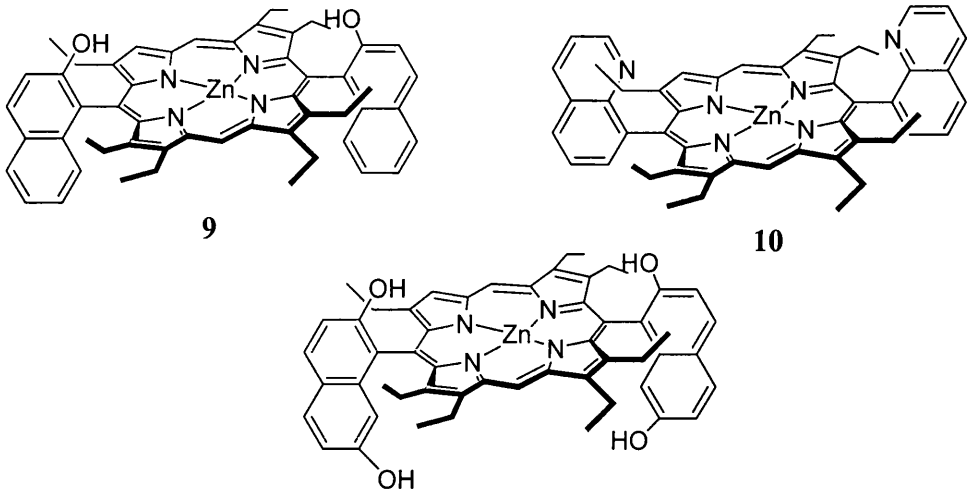

Figure I-6. Porphyrin U-Shaped Receptors **9**, **10** and **11**.

These 3 porphyrin systems contain one Lewis acid site and 2 hydrogen–bonding sites arranged in a similar manner to form a recognition pocket above the porphyrin plane. In $CHCl_3$, systems **9**, **10** and **11** were able to form 1:1 complexes with the glucoside **5**. The association constants K were 180, 2090 and 41400 M^{-1} respectively. The system developed by Kral and co-workers also contain a porphyrin unit (compound **12**).[32] Two different porphyrins entities are linked together by two ionic groups, which enhance the solubility of **12** in water. The cyclic system provides a perfect hydrophobic cage for the carbohydrate. Hydrogen bonding from the hydroxyl groups to the well-hydrated tertiary amide and azonia functions is also possible. This system has a preference for trisaccharides. However, a strong complex is also formed with D-glucose (K = 1380 M^{-1}). This is a very encouraging result for saccharide recognition in water.

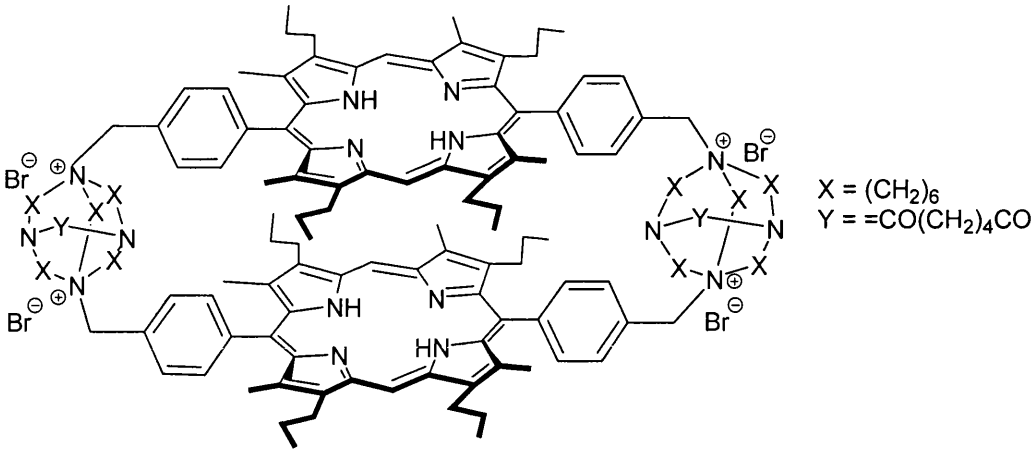

12

The next two systems **13** and **14** utilise a naphthyridine unit for saccharide recognition. These compounds were developed by Diederich *et al.*[33] but are in fact the extension of Cabell and Inouye's work, who used a 2-aminopyridine moiety.[34,35] Compounds **13** and **14** bind glucosides **4** and **5** in $CDCl_3$ with binding constants K ranged between 180 and 1270 M^{-1}.

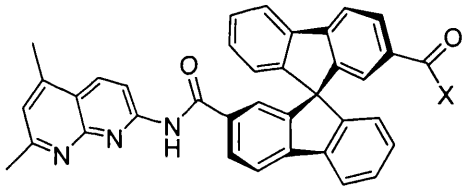

13 X =

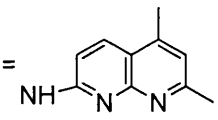

14 X = OCH_3

Figure I-7. Receptors **13** and **14** using a Naphthyridine Unit.

The last system presented contains phosphonate groups. They are part of the receptor framework and provide H-bond acceptor sites capable of binding diol units. Das and Hamilton synthesised receptors **15** and **16**, which showed very good selectivity for glucosides **4** and **5** (K = 4400 and 3220 M^{-1} in CD_3CN respectively).[36,37]

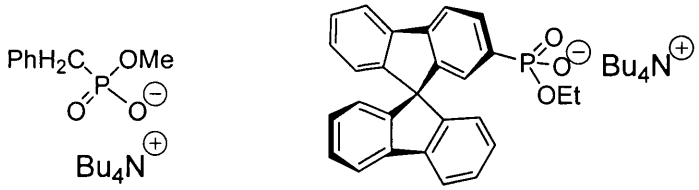

15 **16**

Figure I-8. Receptors **15** and **16** using an Anionic Center (phosphonate) for Recognition.

I-2.2.2 Saccharides Receptors using Covalent Interactions: Boronic Acid Sensors

Phenyl boronic acid **17** was first synthesised by Michaelis and Becker in 1880.[38]

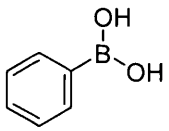

17

However, the interactions between boronic acid and saccharides were only investigated 74 years later when, in 1954, Kuivila *et al.* noticed the ability of boronic acids to solubilise polyols and saccharides.[39] The hypothesis of the formation of a cyclic boronate ester with saccharide was then suggested and confirmed by Lorand and Edwards who published the first quantitative evaluation of saccharide-boronic acid interactions in 1959.[40] In spite of the fact that the structure of the complex formed between boronic acids and saccharides in aqueous solution is still disputed,[41] the use of boronic acids in the design of sensors for saccharides has recently gained a great deal of interest among a variety of research groups.[42-46]

Boronic acids covalently react with 1,2 or 1,3 diols to form five or six membered cyclic esters in non-aqueous or basic aqueous media (Scheme 1.2).

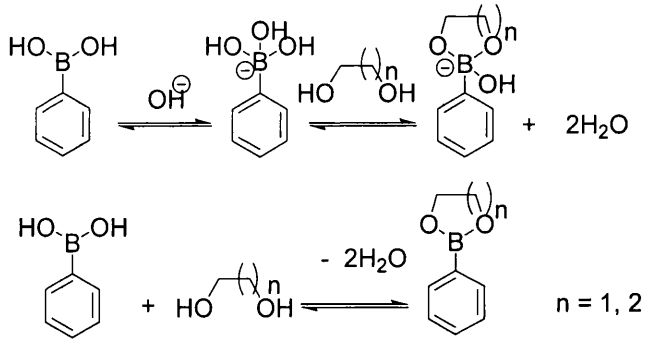

Scheme 1.2 - Formation of Cyclic Boronate Ester at High pH or Non-Aqueous Media.

To avoid problems encountered in a high pH media, a neighbouring amine group can be incorporated into the molecule (Scheme 1.3). This boron-amine interaction was first proposed by Wulf.[47]

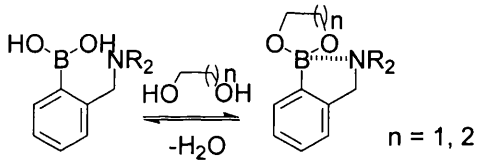

Scheme 1.3 - Effect of an Amine Neighbouring the Boronic Acid.

Boronic acids have a sp^2 hybrization and therefore the angle between bonds is 120°. However, when a five membered cyclic boronate ester is formed, the angle is reduced to 108°, which is closer to sp^3 hybrization (angle 109°). This increase in the *s* character of the free boron orbital results an enhancement of the Lewis acidity of the original boronic acid. This means that the cyclic boronate ester formed is more acidic than the boronic acid. A strong acid-base B-N interaction takes place between the boronic acid and the neighbouring amine, which facilitates the formation of stable boronic acid-saccharide complexes under neutral conditions. The particular feature of boronic acids to bind covalently, rapidly and reversibly with saccharides make them very attractive as

receptors in the design of saccharide sensors. However, the sensing tool can differ. In this part we have chosen to describe receptors using CD (circular dichroism) or a change of colour property induced by saccharide recognition. An important number of receptors uses fluorescence as a sensing tool. This method of sensing will be discussed in the final part of this chapter. Some receptors utilise CD activity induced by the formation of the complex between the saccharide and the boronic acid. Receptors containing two boronic acid units can bind one molecule of saccharide by its head and tail forming a rigid 1:1 complex (i.e. compounds **18** and **19**, Figure I-9).

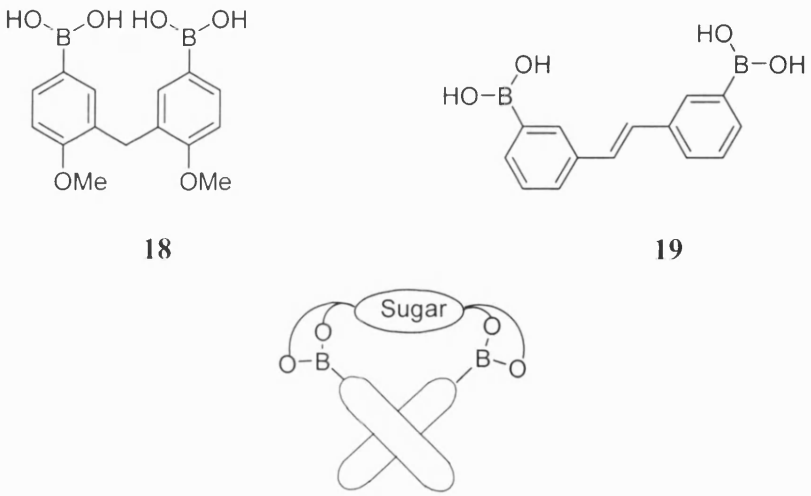

18 **19**

Figure I-9. 1:1 Complex Formed between a Saccharide and a Diboronic Acid.

CD activity is induced by the formation of this complex. The receptor molecule (boronic acid) has to be achiral and chromophoric and the guest molecule chiral and non-chromophoric, which is the case for saccharides (Scheme 1.4).

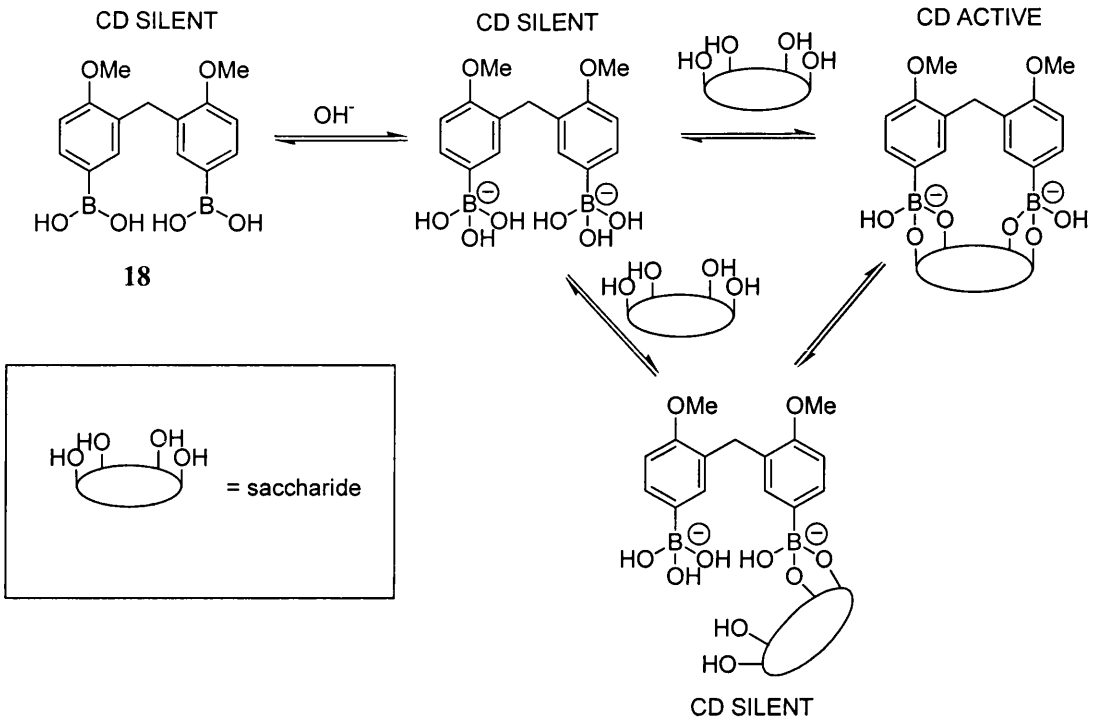

Scheme 1.4 - Effect of the 1:1 Complex Formation on the CD Activity.

The formation of the bidentate 1:1 complex with one enantiomer imposes a fixed position for the dipolar moment of the complex. The other enantiomer induces the symmetrically inverted position. This can be determined by CD spectroscopy, where D- and L- saccharides give positive and negative exciton coupling respectively.[48,49]

Colour changes on the addition of saccharide represent another way of sensing using boronic acid receptors. If a system with a large colour change can be developed it could be incorporated into a diagnostic test paper for D-glucose, similar to universal indicator paper for pH. Such a system would make it possible to measure D-glucose concentrations without the need for specialist instrumentation. For example, the boronic acid appended spirobenzopyran **20** undergoes changes in the absorption spectrum upon saccharide addition.[50] The binding of the saccharide changes the position of the merocyanine (MC) to spyropyran (SP) equilibrium and hence the colour of the system. With added saccharide, the SP structure **20d** is favoured over the MC

structure **20c** due to a stronger B-N interaction in the saccharide complex **20d** (Scheme 1.5).

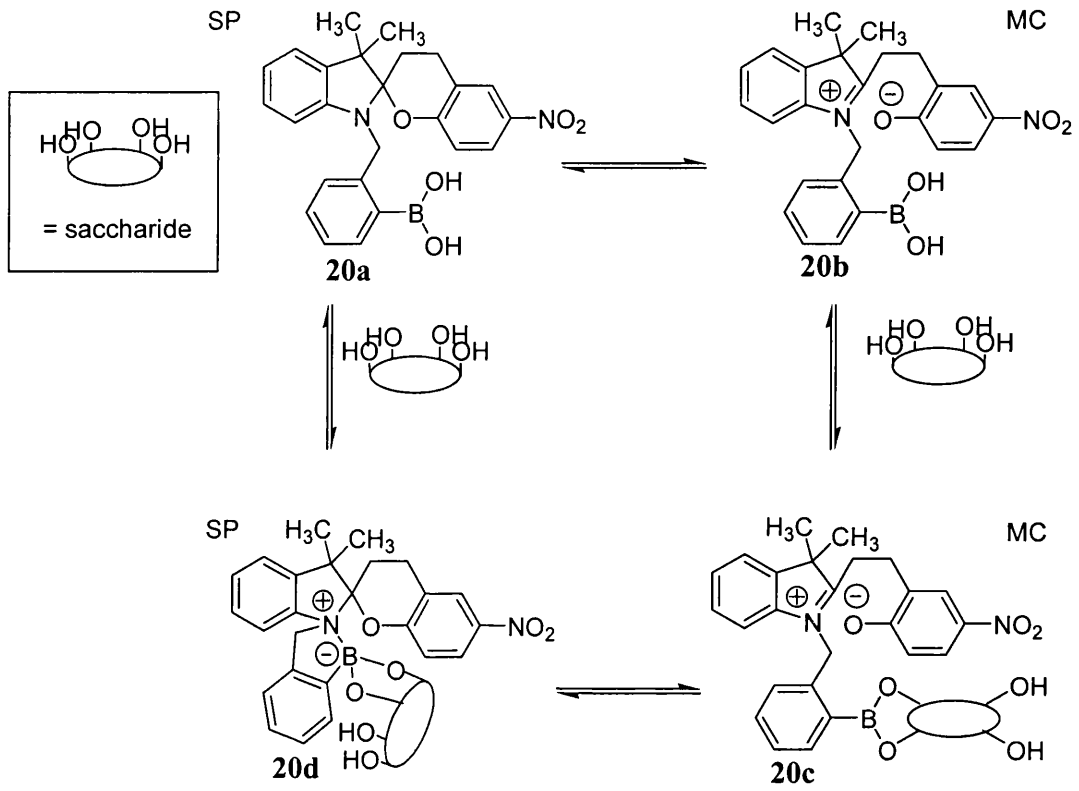

Scheme 1.5 - Effect of the Addition of a Saccharide Favouring the SP Formation.

The diazo dye system **21** is a particularly interesting example because a large visible colour change from purple to red can be observed on the addition of saccharides.[51]

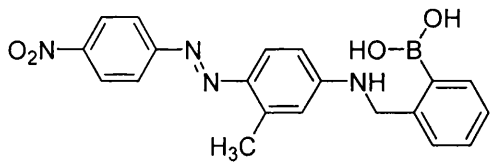

21

In the absence of saccharide, at pH 11.32, the observed colour is purple and in the presence of saccharide the colour is red. The equilibrium represented in Scheme 1.6 shows the different existing species before and after the binding of the saccharide.

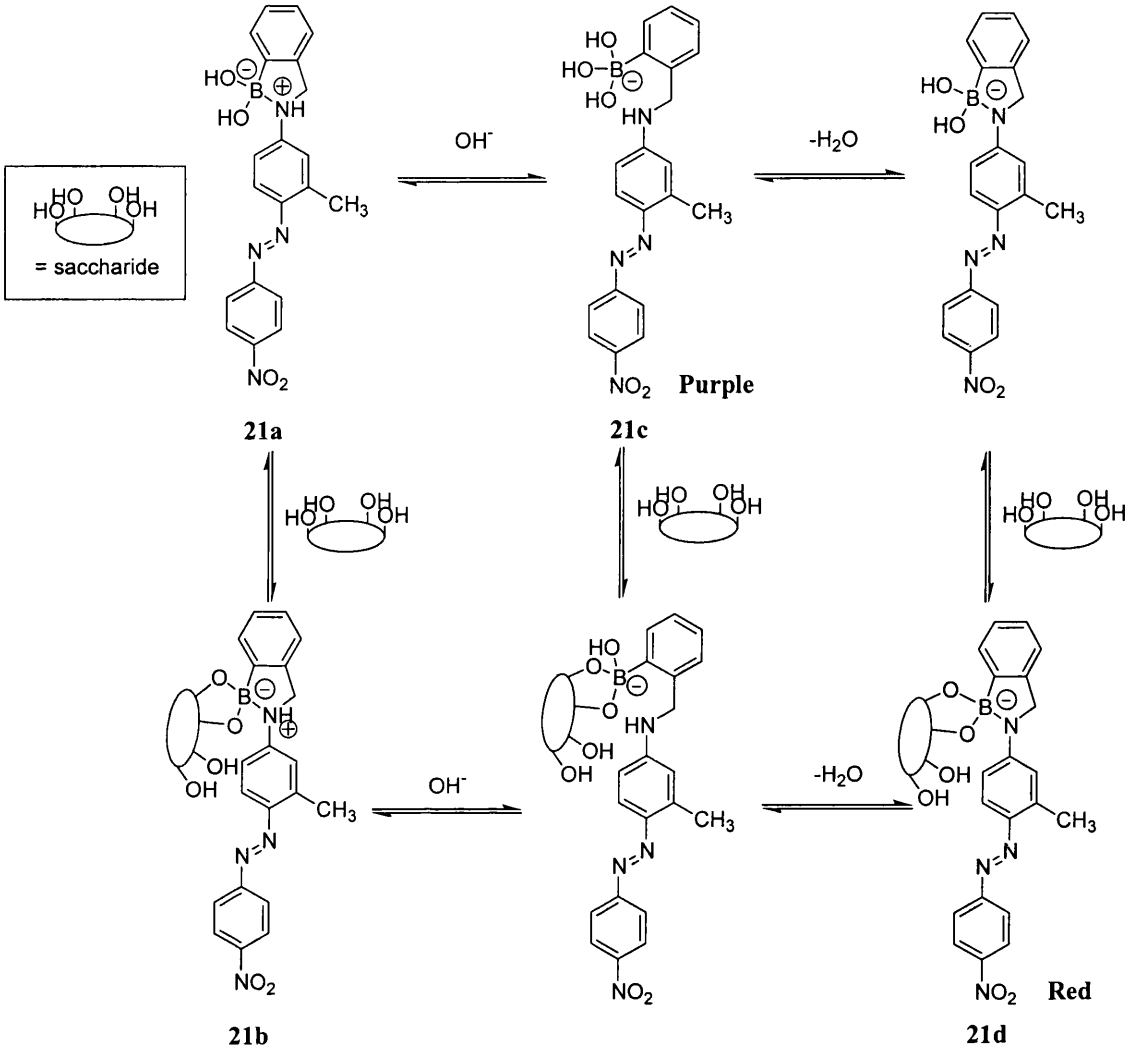

Scheme 1.6 - Existing Species at pH 11.32.

As mentioned previously, cyclic boronate esters (formed by saccharide binding) are more acidic than free boronic acids. This means that the B-N acid-base interaction is stronger in the species **21b** than **21a**. Therefore, the N-H proton of species **21b** is more acidic than the corresponding proton of **21a**. Consequently, at higher pH, species **21b** will deprotonate to form the red species **21d**, whereas the weaker B-N bond in **21a** is broken by hydroxide ion to form the purple coloured species **21c**.

I-3 Fluorescent Sensors

I-3.1 Fluorescence

Fluorescence was first reported in 1565 by Nicolas Monardes, a Spanish physician and botanist, who noticed a strange blue glimmer from water contained in a cup made from a specific wood (*Ligirium nephiticiem*). However the understanding of the process only started in the late 19th century with George Stokes' work. He was the first to establish that fluorescence emission occurs at a longer wavelength than the absorption. Figure I-10 shows the various absorption and emission processes which can occur in a molecule.[52] The singlet state and the triplet state of the electronic energy level of a molecule are presented as $^1\Sigma$ and $^3\Pi$, respectively. The first excited state is represented by $^2\Sigma$. Each electronic level has a series of vibrational states, labelled by ν_1, ν_2, ν_3 etc. The absorption of a quantum of light by a molecule results in the elevation of an electron from the molecule's ground electronic state ($^1\Sigma$) to one of several vibrational levels in the electronically excited state. In solution, the excited state molecule rapidly relaxes to the lowest vibrational level of the lowest electronic state ($^2\Sigma$). This relaxation corresponds to non-radiative or internal conversion (IC) transitions shown as wavy lines within the excited state in Figure I-10. The energy is lost in collisions with other atoms or molecules, appearing in the other particles as kinetic energy of motion or in excited vibrational states. After relaxing thermally to the lowest vibrational level of the $^2\Sigma$ the electron may return to the $^1\Sigma$ state with light emission (fluorescence). However, if the molecule is sufficiently long-lived in the $^2\Sigma$ state, it may cross into a lower energy triplet state ($^3\Pi$). Since transitions between two electronic states of different multiplicity are not allowed (quantum mechanics rules), Inter-System Crossing (ISC) is the only way for an electron to be in a triplet state. Relaxation from the $^3\Pi$ state to the

$^1\Sigma$ state can also occur with light emission in solids (phosphorescence), by the release of energy (radiationless transition), or by chemical reaction The phosphorescence is a slow process, it continues long after the excitation radiation is removed, sometimes for a matter of seconds or even minutes. The fluorescence emission, however, is a very rapid transition, requiring less that 10^{-8} seconds to occur.

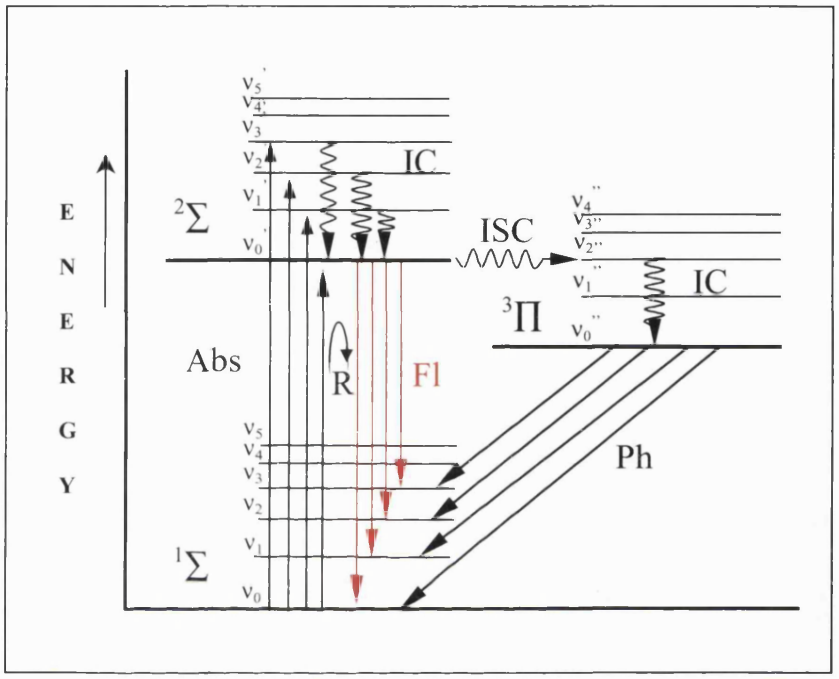

Figure I-10. A Molecular Energy Level Diagram showing Absorption (Abs), Resonance Emission (R), Fluorescence (Fl), Inter-System Crossing (ISC), Internal Conversion (IC) and Phosphorescence (Ph).

The extreme rapidity (quasi-instantaneous) of the fluorescence process allows immediate detection of saccharides and represents one of the numerous advantages that its use in molecular recognition offers. The high sensitivity of the fluorescence technique also means that only very small amounts of sensor molecule (typically 10^{-6} M) are required. Moreover, fluorescence spectrometers are cheap and widely available. An increase or decrease in the fluorescence intensity, or shifts in the absorption or emission spectra are the main changes observed when binding occurs. These changes

are based on a variety of photophysical processes. The most important of these are described in the following section.

I-3.2 Fluorescence Enhancement by Alkali-Metal Ions

This section describes three examples of alkali-metal ions receptors, which observe fluorescence enhancement when ions are added. Whilst these examples illustrate three different photophysical processes, various others exist. It is also important to note that sometimes the exact nature of the fluorescence is unknown. The first concept to be considered involves the modification of the energy levels of the electronic excited states by the formation of a complex between a cation and the receptor. This can lead to a decrease in the triplet energy level relative to the fluorescent singlet state and the ground state. This decreases the probability of Inter-System Crossing (ISC) occurring leading to an increase in the fluorescence emission. In the example described below, the complexing of a sodium cation by the four carbonyl units of the triester **22** affects the level of the n (non-bonding) state and π^* (bonding) excited state.[53]

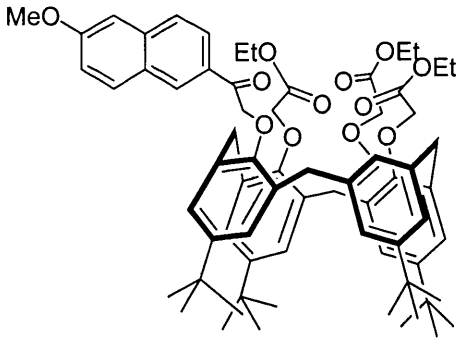

22

When sensor **22** is uncomplexed, the lowest excited state can be reached by a $n\pi^*$ transition. The $n\pi^*$ excited state has a much longer lifetime than $\pi\pi^*$ and so there is a much greater chance of ISC taking place and consequently a decreasing of the fluorescence intensity. In the presence of a cation, which strongly interacts with the

lone pairs of the carbonyl groups, the n is likely to be shifted to a higher energy level so that the lowest excited state becomes $\pi\pi^*$.

The second photophysical process suggested for fluorescence enhancement is the displacement of a cation complexed quencher by another non-quencher cation. Scheme 1.7 illustrates this concept.[54]

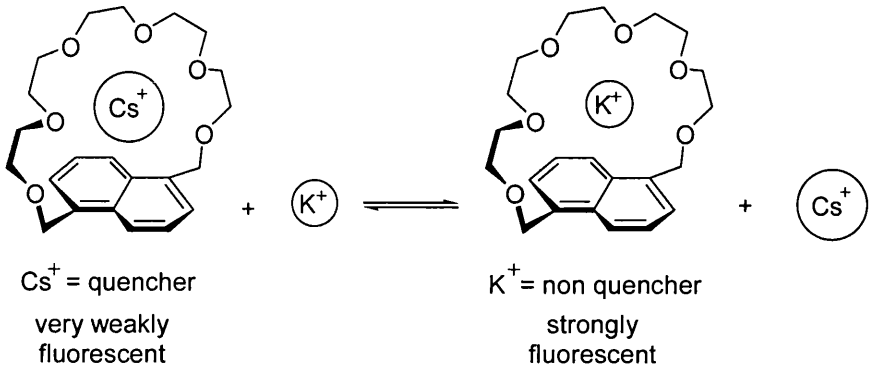

Scheme 1.7 - K^+ Displacement of a Complexed Fluorescence Quencher.

The heavy atom ion Cs^+ was selected as a quencher because of its ability to increase Inter-System Crossing. The crown ether forms a band above the naphthalene. This structure is ideal to hold Cs^+ against the π system of the naphthalene chromophore, a favourable interaction for fluorescence quenching. A potassium ion K^+, which is not a quencher, replaces the Cs^+, thus preventing fluorescence quenching. It has been shown that the addition of a 0.1 M concentration of potassium ion causes an 80 percent increase in fluorescence intensity.

The last example to be presented in this part involves the interruption of an intramolecular quenching process by the addition of a cation. Scheme 1.8 shows how the complexation of a cation by the receptor can separate the chromophore from the quencher contained within the same molecule. This results in an increase of the fluorescence intensity.[54]

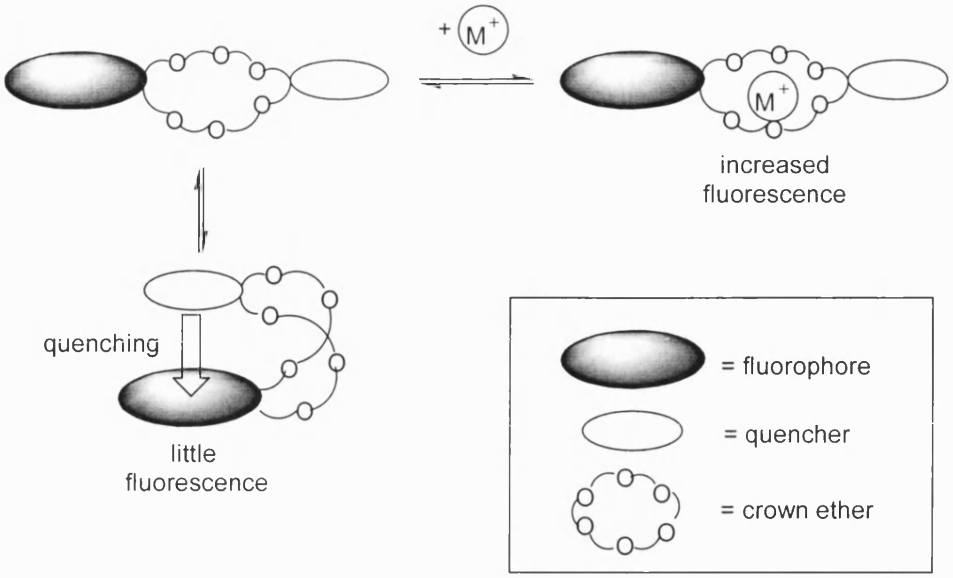

Scheme 1.8 - Cation-Fostered Interruption of Quenching in a Crown Ether Containing both a Fluorescent Chromophore and a Quencher.

The azacrown ether **23** is an example of sensor producing an enhanced fluorescence according to the process described in Scheme 1.8. It contains a fluorophore unit (naphthalene) and a quencher unit (aniline). When a potassium cation is complexed by the crown ether, it forces the aniline and the naphthalene units apart, preventing fluorescence quenching and enhancing the fluorescence emission. The addition of a 0.16 M solution of K^+ produces an increase of 55 % in the fluorescence intensity.

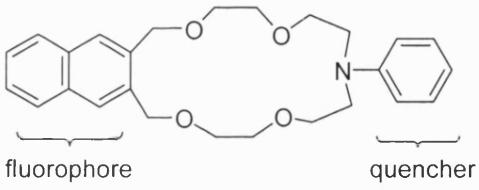

23

I-3.3 Photoinduced Charge or Energy Transfer[55]

Many common examples of heteroatom-containing π-systems have enlarged dipoles in their excited states due to Internal Charge Transfer (ICT). The electronic environment (i.e. solvent) can cause modifications of the electronic excited states. It can thus be anticipated that cations in close interaction with the donor (D) or the acceptor (A) moiety of a receptor will change the photophysical properties of the latter. The complexation of a cation affects the efficiency of the ICT within the molecule which will affect the fluorescence.[56] When the cation interacts with the donor group, Figure I-11 (a) below, the electron donating character of the donor D is reduced and the complex is destabilised (higher energy). The larger the dipole moment in the excited state relative to the ground state, the greater the destabilisation of the excited state. This results in a 'blue shift' in the absorption wavelength (higher frequency). When the cation interacts with the acceptor group, Figure I-11 (b), the excited state is more stabilised by the cation than is the ground state, leading to a 'red shift' of the absorption spectrum (lower frequency).[57]

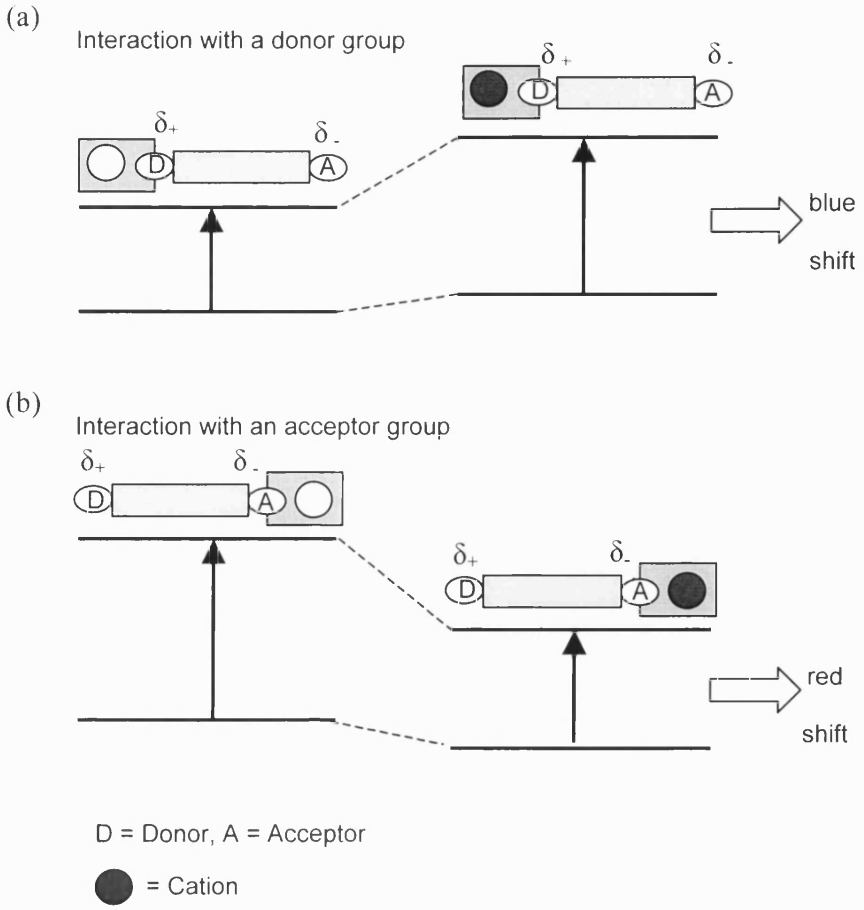

Figure I-11. Interaction of a Cation with a a) Donor Group (D) or b) Acceptor Group (A).

In the azacrown ether **24**,[58-60] the donor group is represented by the crown ether and the acceptor by the dicyanomethylene. When a cation is complexed by the crown ether, there is an effect due to the interaction of the cation with the donor group of the molecule. As expected a 'blue shift' in the absorption and emission (fluorescence) spectra is observed upon addition of alkali metal ions. However, the 'blue shift' of the fluorescence emission is less pronounced than the shift in the absorption spectrum. A decrease of the fluorescence intensity is also observed. In this example, changes in the fluorescence intensity are due to the ejection of the cation after photoabsorption.

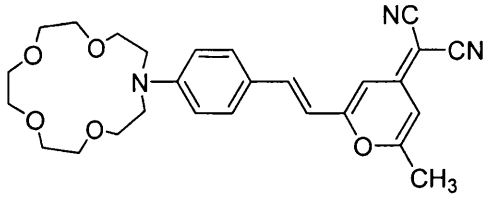

24

The second example (compound **25**[61]) shows similar blue shifts in the absorption and emission spectra resulting from the interaction between the cation and the donor (azacrown ether). However, in this case, the fluorescence intensity increases upon the addition of the cation. This is the result of the formation of a TICT (twisted internal charge transfer) state formed by single bond twisting upon excitation (the single bond connecting benzoxazinone and ethylene).

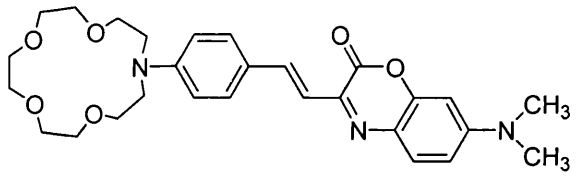

25

Compound **26**[62-64] illustrates the case of a bound cation interacting with an electron-withdrawing group of the molecule.

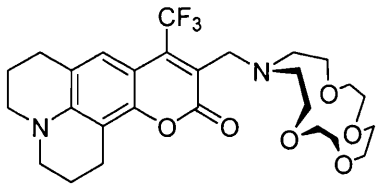

26

Upon excitation, there is a charge transfer from the nitrogen atom of the julolidyl ring to the carbonyl group, and the complexation of a cation, intensifying the acceptor character of the carbonyl which enhances this charge transfer. Red shifts in the absorption and emission spectra are thus observed. This shift mirrors exactly the order of increased

charge density of the cation. As well as the shift in the fluorescence, the intensity is also modified and increases upon addition of Li^+, Na^+ and Ba^{2+}. In the free ligand, the crown ether can interact with the coumarin ring, which results in some quenching. Upon complexation, the crown ether and the coumarin are placed in such a position that they can no longer interact and the fluorescence increases.

I-3.4 Photoinduced Electron Transfer (PET)

Fluorescent Photoinduced Electron Transfer (PET) sensors represent an important class of fluorescent sensors for the recognition of neutral or cationic molecules. They can be formalised as 'fluorophore-spacer-receptor' systems as schown in Figure I-12 (a).[56] A fluorophore module is the site of both excitation and emission, the receptor is responsible for the guest complexation and decomplexation and a spacer module holds the fluorophore and the receptor close to, but separate from, each other.

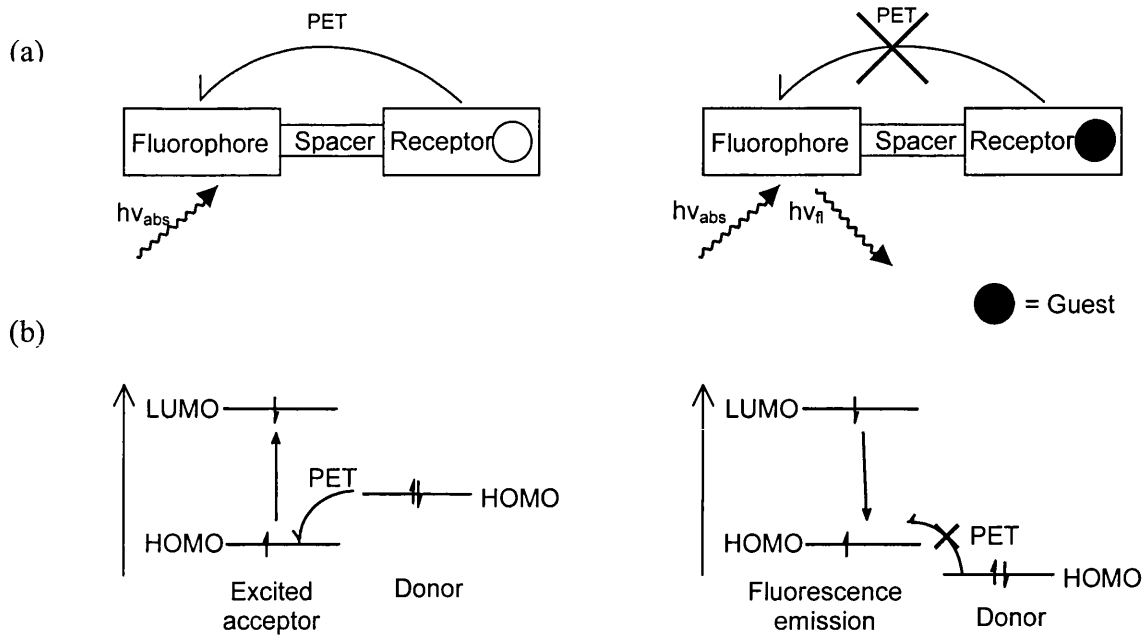

Figure I-12. (a) Schematic of a PET Sensor, (b) PET explained using Simple Frontier Molecular Orbital.

Upon excitation of the fluorophore, an electron in the highest occupied molecular orbital (HOMO) is promoted to the lowest unoccupied molecular orbital (LUMO). This enables PET from the HOMO of the donor (belonging to the free receptor) to the HOMO of the fluorophore, causing fluorescence quenching. Upon guest binding, the redox potential of the donor is raised so that the relevant HOMO becomes lower in energy than that of the fluorophore. Consequently PET is not possible anymore and fluorescence quenching is suppressed. Therefore, fluorescence intensity is enhanced upon guest binding and these systems are called "Off-On" systems. PET systems employ thermal back-electron transfer as a self-repair mechanism following the potentially damaging PET process. Lone pairs of electron on amine or carbonyl groups are usually used as donor in PET systems.

The history of PET sensors began in the late 70's with the methylamines **27** and **28**.[65,66] They both undergo an enhancement of fluorescence intensity due to protonation of nitrogen atoms.

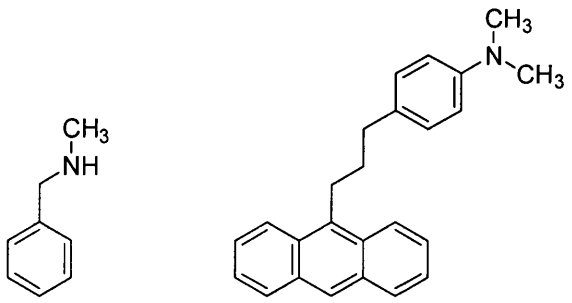

27 **28**

Most PET systems function following the "Off-On" principle illustrated in Figure I-12 above. Cationic sensors largely dominate in the literature but we can also find PET sensors for neutral molecules. Some examples of "Off-On" PET sensors are presented below in Figure I-13.

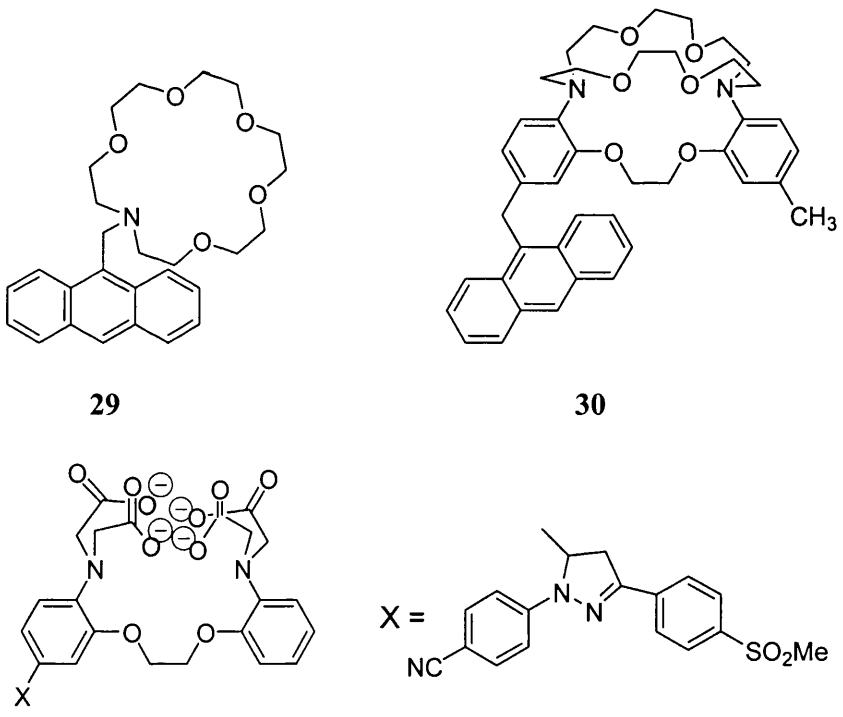

29 **30**

31

Figure I-13. Examples of "Off-On" Sensors.

Compounds **29**, **30** and **31** are all cation sensors but they have different modes of operation. Azacrown ether **29**[67] is the first and simplest coronand PET sensor. Its fluorescence quantum yield increases from 0.003 to 0.14 upon binding of K^+ in methanol. Cryptand **30** is an example of macrobicyclic structure expected to be more selective toward alkali cations than simple macrocyclic structures. The cavity in **30**[68] is ideally suited to binding K^+ and also has the advantage of having a lower pK_a than aliphatic amines (i.e. **29**). This allows it to overcome the problem of pH sensitivity *via* protonation of the nitrogen atoms. Chelator **31**[69] is a chelating PET sensor selective for Ca^{2+} cations. It uses the 5-methine group as a spacer and the 4 carboxylic acid groups as chelators. Naphthalen-1-yl-methylamine **32** is one example of a fluorescent PET sensor for neutral molecules.

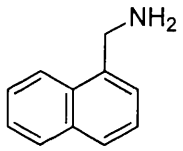

32

This kind of PET sensor is known to be quenched by unprotonated amines.[65] Lakowicz *et al.* studied the fluorescence behaviour of **32** in organic solution in the presence of gaseous carbon dioxide.[70] They observed an enhancement of the fluorescence when CO_2 was dissolved in solution. This is a result of a decrease in amine quenching. The interaction between the amine and CO_2 are currently under investigation but compound **32** seems to be a promising CO_2 sensor.

Another variant of the PET sensor is to use opposite "On-Off" systems. In this case the binding of the guest molecule leads to fluorescence suppression of the fluorophore, caused by the formation of a strong PET acceptor, Figure I-14.

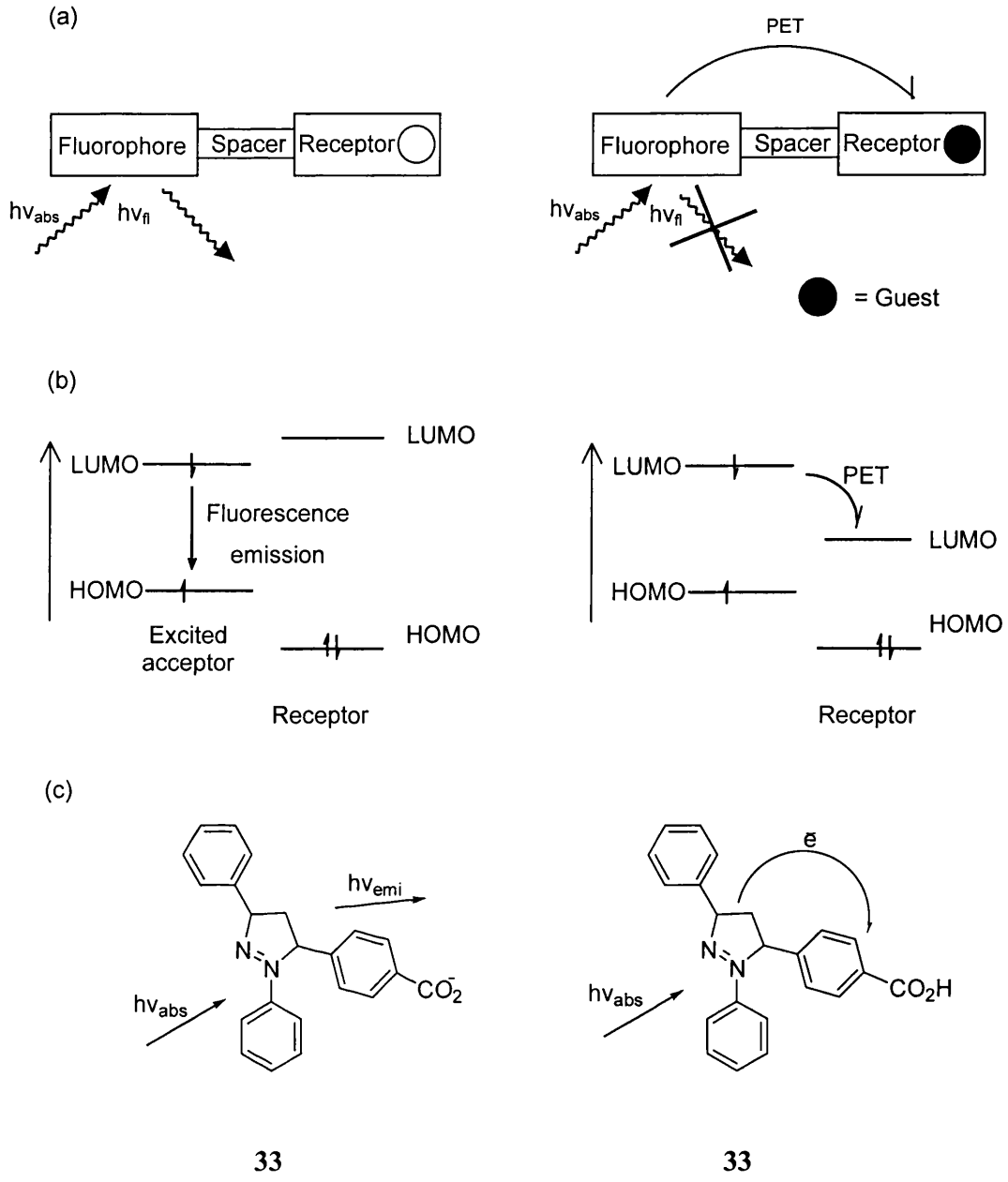

Figure I-14. (a) Schematic Model of a PET "On-Off" System, (b) Frontier Molecular Orbital Representation, (c) Example of a PET "On-Off" System.

In the Figure I-14 (c), protonation of the carboxylate of **33**,[71] is responsible for the lowing of its LUMO. The change in the LUMO energy enables PET from the fluorophore to the receptor. Recently Vogtel and co-workers developed an "On-Off" PET system using a dendrimer structure containing 32 dansyl units at the periphery and 30 aliphatic units in the interior.[72] The strong fluorescence of all the dansyls units is

quenched when a Co^{2+} ion is incorporated into the dendrimer. Shinkai *et al* also investigated the idea of an "On-Off" system.[73] However, the Shinkai system is based on a different principle. They use the steric crowding of the porphyrin **34** to switch the fluorescence "On" or "Off".

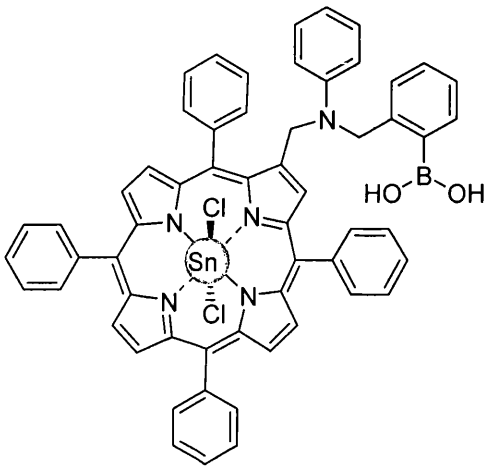

34

Upon binding of saccharides to the boronic acid moiety, the ligands are suspended over the planar structure of the porphyrin, which places the boron and the nitrogen too far apart to interact. PET can then occur from the amine to the porphyrin and the fluorescence is switched "off". However, when the boronic acid is unbound, the boron and nitrogen can come close enough to interact. This results in the suppression of PET and fluorescence recovery.

"Off-On" and "On-Off" principles can also be combined to design even more elaborate "Off-On-Off" systems. The design of this type of sensor requires a combination of 3 distinct units each playing a key role in the system. A fluorophore, where emission and electron transfer takes place, is linked to two different receptors. One receptor is responsible for an electron transfer to the fluorophore and the second receptor is a strong PET acceptor. The action of each receptor is only activated within a specific range of guest concentrations. Spacers also play an important role in the functioning of

the system as the two receptors have to be close enough to the fluorophore to allow electron transfer, but separated enough, in order to avoid other possible transfers. DeSilva exploited the idea by developing an "Off-On-Off" PET system which displays strong fluorescence within certain pH windows.[74,75] The different structures and electron transfers occurring in the system at different pH are depicted in Figure I-15.

Low pH: (≤ 4.4) non-fluorescent

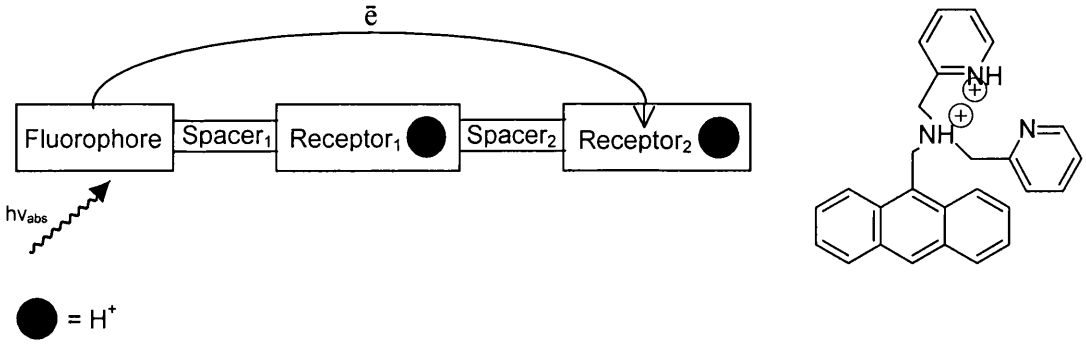

Mid pH: (4.4 – 7.5) fluorescent

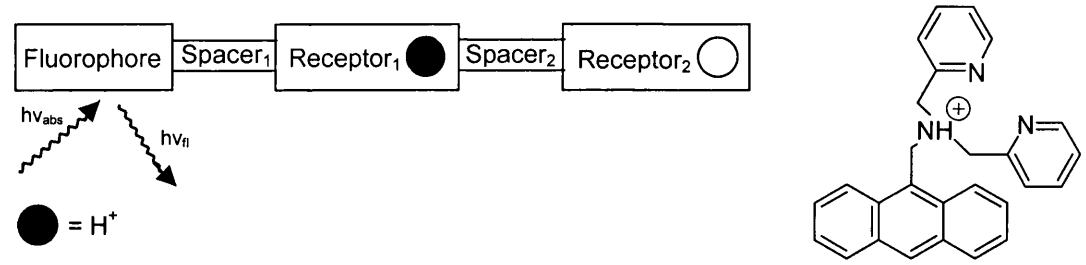

High pH: (≥ 7.5) non-fluorescent

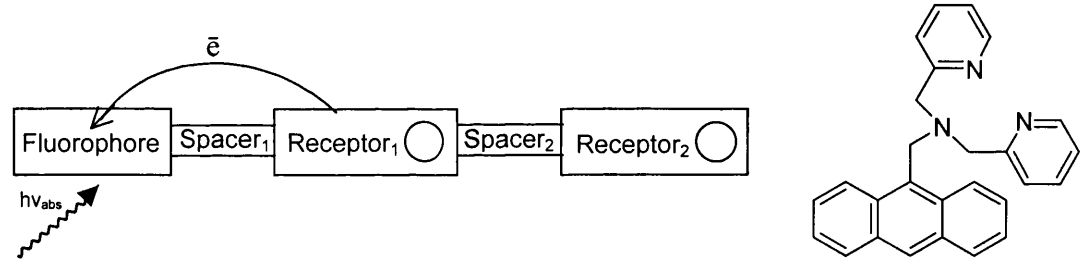

Figure I-15. Schematic Representation of the Different Structures and Electron Transfers Occurring in a "Off-On-Off" PET System at Different pH.

$Receptor_1$ is PET active according to the normal logic for an "Off-On" system. This means that at high pH (pH ≥ 7.5), when the tertiary amine is not protonated, PET occurs from $Receptor_1$ to the anthracene. Protonation of the amine at mid pH (4.4 ≤ pH ≤ 7.5) prevents PET and the fluorescence is switched "on". Decrease in pH leads to protonation of the pyridine of $Receptor_2$ leading to a significant change in its reduction

potential, which favours the second PET process from the fluorophore to $Receptor_2$. This is the principle of "On-Off" systems described earlier. The pK_a values for the protonation of the tertiairy amine and the pyridine ring are 7.5 and 4.4 respectively.

I-4 PET Fluorescent Sensors using Boronic Acid as Saccharide Receptor

I-4.1 Introduction

We have seen in Section I-2.2.2 that boronic acids have been widely used in the design of sensors. They covalently react with 1,2 or 1,3 diols to form cyclic esters in non-aqueous or basic aqueous media (Scheme 1.2, p17). The disadvantage of a high working pH in aqueous solution can be overcome by introducing a neighbouring amine group. The latter, by its interaction with the boron, lowers the pK_a of the molecule. The amine neighbouring the fluorophore also provides an electron-rich centre for PET processes. Figure I-16 shows the functioning of a boronic acid PET sensor.[76]

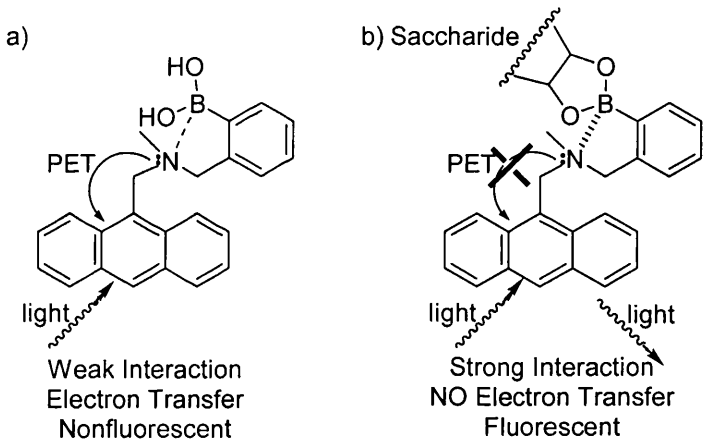

Figure I-16. Example of a Boronic Acid PET Sensor a) unbound and b) with saccharide bound.

The structure of the sensor in Figure I-16 agrees with the general model 'fluorophore-spacer-receptor' of "Off-On" PET systems (Figure I-12). The fluorophore is represented by an anthracene unit and the saccharide receptor by a boronic acid moiety. The lone pair of electrons on the nitrogen of the amine is responsible for quenching the fluorescence *via* a PET process. Upon saccharide binding, the PET stops and the fluorescence is switched "on". This can be interpreted as follows. When the boronic

acid binds the saccharide, forming a cyclic boronate ester, the Lewis acidity of the boronic acid is enhanced. Therefore, the Lewis acid-base interaction between the tertiary amine and the boron is stronger. The strength of this interaction modulates the PET from the amine (acting as a quencher) to the anthracene. These fluorescent sensors show increased fluorescence at neutral pH through suppression of the PET from the amine upon saccharide binding. Figure I-17 illustrates this concept by using simplified molecular orbital theory.

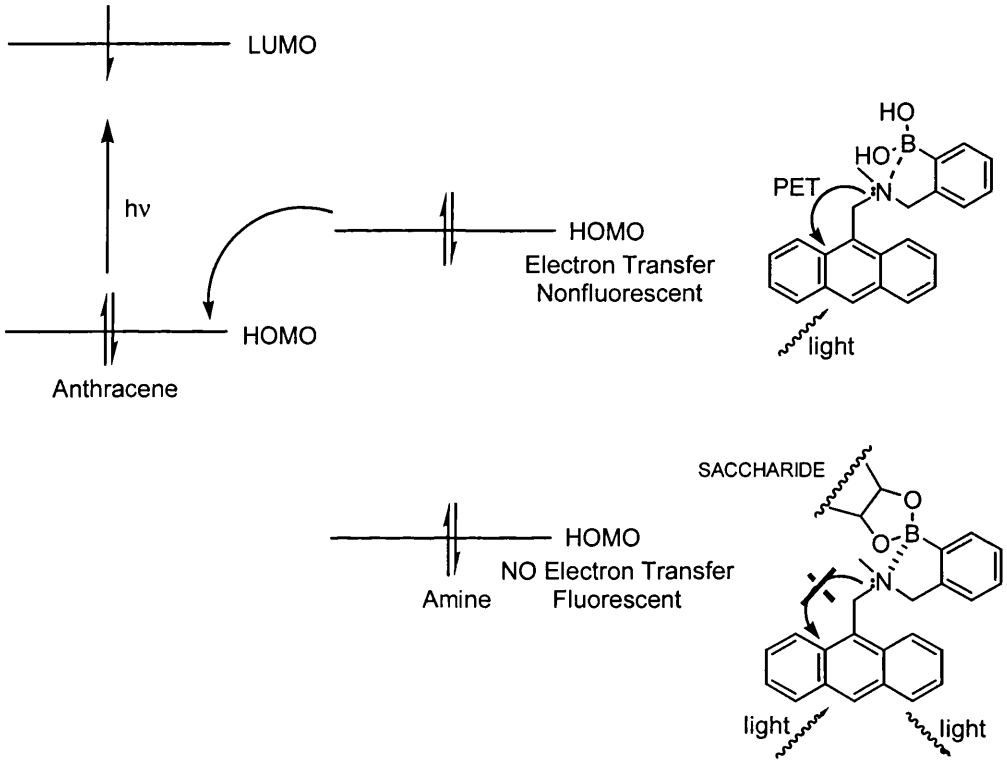

Figure I-17. Changes of the Oxidation Potential of a Neighbouring Amine upon Saccharide Binding.

I-4.2 Evolution of the Sensors

The first fluorescent PET sensors for saccharides contained only a fluorophore and a boronic acid. In 1992, Czarnik showed that 2- and 9- anthrylboronic acid **35** and **36** could be used to detect the presence of saccharides.[77] The PET from the boronate anion formed is believed to be the source of the fluorescence quenching. Therefore, the first examples of PET sensors were using an "On-Off" process. Similarly, Aoyama showed that 5-indolylboronic acid **37** undergoes fluorescence decrease upon the addition of saccharides.[78] The selectivity of this type of sensor is in line with the selectivity of phenyl boronic acid. However, the fluorescence change upon the binding of saccharide was very small [I (in the presence of saccharide)/I_0 (in the absence of saccharide) = 0.7].

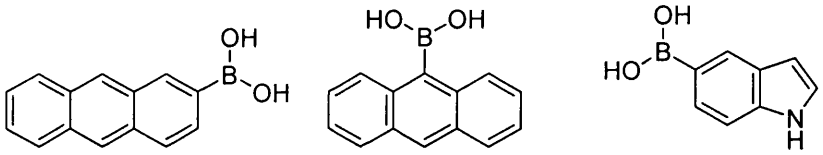

35 **36** **37**

Figure I-18. First PET Fluorescent Sensors for Saccharides.

The introduction of an amine group to the molecule to lower the working pH of sensor molecule also allows the development of new PET systems. The fluorescence enhancement of this type of sensors makes them "Off-On" PET sensors for saccharides. The first of the series, the boronic acid **38** below was prepared in 1994 by James and Shinkai.[79] Compound **38** shows a selectivity order, which is inherent to all monoboronic acids.[40]

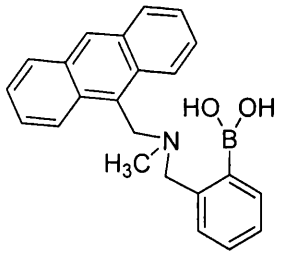

38

The glucose selectivity of "Off-On" fluorescent PET systems was reached later by the introduction of a second boronic acid group to produce the diboronic acid **39**.[80] The relative spatial orientation of the two boronic acids in **39** favours the binding of D-glucose. Glucose can be bound in two different modes forming a 1:1 or 2:1 complex (Scheme 1.9).

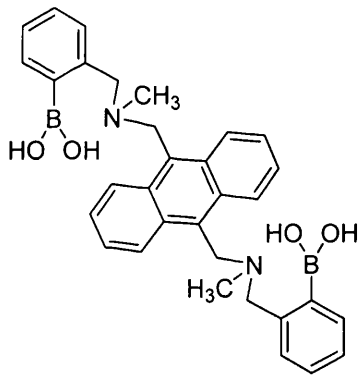

39

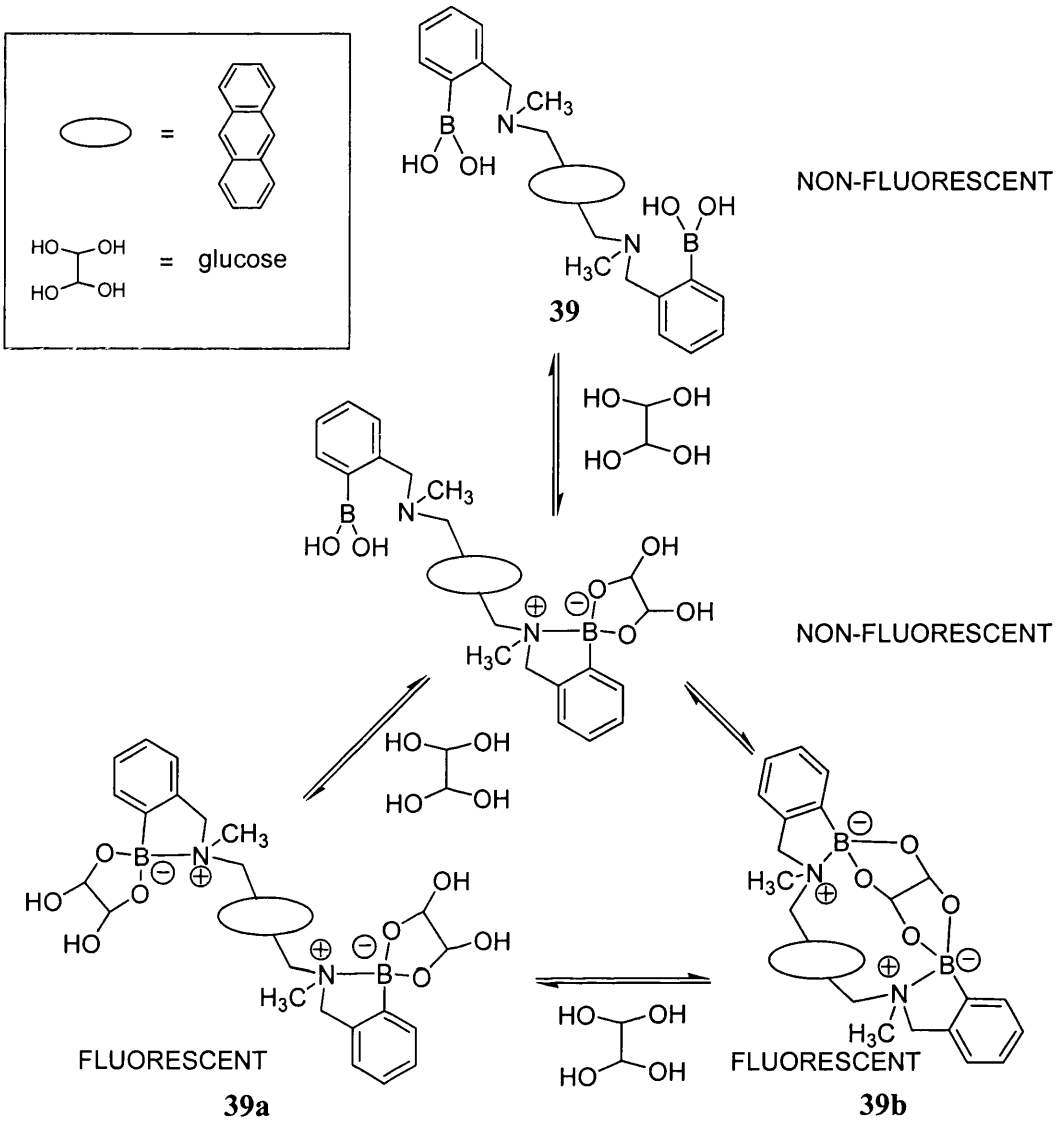

Scheme 1.9 – Formation of two Different Complexes (1:1 and 1:2) between **39** and D-Glucose.

Norrild has carried out more detailed investigation of this system in order to confirm the chemical structure of the bound glucose.[41] Norrild was interested in the system since the ^{1}H NMR spectrum reported indicated that D-glucose bound to the receptor in its pyranose form.[80] From ^{1}H NMR spectrum observations it was concluded that the diboronic acid **39** initially interacts with the pyranose form of D-glucose and over time the bound glucose converts to the furanose form. The Norrild experiments were carried out using 1:1 D-glucose and diboronic acid, whereas the fluorescence titrations reported

involve a 10-100 fold excess of D-glucose.[80] Therefore, in the D-glucose fluorescence titrations, it is possible that the furanose form will be replaced by a new glucose molecule in the pyranose form as the furanose is formed. The diamine diboronic acid **40** is one of the diboronic acid derivatives of sensor **39**.[81] It has a flexible spacer but behaves similarly to **39**. The two pyrene units, which are able to form excimers, give information on both the saccharide concentration and the structure of the complex. The 1:1 binding of a saccharide to **40** leads to an increase in fluorescence intensity over that of the monomer. This increase is produced partially by less excimer formation and partially by the increased overall fluorescence quantum yield because of the suppression of the PET process. The 1:2 binding of **40** to saccharides, on the other hand, increased the excimer:monomer fluorescence intensity ratio. The selectivity of **40** is similar to **39**.

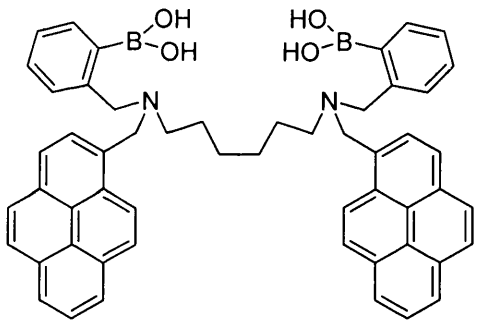

40

Two other diboronic acid sensors **41**[82] and **42**[83] have been synthesised, respectively for the recognition of saccharides at high concentrations and for small saccharides (i.e. D-sorbitol). Sensor **41** with a larger space between the two boronic acid groups loses selectivity and sensitivity. It can detect an important variety of saccharides in solution *via* the formation of a 1:2 complex. Based on data obtained from studies with the diboronic acid **41**, the diboronic acid **42** was synthesised. The distance between the two boronic acids groups has been reduced, which modifies the selectivity of **42** towards small saccharides.

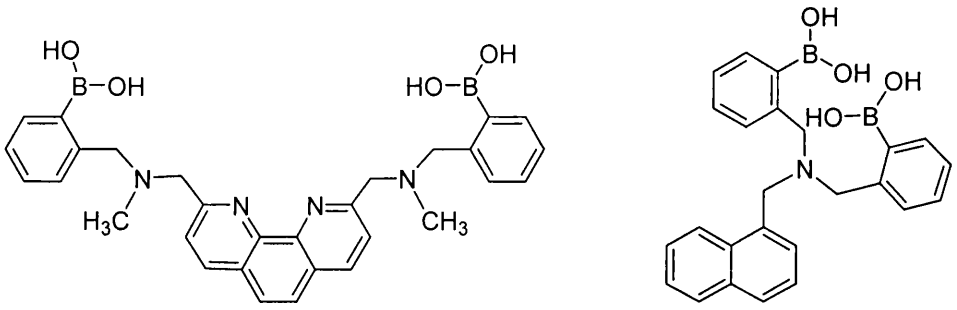

41 **42**

Figure I-19. Further Examples of PET Fluorescent Sensors Diboronic Acids.

The research I have undertaken during the last three years is an extension of previous studies in the field of diboronic acid PET fluorescent sensors. It consisted, initially, of the synthesis of novel modular diboronic acid fluorescent sensors for saccharides. The modular design of the systems was chosen to allow the synthesis of a whole family of sensors using a single synthetic route. The following section describes the synthetic work carried out to prepare two series of sensors and analytical experiments providing information on the interactions of the sensors with saccharides.

II Results and Discussions

II-1 Introduction to the project

The aim of the project was to synthesise a novel modular diboronic acid PET fluorescent sensor for saccharides. The design of this new molecule was based on the structure of sensor **39**, schematically represented in Figure II-1.

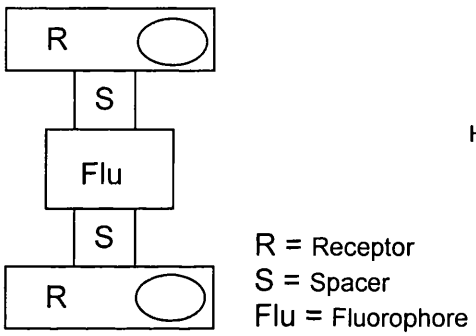

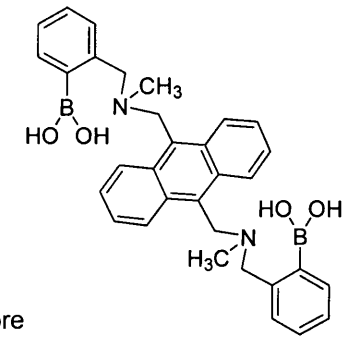

39

Figure II-1. Schematic Representation of PET Sensor **39**.

The characteristics of the structure of compound **39** clearly appear on the schematic representation above. The fluorophore Flu (the anthracene unit) is placed at the centre of the molecule and the two receptors (phenyl boronic acid units) are arranged symmetrically to either side of the anthracene unit. In compound **39**, the fluorophore and receptors are separated by an identical spacer (S). The main rationale behind the design of the new target molecule was to use a modular approach to allow variation of the nature of the fluorophore and variation of the distance between the two boronic acids. Figure II-2 (a) shows a representation of the target molecule.

a) b)

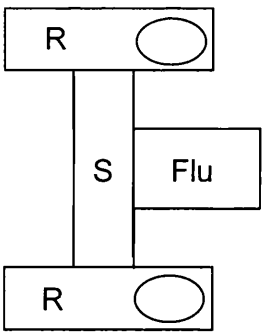

R = Receptor
S = Spacer
Flu = Fluorophore

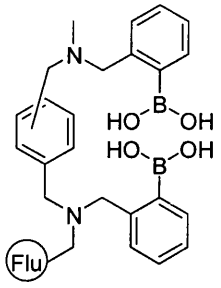

43, **44**, **45** (*para* series)
46, **47**, **48** (*meta* series)

Figure II-2. Schematic Representations of Target Compounds.

As we can see, the main structural difference between compound **39** and the target molecules **43-48** is the position of the fluorophore. The fluorophore is no longer in the centre of the molecule. It is clear in Figure II-2 (a) that the fluorophore (Flu) and the two boronic acid moieties (R) of the new target molecule are placed around a spacer (S). This modular design provides an advantage in the synthesis of a series of different sensors. The sensor is not built around the fluorophore as with compound **39**, which means that the fluorophore and the two boronic acid units can be added to the molecule in the final stages of the synthesis. This results in a logical approach to the construction of the target sensors **43-48** by dividing the synthesis into 3 different steps: the initial formation of the core unit, followed by the addition of the fluorophore and finished by the addition of the boronic acid units in the last stage of the synthesis. Therefore, one unique synthetic route to make a core molecule (the spacer in this case) can be used to synthesise a variety of sensors with different fluorophores. Figure II-2 (b) shows the chemical structure of the new modular compounds.

The *para* or *meta* diaminomethyl-benzyl represents the core unit of the sensor. Both boronic acid groups and fluorophore unit are added to this core structure *via* an amine

group. Changing the nature of the fluorophore (naphthalene, anthracene, pyrene) and the position of the two aminomethyl groups (*para* for sensors **43**, **44**, **45** and *meta* for sensors **46**, **47**, **48**) will allow the synthesis of two different series (*para* and *meta* series).

The use of different fluorophores allows different wavelengths to be used in detection. This flexibility could become essential when the fluorescent sensor is used *in situ*. The environment containing D-glucose (for example blood) could contain some species able to absorb at the same wavelength as a particular fluorophore. The possibility of changing the fluorophore can be a solution to avoid this interference. The spacing between the two boronic acid directs the selectivity of the sensor. By moving the position of the two aminomethyl groups (*para* or *meta*), the selectivity of the sensor can be varied.

The first target of the project was to find a modular synthetic route to obtain two series of sensors **43-45** and **46-48**. Further experiments will then permit the evaluation of the saccharide detecting ability.

The following section contains an initial synthetic section, in which the synthesis of sensors **39**, **111** and the two series of sensors (**43**, **44**, **45** for the *para* series and **46**, **47**, **48** for the *meta* series) are detailed. In sensor **111** the group Flu-CH_2 is replaced by a methyl group, CH_3. The main rationale behind the synthesis of **111** was to use **111** as a reference compound in the study of the various interactions of the two series of sensor. The analytic section will then discuss the fluorescence and CD (Circular Dichroism) measurements carried out to evaluate the saccharides sensing activity of the sensors.

II-2 Synthesis of Sensors 43, 44 and 45

The first target of the research was the synthesis of the *para* series of sensors (with the 2 aminomethyl groups of the molecule in a *para* position to each other). The three sensors belonging to this series (compounds **43**, **44** and **45**) only differ by the nature of their fluorophores, which are respectively a naphthalene, an anthracene and a pyrene unit. A retrosynthetic analysis of the target molecules (**43**, **44**, **45**) is depicted in Scheme 2.1.

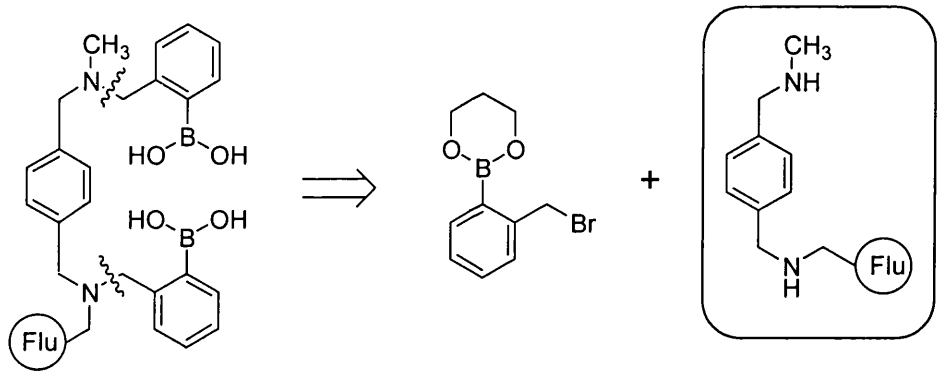

43 Flu = naphthalene
44 Flu = anthracene
45 Flu = pyrene

49

Flu = fluorophore

50 Flu = naphthalene
51 Flu = anthracene
52 Flu = pyrene

Scheme 2.1 - Retrosynthetic Analysis of Target Compounds **43-45**.

Retrosynthetic analysis of the target compounds **43**, **44** and **45** suggested disconnections of the two N-CH_2 bonds to give the cyclic boronate ester **49** and the diamine **50**, **51** and **52** as fragments. The reaction between the benzyl bromide **49** and secondary amines are well known in the literature.[80] Attention, therefore, was focussed on the synthesis of the diamine fragments **50-52**. Scheme 2.2 shows three possible disconnection strategies, A, B and C.

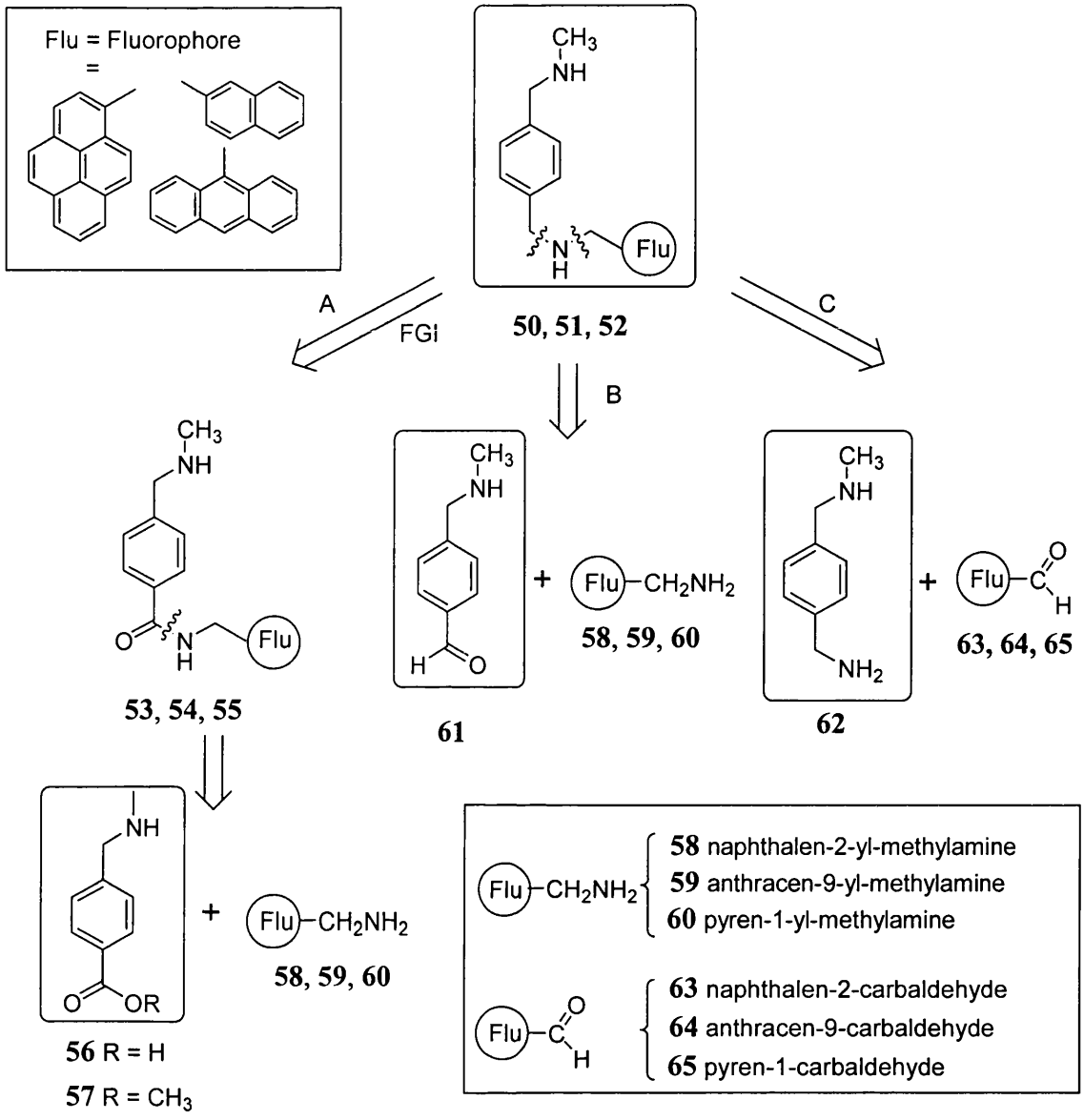

Scheme 2.2 - Retrosynthetic Analysis of Building Block **50-52**.

Strategy A involves the functional group interconversion of the amine **50**, **51** or **52** to the amide **53**, **54** or **55**. The amides **53**, **54** and **55** can be either synthesised from the carboxylic acid **56** or the ester **57** and the amines **58**, **59** or **60**, depending on which fluorophore is required. Strategy B involves disconnection of a CH_2-N amine bond to produce two fragments, the aldehyde **61** and the amine carrying the fluorophore (**58**, **59** or **60**). These can be reacted together under reducing conditions to form the respective

amines **50**, **51** or **52**. Strategy C involves a similar disconnection to strategy B to afford the amine **62** and the three different aldehydes **63**, **64** or **65** depending on which particular final compound is targeted, respectively amines **50**, **51** or **52** leading to sensors **43**, **44** and **45**.

II-2.1 Route A

II-2.1.1 Introduction

The retrosynthetic strategy A suggests the synthetic route A depicted in Scheme 2.3. This is the longest of the proposed strategic routes to obtain amines **50**, **51** and **52**. The addition of the fluorophore *via* the amines **58**, **59** and **60** on the core unit **56** or **57** involves the formation of amides **53**, **54** and **55**. The reduction of these amides leads to the targeted diamines **50**, **51** and **52**. The two boronic acid groups are finally added to these diamines *via* the cyclic boronate ester **49** to give the three targeted sensors **43**, **44** and **45** of the first *para* series.

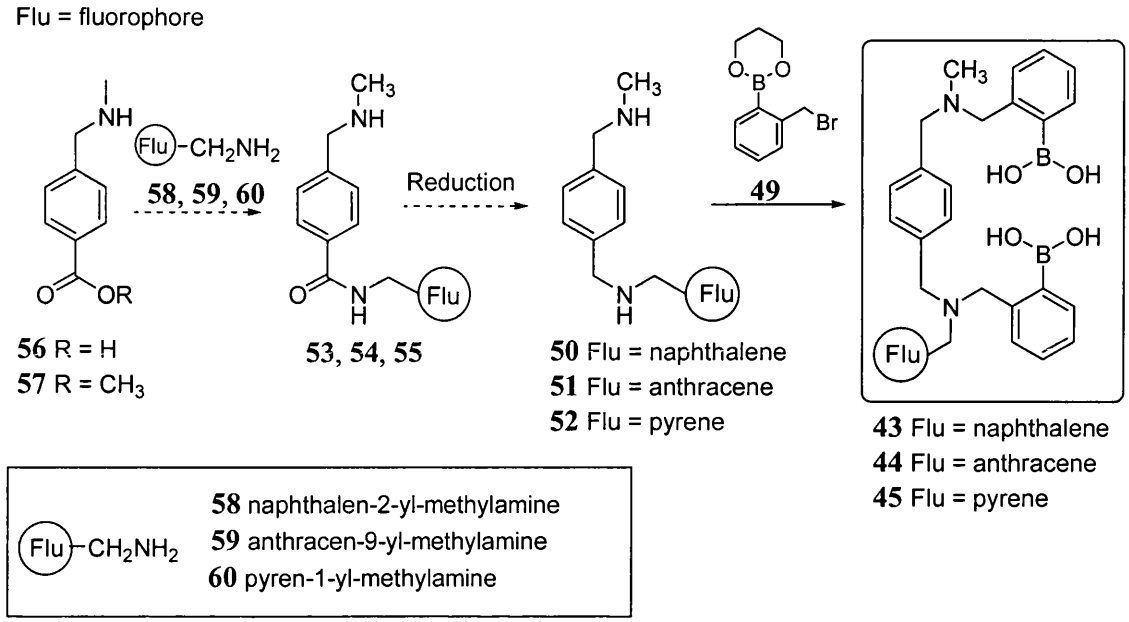

Scheme 2.3 - Route A: First Synthetic Strategy to obtain Sensors **43-45**.

Attention was initially focused on core units **56** and **57** representing the starting material of strategy A.

II-2.1.2 Attempted Synthesis of Core Unit 56

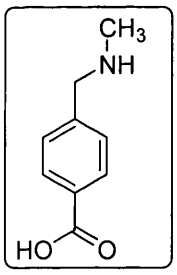

56

Scheme 2.4 shows the attempted synthesis of core unit **56**.

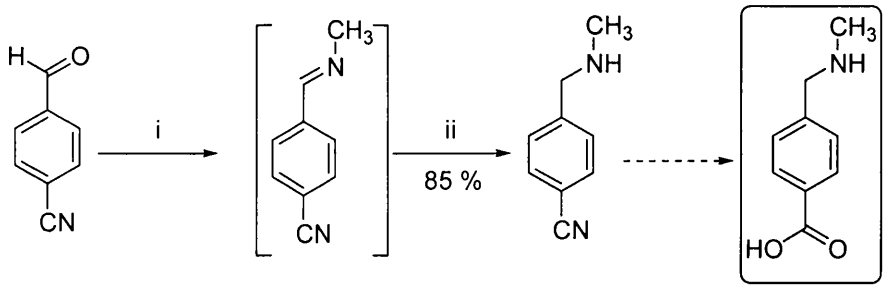

66 67 68 56

Reagent and conditions: i) CH_3NH_2/ methanol, rt; ii) $NaBH_4$/ methanol, rt.

Scheme 2.4 - Attempted Synthesis of Core Unit **56**.

The commercially available 4-cyanobenzaldehyde **66** was treated with a solution of methylamine in methanol to give the intermediate imine **67** which was not isolated. Reduction of the imine with sodium borohydride in methanol afforded the amine **68** in 85 % yield over the two steps. The hydrolysis of the nitrile **68** to the carboxylic acid **56**, was attempted under both basic[84] (20 % aqueous solution of NaOH in EtOH, heat, 48 hours) and acidic[85] (20 % aqueous solution of H_2SO_4, heat, 8 hours) hydrolysis conditions, but was unsuccessful. Attention was therefore turned to the preparation of the core unit **57**, which could also be used for the formation of the amides **53**, **54** and **55** by reaction of an amine with the ester.

II-2.1.3 Attempted Synthesis of Core Unit 57

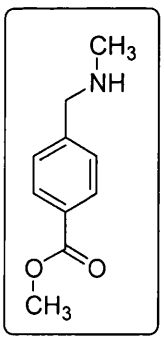

57

Methyl 4-formylbenzoate **69** was used as starting material, Scheme 2.5.

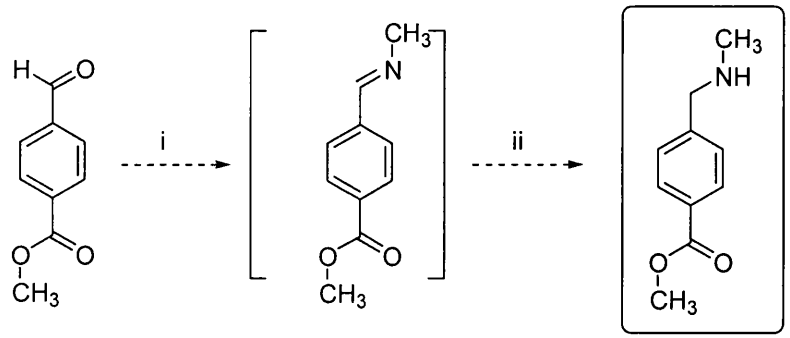

69 **70** **57**

Reagents and conditions: i) CH_3NH_2/ methanol, rt; ii) $NaBH_4$/ methanol, rt.

Scheme 2.5 - Attempted Synthesis of Core Unit **57**.

Encouraged by the successful conversion of the aldehyde group of methyl 4-formylbenzoate **69** to an amine using the method of Cambon *et al.*,[86] identical reagents and conditions were used in order to form the amine group of the core unit **57**. However, the addition of the methylamine solution in methanol resulted in the formation of the imine **70** but also gave 40 % of extra by-products. The NMR spectrum showed a signal at 2.91 ppm corresponding to the $CH_3NHC(O)$ signal. It was therefore suggested that the methylamine also reacted with the ester groups of aldehyde **69** and imine **70** to form amides **71** and **72**.

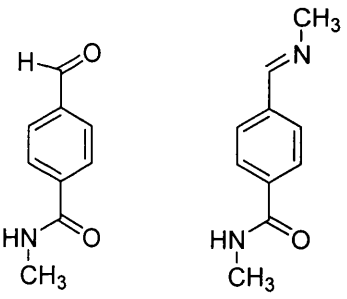

71 **72**

Figure II-3. Possible By-Products formed during the Formation of Imine **70**.

The isolation of compound **57** from the by-products would afford an unsatisfactory low yield of core unit. This is against the features targeted for the successful synthesis of

our modular system: the synthesis has to be quick and facile. Due to the failure to synthesise the amines **56** and **57**, attention was turned to the second synthetic strategy (route B, Scheme 2.6)

II-2.2 Route B

II-2.2.1 Introduction

The retrosynthetic approach B in Scheme 2.2 (p 50) suggested the formation of sensors **43-45** *via* Route B described below, Scheme 2.6.

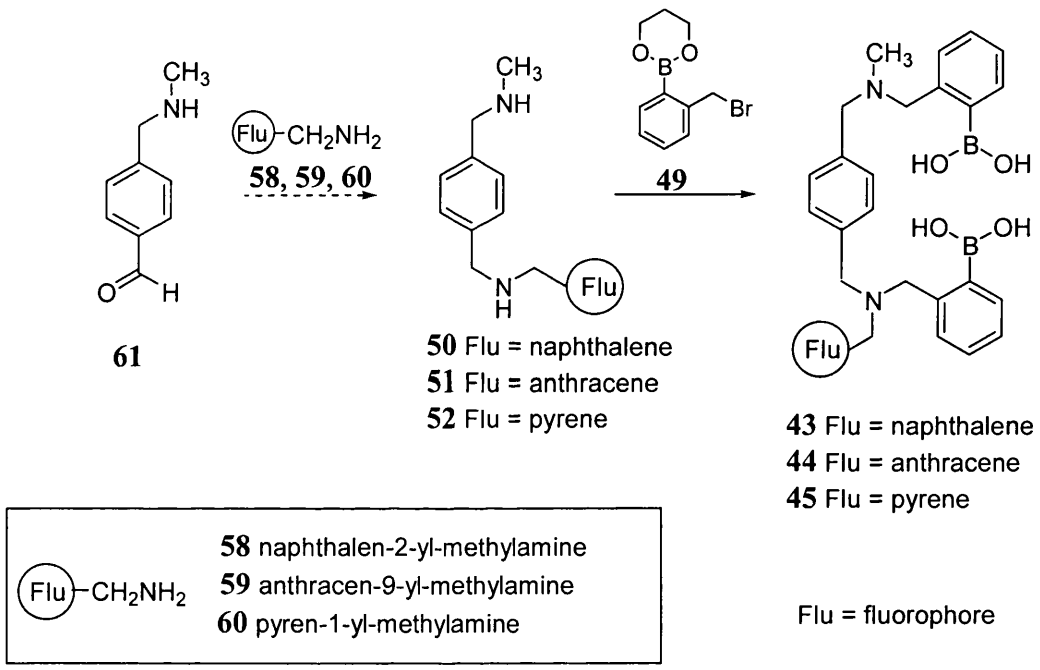

Scheme 2.6 - Route B: Second Synthetic Strategy to obtain Sensors **43-45**.

Route B is slightly shorter than route A described previously, Scheme 2.3. The fluorophore is added onto the aldehyde **61** using the same three amines **58, 59** and **60** carrying respectively a naphthalene, an anthracene and a pyrene unit. However, in this case the primary amine groups of compounds **58, 59** and **60** react with the aldehyde group of core unit **61** and form, after reduction of the intermediate imine, respectively

the diamines **50**, **51** and **52**. The same reaction conditions as with route A are used to add the two boronic acids units to compounds **50**, **51** and **52**. The initial target molecule of the synthetic route B was the aldehyde **61**.

II-2.2.2 Formation of Core Unit 61

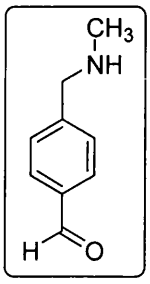

61

Compound **61** plays the role of a proper core unit since both the fluorophore and the two boronic acids are added on to it. Scheme 2.7 shows the initial synthetic route attempted to form **61**.

- First Synthetic Route Attempted to Form Core Unit **61**

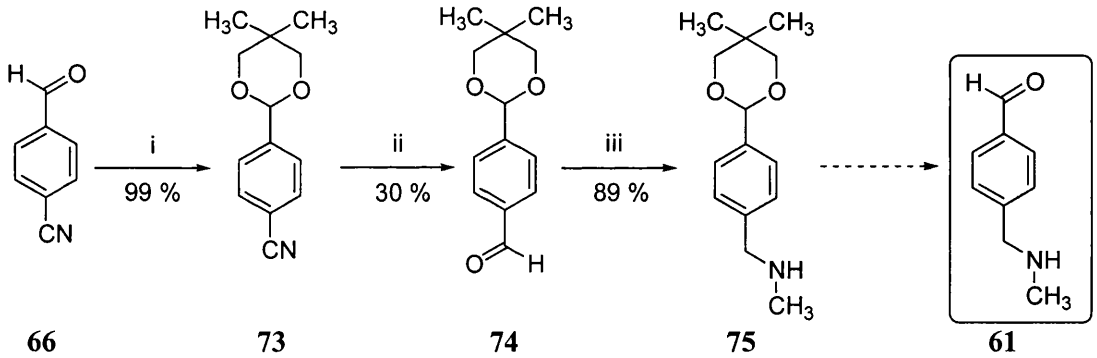

66 **73** **74** **75** **61**

Reagents and conditions: i) 2,2-Dimethyl 1,3-propanediol, TsOH/ toluene, Δ; ii) DIBAL-H/ dry THF, benzene, 0 °C; iii) a. CH_3NH_2/ methanol, rt; b. $NaBH_4$/ methanol, rt.

Scheme 2.7 - First Synthetic Route Attempted to form Core Unit **61**.

A 4 step synthesis starting from 4-cyanobenzaldehyde **66** was envisaged (Scheme 2.7). The protection of the aldehyde group was necessary before the reduction of the nitrile to

prevent conversion of the aldehyde to the alcohol. This protection was first attempted with 1,3-propanediol in the presence of TsOH as an acid catalyst. However, the analysis of the NMR spectrum showed several unexpected signals between 3.5 and 4.5 ppm and TLC confirmed the presence of extra products. These extra products could be the result of different additions onto aldehyde **66**. For example, two different hydroxy groups of two different molecules of 1,3-propanediol can react with aldehyde **66** giving an acetal other than **73**. The hemiacetal formed after addition of one hydroxy group of one molecule of 1,3-propanediol could also be one of the by-products observed in the NMR spectrum. Trituration with a number of solvents such as ethanol, dimethyl ether and DCM were attempted, but no precipitation was observed. An attempted recrystallisation from benzene failed and led to the formation of an oil. Another diol, 2,2-dimethylpropan-1,3-diol, was then chosen as the aldehyde protecting group. Using 2,2-dimethylpropan-1,3-diol, the protection of the aldehyde was achieved affording the pure acetal **73** in 99 % yield. The formation of acetal **73** resulting from the intramolecular addition of the two hydroxy groups of one molecule of 2,2-dimethylpropan-1,3-diol is complete in this case. The bulk of the two methyl groups of the diol may be a factor preventing the addition of another diol molecule to the hemi-acetal already formed. Reduction of the cyano group of **73** to an aldehyde group was done using diisobutylaluminium hydride (DIBAL-H, 1.25 eq.) at 0 °C in benzene.[87] Purification of the reaction mixture by silica gel column chromatography afforded the aldehyde **74** in 30 % yield. The amine **75** was obtained in 88 % yield over 2 steps by sequential addition, at room temperature, of a solution of methylamine in methanol followed by the reduction of the imine *in situ* with sodium borohydride. Core unit **61** could finally be obtained by the removal of the diol protecting group. However this final step caused more difficulties than expected. Several different acids such as HCl,

PPTS (pyridinium *p*-toluenesulfonate), H_2SO_4, and TFA were used under various conditions, but resulted in either decomposition of compound **75** or no deprotection. The various conditions used for the deprotection are summarised in Table 2.1.

Table 2.1- Conditions Attempted for the deprotection of Amine **75**.

Acid	Solvent	Temperature	Time (hours)	Result
HCl (3 eq.)	Methanol	rt	12	No deprotection
HCl (3 eq.)	Methanol	reflux	12	No deprotection
HCl (6 eq.)	Methanol	reflux	12	No deprotection
HCl[88] (10 eq.)	THF	rt	20	No deprotection
PPTS[89]	H_2O/ Acetone (1/15)	50 °C	12	No deprotection
H_2SO_4[90] (10%)	CF_3COOH	rt	5	Decomposition
H_2SO_4 (aq. 10%)	CF_3COOH	0 °C	3	Decomposition

At this stage of the synthesis, the difficulty of the removal of the protecting group of the amine **75** combined with the low yield (30 %) of the formation of the aldehyde **74** prompted us to focus on a different synthetic route to obtain core unit **61**, Scheme 2.8.

- Second Synthetic Route to Form **61**

As seen earlier with the attempted synthesis to core unit **57** (Scheme 2.5), the methylamine reacts easily with an ester group to form an amide. Therefore a new synthetic route, shown below, was envisaged (Scheme 2.8).

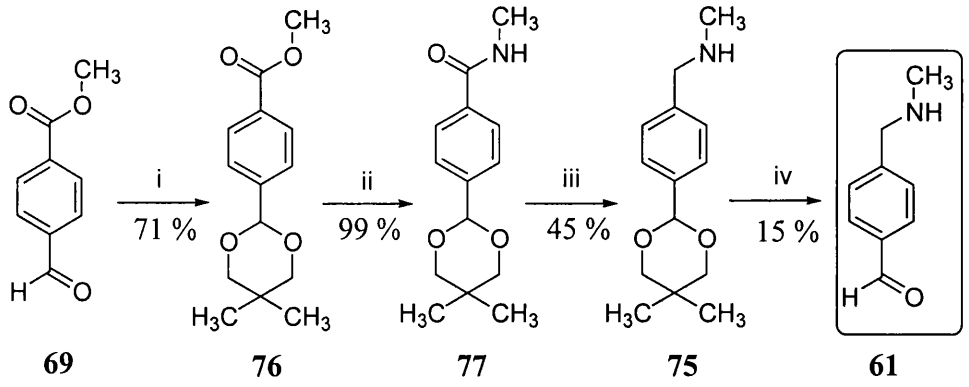

Reagents and conditions: i) 2,2-Dimethyl 1,3-propanediol, TsOH/ Toluene, Δ; ii) CH_3NH_2/ methanol, rt; iii) $LiAlH_4$/ dry THF, Δ; iv) HCOOH, 50 °C.

Scheme 2.8 - Second Synthetic Route Attempted to form **61**.

The commercially available methyl 4-formylbenzoate **69** was used as the starting material. The aldehyde group was protected using 2,2-dimethyl 1,3-propanediol to afford the acetal **76** in 71 % yield. The acetal **76** was converted to the amide **77** by nucleophilic substitution of the methoxy group by methylamine. The formation of the amide **77** was successfully achieved with 99 % yield under mild conditions (no activation was required and the reaction was carried out at room temperature). Reduction of amide **77** by lithium aluminium hydride in dry THF gave the desired amine **75** in 45 % yield[91] and further investigations in order to remove the acetal protecting group were carried out. As mentioned earlier (Table 2.1, p 58) several acids failed to deprotect compound **75**. All reactions either resulted in the decomposition of the amine **75** or gave no result. The deprotection of the aldehyde group was finally achieved using pure formic acid at 50 ^{0}C, leading to the formation of the crude aldehyde **61**. The crude product **61** was contaminated with unreacted formic acid and by product of the deprotection. Purification by column chromatography was attempted, as similar compounds (2-aldehyde-4-substituted quinolines) have been purified by this method.[92] However, the compound decomposed on the column. In order to remove the formic

acid, the crude aldehyde **61** was washed with a 2 moldm^{-3} solution of $NaHCO_3$. Unfortunately, this lead to decomposition of **61**. A water wash was also attempted, but the isolation of core unit **61** was not possible because of its high solubility in water. Faced with the difficulties of isolating core unit **61**, a new synthetic route was developed (Scheme 2.9, below).

- Third Synthetic Route Attempted to Core Unit **61**

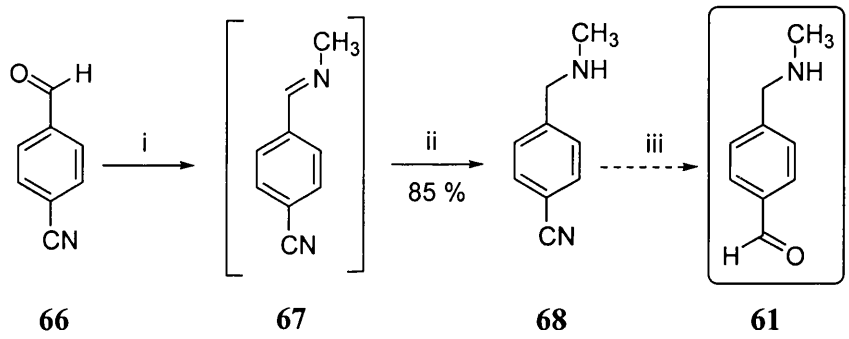

66 **67** **68** **61**

Reagents and conditions: i) CH_3NH_2/ methanol, rt; ii) $NaBH_4$/ methanol, rt; iii) DIBAL-H/ dry THF/ dry benzene, rt.

Scheme 2.9 - Third Synthetic Route Attempted to Core Unit **61**.

Reaction of 4-cyanobenzaldehyde **66** with 6 equivalents of methylamine in methanol afforded, after reduction of the intermediate imine **67**, 4-methylaminomethyl-benzonitrile **68** in 85 % yield. It was envisaged that subsequent reaction of the methylamine **68** with DIBAL-H in tetrahydrafuran would afford the aldehyde **61**.[87] The methylamine **68** was treated with 1.25 equivalents of DIBAL-H in tetrahydrofuran to afford crude **61**. However, subsequent work up involved treatment with HCl, causing protonation of the amine resulting in migration of the product to the aqueous layer. Subsequent neutralisation with 2 moldm^{-3} NaOH caused decomposition of the product, as judged from NMR spectroscopy.

Due to the difficulties encountered during the various attempts to synthesised core unit **61**, attention was turned towards route C involving the synthesis of a new core unit **62** (Scheme 2.10).

II-2.3 Route C

II-2.3.1 Introduction

The strategic disconnection C depicted in Scheme 2.2 (page 50) involves the use of core unit **62** as starting material. The fluorophore and the two boronic acid groups are consecutively added onto the core unit **62**, as shown on Scheme 2.10.

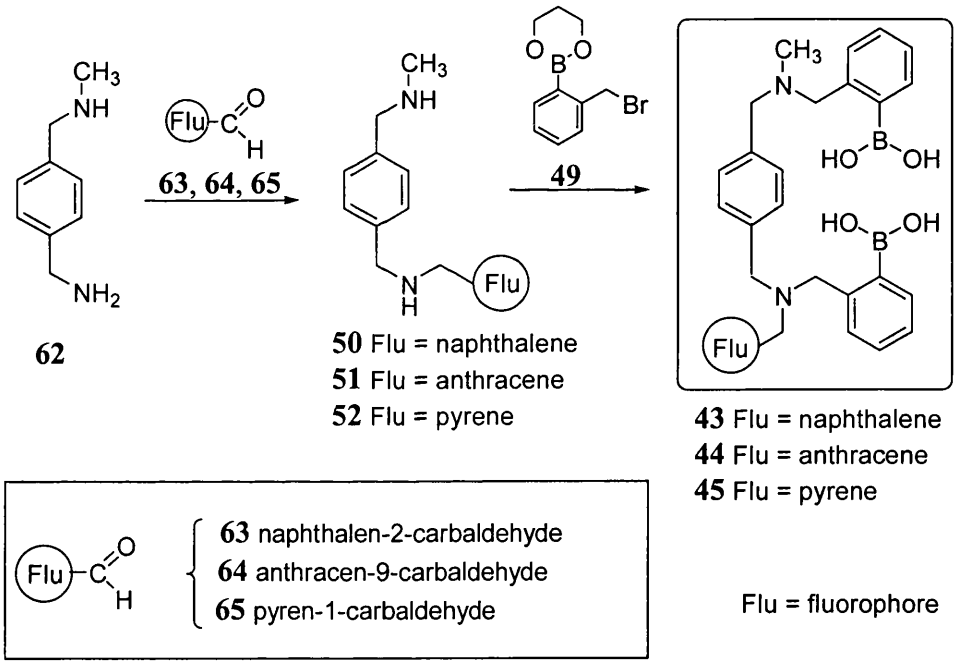

Scheme 2.10 - Route C: Third Synthetic Strategy to obtain Sensors **43-45**.

The fluorophore is added to diamine **62** *via* the reaction between the primary amine group of **62** and the aldehyde group of naphthalen-2-carbaldehyde **63**, anthracen-9-carbaldehyde **64** or pyren-1-carbaldehyde **65**. The similar method of addition, involving an aldehyde and a primary amine group, was used in Route B. However in

this case, the fluorophore (naphthalene, anthracene or pyrene) contained an aldehyde group (**63**, **64** and **65**) and the core unit **62** contained the primary amine group. In contrast, in Route B, the fluorophores contained primary amine compounds (**58-60**) and the aldehyde was part of the core unit **61**. The two boronic acids groups are finally added to the diamine compounds **50**, **51** and **52** by using a nucleophilic substitution with cyclic boronate ester **49**. The success of Route C depended initially on the synthesis of core unit **62**.

II-2.3.2 Formation of the Core Unit 62

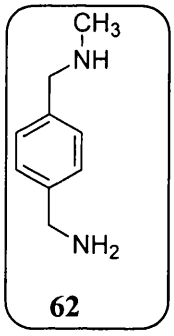

62

The core unit **62** contains two amine groups (one primary and one secondary), and it was hoped that this diamine would present fewer synthetic problems than the aldehyde **61**. Core unit **62** plays a similar role to core unit **61** in the synthesis of building block **50-52,** since **50-52** can be directly assembled from **63**, **64** or **65** and compound **62**. The first strategy approached to obtain core unit **62** is shown in Scheme 2.11 below.

- First synthetic Route Attempted to Form Core unit **62**

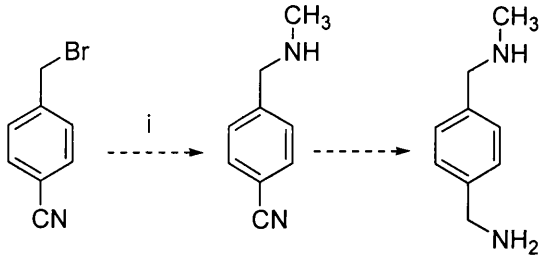

78 **68** **62**

Reagents and conditions: i) CH_3NH_2/ methanol/ dioxane, rt.

Scheme 2.11 - First synthetic Route Attempted to Form Core unit **62**.

It was envisaged that the amine **62** would be prepared in a two step procedure using 4-cyanobenzylbromide **78** as starting material. Nucleophilic substitution of the bromine by methylamine would afford 4-cyanobenzylmethylamine **68**. Those conditions were used by Bardsley and Ashford with the same compound with a solution of methylamine in ethanol and dioxane.[93] Analysis by NMR spectroscopy suggested formation of the intended product **68**. However, the analysis by mass spectrometry showed a different mass from that expected. A signal at *m/z* 261 does not correspond to the secondary amine **68**, but to the tertiary amine **83**, Scheme 2.13. The newly formed 4-cyanobenzylmethylamine **68** (Scheme 2.12) can react with another equivalent of 4-cyanobenzylabromide to form the tertiary amine *bis*(4-cyanobenzyl) methylamine **83**, Scheme 2.13.

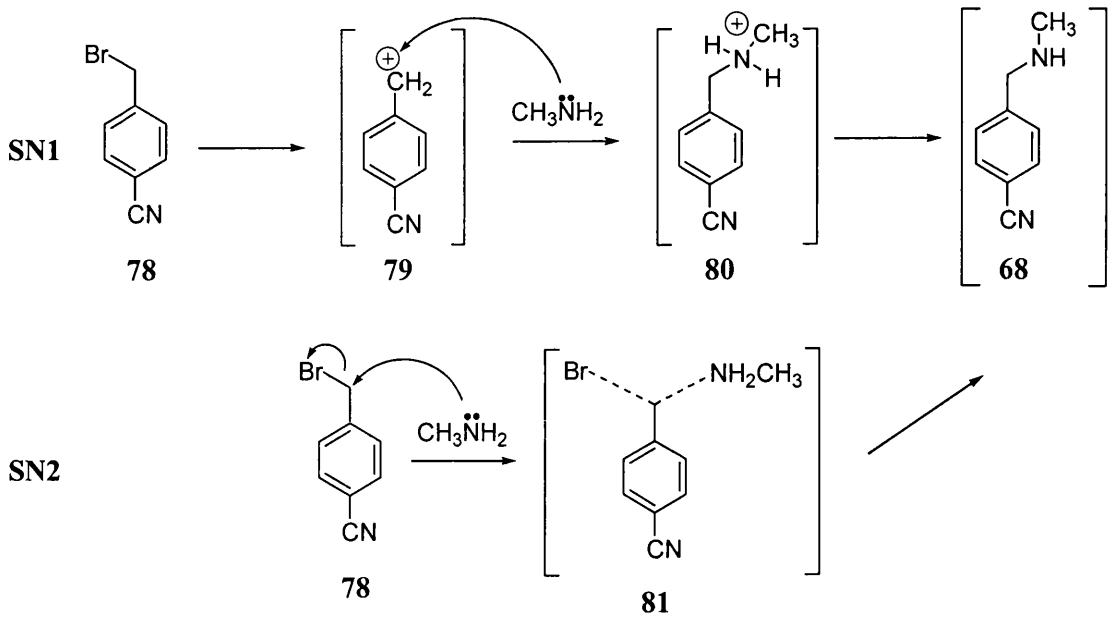

Scheme 2.12 - Formation Of Compound **68**.

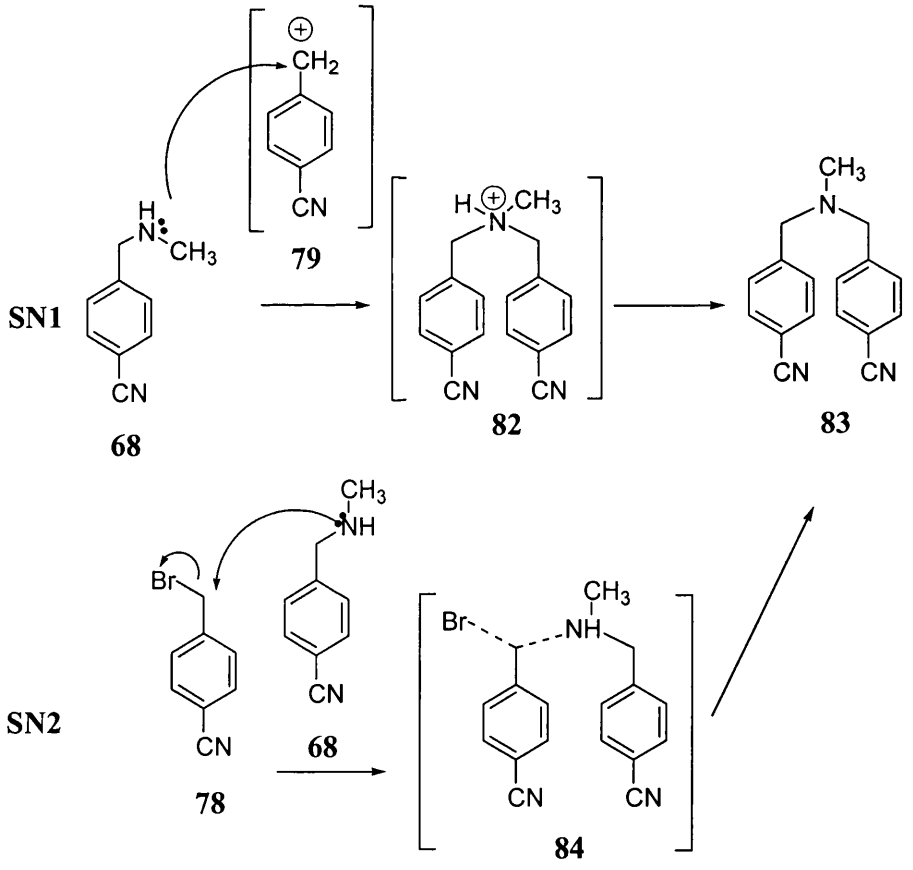

Scheme 2.13 - Formation *in situ* of Tertiary Amine **83**.

Both SN1 and SN2 mechanisms have been suggested for each nucleophilic substitution (Scheme 2.12 and 2.13). The first nucleophilic substitution resulting in the formation of **68** and the second in the formation of **83**. Increasing the equivalents of methylamine used could have allowed to obtain a mixture of tertiary amine **83** and the desired product **68**. However, the isolation of compound **68**, followed by the reduction of the latter to give core unit **62** would have led to an unsatisfactory yield of the diamine **62**. The rationale behind the synthesis of the core units is that the synthesis should be simple and high yielding. Therefore attention was turned to a different synthetic route to core unit **62**, Scheme 2.14.

- Second Synthesis of Core Unit **62**

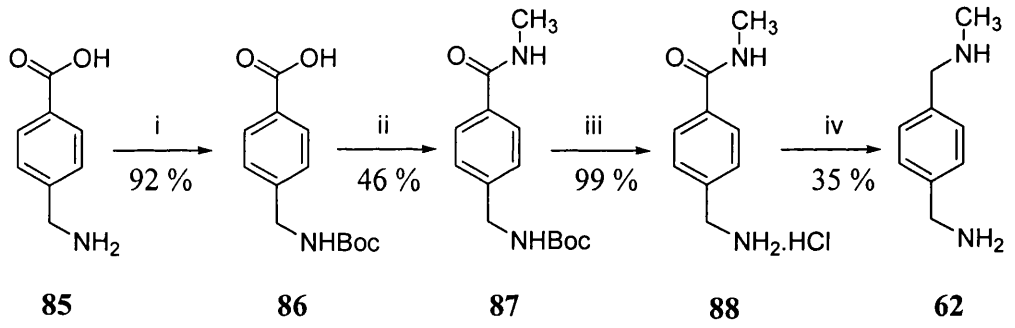

Reagents and conditions: i) Boc_2O/ NaOH/ Propan-2-ol, rt; ii) a, HOOBt.CH_3NH_2 salt/ DMF, b, DCC/ DMF, rt; iii) HCl (32 %)/ Et_2OAc, rt; iv) $LiAlH_4$/ dry THF, Δ.

Scheme 2.14 - Synthesis of Core Unit **62**.

The target compound 4-aminomethylbenzylmethyl amine **62** was successfully synthesised from 4-(aminomethyl)benzoic acid **85** in 13 % overall yield over 4 steps. The commercially available 4-(aminomethyl)benzoic acid **85** was treated with a solution of 1.1 equivalents of di-*tert*-butyl dicarbonate (Boc_2O) to afford the protected amine **86** in 92 % yield. This protection is a standard protocol in peptide synthesis to avoid the polycondensation of the amino acid. The next step is the amidation of the carboxylic

acid. The amidation method used by Kao and Barfield[94], who initially converted the carboxylic acid to an *o*-carboxylchloride with thionyl chloride, failed to give compound **87** and removed the Boc protecting group.

The method used for the amidation of protected amino acid **86** requires the prior formation of the reagent methylammonium salt of 3-hydroxy-1,2,3-benzotriazin-4(3*H*)-one (HOOBt) **89**.[95]

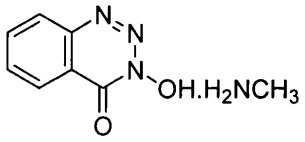

89

This was achieved by direct addition of a solution of methylamine in methanol to a solution of HOOBt in methanol. The solid salt **89** was rapidly formed and was used immediately after filtration. The salt **89** reacted with carboxylic acid **86** in the presence of 1.1 equivalents of DCC in DMF to give amide **87** in a 46 % yield after trituration in hexane and ethyl acetate. The *tert*-butoxycarbonyl (Boc) protecting group of amide **87** was successfully removed by a solution of hydrochloric acid (32 % aqueous solution) in ethyl acetate to afford amide **88** as the hydrochloride salt in 99 % yield.[96] The Boc deprotection method described by Schmidt *et al.* who used a solution of TFA in DCM at low temperature (0 °C)[97] was also attempted, but resulted in the decomposition of amide **88**. The synthesis of core unit **62** was successfully achieved by treatment of amine **88** with lithium aluminium hydride, which reduced the amide group to an amine in 35 % yield (13 % yield over the 4 steps).

Compound **62** would then be used as a core unit and undergo the addition of the fluorophore and the 2 boronic acid groups in order to form the *para* series of sensors **43-45**.

A variant to route C was also attempted, Scheme 2.15. In this variant, the reduction of the carbonyl group of compound **88** was carried out after addition of benzaldehyde (a) or the fluorophores **63-65** (b). The addition of benzaldehyde onto compound **88** led to amide **90** and the reduction of the latter gave diamine **91**. The addition of fluorophores **63-65** onto amine **88** gave amides **92-94** but decomposed under reduction of **92-94**, in an attempt to give diamines **50-52**. Therefore it was decided to add the fluorophore after reduction of amide **88** to amine **62**.

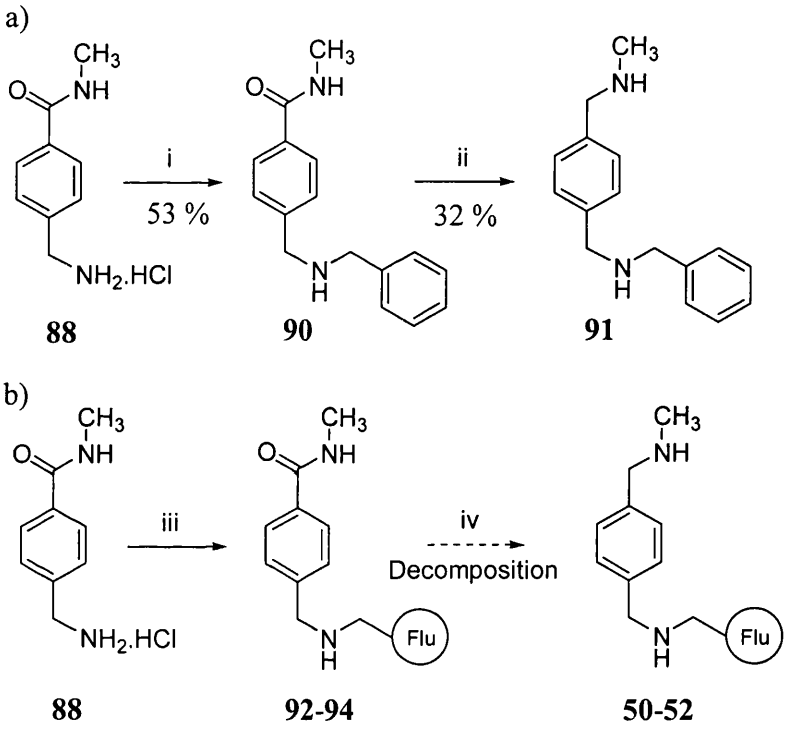

Reagents and conditions: i) a. Benzaldehyde/ methanol, rt; b. $NaBH_4$/ methanol, rt; ii) $LiAlH_4$/ dry THF, Δ; iii) a. Fluorophore **63-65**/ methanol, rt; b. NaBH4/ methanol, rt; iv) $LiAlH_4$/ dry THF, Δ.

Scheme 2.15 - Addition of Benzaldehyde (a) and Fluorophores **63-65** (b) on Amide **88**.

The synthesis detailed in Scheme 2.14 successfully gave core unit **62** but the low yield (13 %) encouraged us to investigate further a higher yielding synthetic route. A shorter 2 step route (Scheme 2.16) was investigated in order to improve the overall yield.

- Third Synthesis of Core Unit **62**

An alternative 2-step procedure to synthesise core unit **62** was investigated, Scheme 2.16. This involved the addition of methylamine to 4-cyanobenzaldehyde **66** to form 4-cyanomethylamine **68**, which can be reduced to the diamine **62** by treatment with $LiAlH_4$.

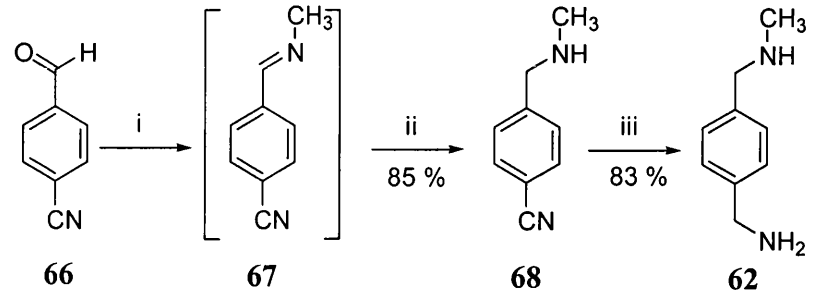

66 **67** **68** **62**

Reagents and conditions: i) CH_3NH_2/ methanol, rt; ii) $NaBH_4$/ methanol, rt; iii) $LiAlH_4$/ dry THF, Δ.

Scheme 2.16 - Third Synthetic Route to Core unit **62**.

Treatment of the commercially available 4-cyanobenzaldehyde **66** with a solution of 6 equivalents of methylamine in methanol gave the intermediate imine **67**, which was not isolated. This was reduced *in situ* with sodium borohydride (5 equivalents) in methanol to give the amine **68** in 85 % yield. The amine **68** was then treated with 5 equivalents of lithium aluminium hydride in dry THF to reduce the nitrile group to a primary amine.[98] This afforded the target amine **62** in a yield of 71 % over 2 steps. After the success of the formation of core unit **62**, it was envisaged that core unit **62** would afford the first series of sensors after addition of the fluorophore and the two boronic acids.

II-2.3.3 Addition of Fluorophore and Boronic acids on Core Unit 62

The quick and mild conditions of preparation of diamine **62** made it an ideal core unit to be used as a foundation for the construction of the first series of sensors **43-45**. The reaction conditions were initially attempted with the addition of benzaldehyde onto core

unit **62** instead of fluorophore **63-65**, as a model reaction. Treatment of the diamine **62** with 1 equivalent of benzaldehyde gave an intermediate imine, which was reduced using 5 equivalents of sodium borohydride to give the diamine **91** in 32 % yield. Treatment of the diamine **91** with 3 equivalents of bromide **49** in dry acetonitrile in the presence of 4 equivalents of K_2CO_3 afforded sensor **95** in 80 % yield after purification (trituration in hexane and chloroform), Scheme 2.17. Sensors **43-45** were obtained in similar conditions.

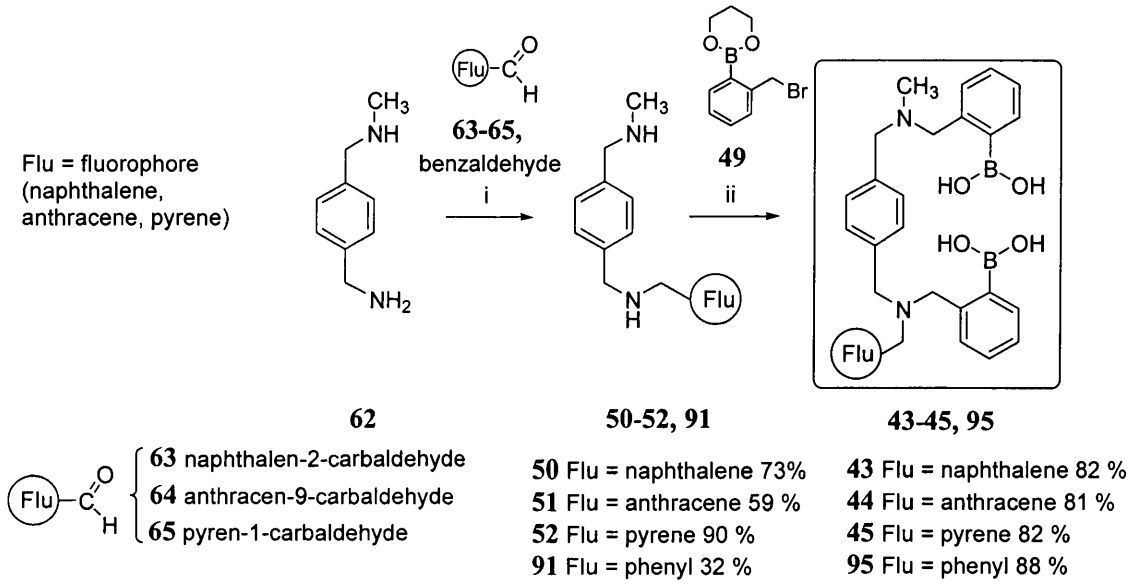

Reagents and conditions: i) a, Benzaldehyde or Fluorophore **63**, **64** or **65**/ methanol, rt; b, $NaBH_4$/ methanol, rt; ii) **49**, K_2CO_3/ dry acetonitrile, Δ.

Scheme 2.17 - Addition of Fluorophores and Boronic acids on to Core Unit **62**.

The addition of the fluorophores (arylaldehydes **63-65**) gave diamines **50, 51** and **52** in 73 %, 59 % and 90 % yield respectively. The addition of the two boronic acids by treatment with bromide **49** afforded the *para* series of sensors **43, 44** and **45** in 72 %, 71 % and 73 % yield respectively after purification (trituration with hexane and chloroform).

Because of the Lewis acidity of the boronic acid, nucleophilic addition to the boron centre are easily carried out even with a weak nucleophile. Therefore, the removal of the diol protecting group of sensors **43-45** are not necessary because they are already deprotected in methanolic solution. This deprotection can even take place during trituration. The mass spectra revealed that various additions can be made to the boron when the sensor is in solution, such as addition of methanol or water and some spectra showed that 1,3 propandiol, the protecting group was still present.

II-3 Synthesis of Sensors 46, 47 and 48

The successful synthesis of the first series of sensors (**43-45**) prompted the investigation of the synthesis of another series of three sensors (**46-48**), Figure II-4. The difference between the first and the second series is the position of the two aminomethyl arms of the sensors. The two aminomethyl arms are in a *para* position in sensors **43-45** and in a *meta* position for sensors **46-48**. As with sensors **43-45,** sensors **46-48** have a different fluorophore unit a naphthalene **46**, anthracene **47** or a pyrene **48** group respectively.

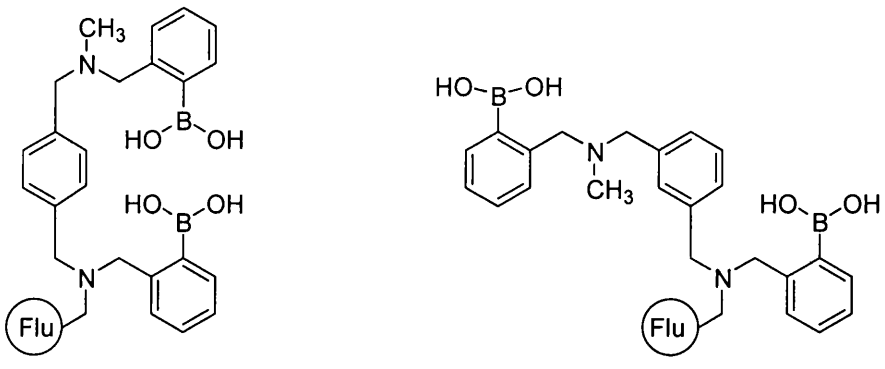

43 Flu = naphthalene
44 Flu = anthracene
45 Flu = pyrene

46 Flu = naphthalene
47 Flu = anthracene
48 Flu = pyrene

Figure II-4. *Para* and *Meta* Series of Sensors.

II-3.1 Route C'

II-3.1.1 Introduction

Route C, represented in Scheme 2.10, page 61, allowed us the successful synthesis of the first series of three sensors **43**, **44** and **45**. This route required the initial synthesis of a core unit **62** and then the successive addition of a fluorophore and two boronic acids onto the core unit **62**. It was therefore intended to use a similar strategy to synthesise the three sensors **46**, **47** and **48** of the second series. Route C' (Scheme 2.18) is also a 3 step reaction and requires the initial formation of core unit **96** (*meta* analogue of core unit **62**). This core unit **96** is used for the addition of the fluorophores, the addition of the two boronic acid groups being carried out in the last stage of the reaction.

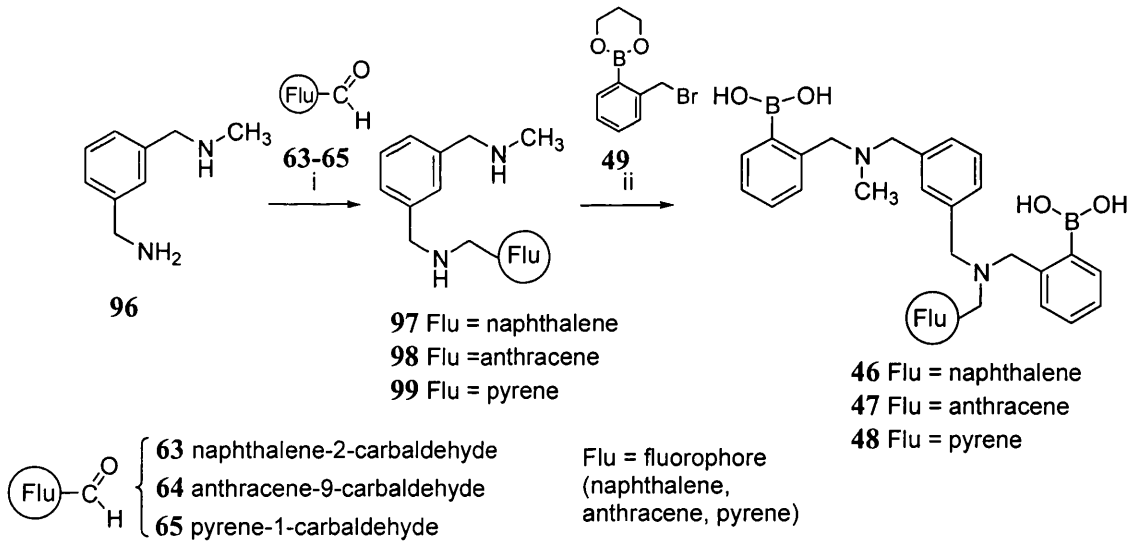

Reagents and conditions: i) a. Fluorophore **63**, **64** or **65**/ methanol, rt; b. $NaBH_4$/ methanol, rt; ii) **49**, K_2CO_3/ dry acetonitrile, Δ.

Scheme 2.18 - Route C': Synthetic Strategy to Obtain Sensors **46-48** (*meta* series).

The formation of the second series of sensors **46-48** initially required the formation of core unit **96**.

II-3.1.2 Synthesis of Core Unit 96

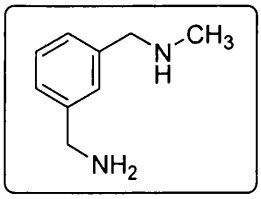

96

Core unit **96** was synthesised in a similar manner to core unit **62**, using 3-cyanobenzaldehyde **100** as starting material, Scheme 2.19.

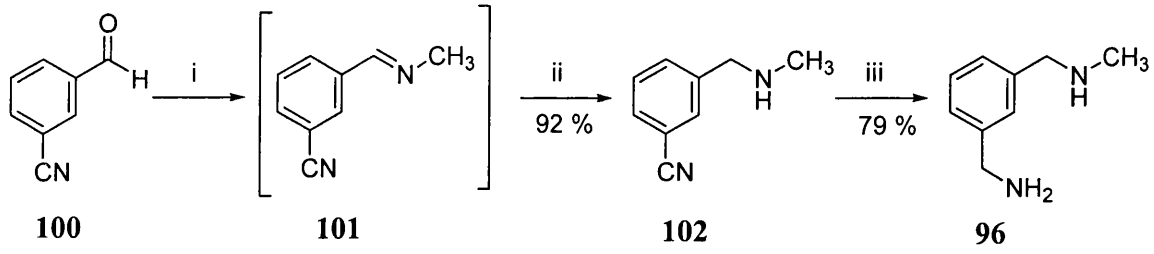

100 **101** **102** **96**

Reagents and conditions: i) CH_3NH_2/ methanol, rt; ii) $NaBH_4$/ methanol, rt; iii) $LiAlH_4$/ dry THF, Δ.

Scheme 2.19 - Formation Of Core Unit **96**.

3-Cyanobenzaldehyde **100** was initially treated with 6 equivalents of methylamine in methanol at room temperature followed by 5 equivalents of sodium borohydride to reduce the intermediate imine **101** and afford 3-methylaminomethyl-benzonitrile **102** in 92 % yield. 3-Methylaminomethyl-benzonitrile **102** was then refluxed with 5 equivalents of $LiAlH_4$ in dry THF to afford the core unit **96** in 79 % yield (73 % over two steps).

II-3.1.3 Addition of Fluorophores and Boronic acids on to Core Unit 96

Core unit **96** was used for the synthesis of the second series of sensors (**46-48**) in a similar manner to the way that core unit **62** was used for the preparation of the first series of sensors **43-45**, Scheme 2.20. As it was done previously with core unit **62**, the

reaction conditions were tested using the addition of benzaldehyde instead of fluorophores **63-65**, Scheme 2.20.

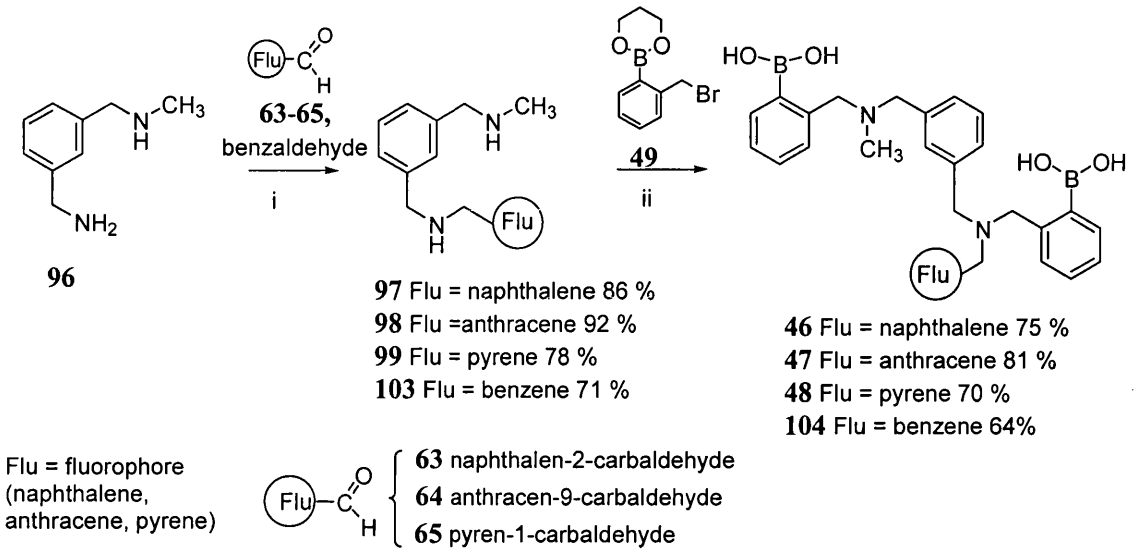

Reagents and conditions: i) a, Benzaldehyde or Fluorophores **63**, **64** or **65**/ methanol, rt, b, $NaBH_4$/ methanol; ii) Bromide **49**, K_2CO_3/ dry acetonitrile, Δ.

Scheme 2.20 - Addition of the Fluorophore and the Two Boronic Acid on to Core Unit **96**.

The core amine **96** was first treated with 1 equivalent of benzaldehyde in methanol followed by reduction with 5 equivalents of $NaBH_4$ in methanol to afford diamine **103** in 71 % yield. Treatment of **103** a manner similar to **50**, **51** and **52** (Scheme 2.17) with cyclic boronate ester **49** in dry acetonitrile in the presence of K_2CO_3 afforded sensor **104** in 64 % yield. The success of the additions of benzaldehyde and the boronic acids suggested that the same conditions could be used for the addition of the fluorophores naphthalen-2-carbaldehyde **63**, anthracen-9-carbaldehyde **64** or pyren-1-carbaldehyde **65**. Accordingly diamines **97**, **98** and **99** were obtained in a 87, 92 and 78 % yield respectively. Treatment of **97-99** with cyclic boronate ester **49** gave the second series of sensors **46**, **47** and **48** in 87 %, 92 % and 78 % yield respectively.

II-4 Synthesis of Sensor 39

II-4.1 Introduction

Sensor **39** was presented in the introduction as the first PET fluorescent sensor selective for D-glucose.[80] The selectivity of the sensor was due to the spatial arrangement of the two boronic acids. The behaviour of sensor **39** with saccharides was chosen as a reference for comparison with the two new series of sensors **43-45** and **46-48**. The distance between the two boronic acids of sensor **39** is identical to the first series of sensors **43-45**, with the two aminomethyl groups in a *para* position. This distance is smaller for the second series of sensors **46-48**. The preparation of sensor **39** by the method of James *et al.* who utilised 9,10-*bis* (chloromethyl) anthracene to synthesise diamine **107** was not used.[80] A different synthetic route was chosen (Scheme 2.21) using milder conditions with 9,10-dialdehyde anthracene **105** as starting material.

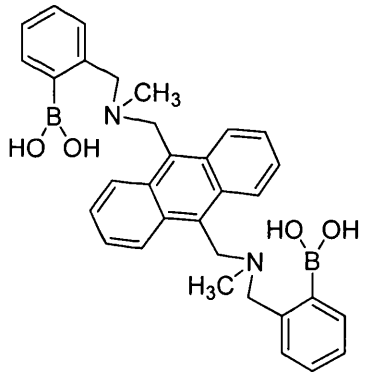

39

II-4.2 Synthesis

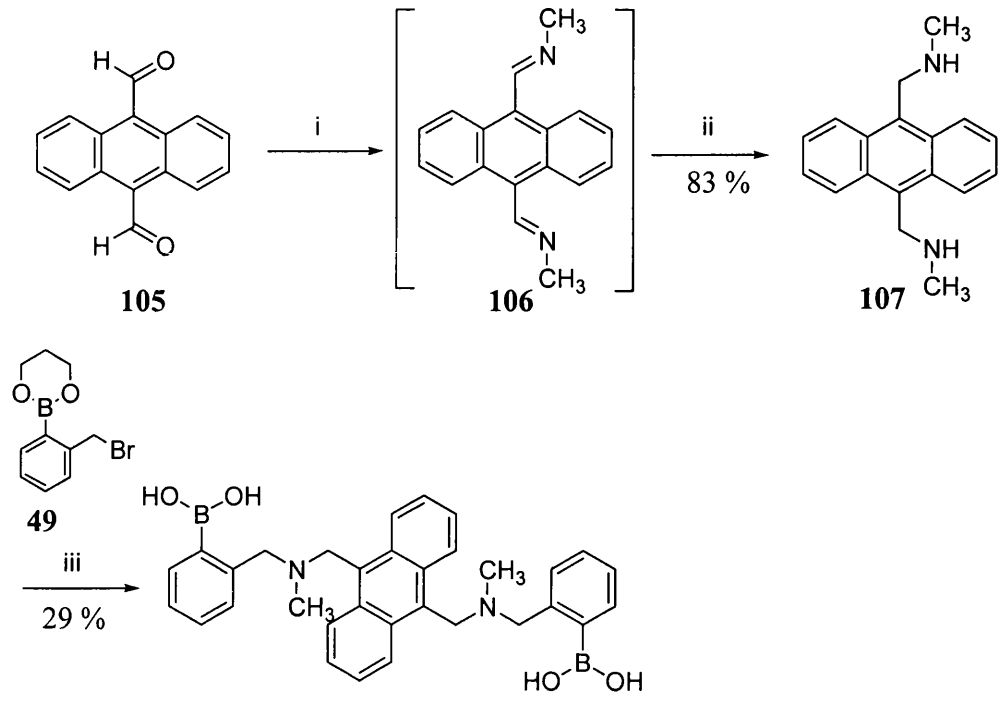

Reagents and conditions: i) CH_3NH_2/ methanol, rt; ii) $NaBH_4$/ methanol, rt; iii) Bromide **49**, K_2CO_3/ dry CH_3CN, Δ.

Scheme 2.21 - Synthesis of Sensor **39**.

9,10-Dialdehyde anthracene **105** was treated with a solution of methylamine (6 equivalents) in methanol at room temperature to give the intermediate imine **106** which was not isolated. The imine was then reduced *in situ* with sodium borohydride (5 equivalents) in methanol at room temperature to form the diamine **107**. Treatment of diamine **107** with 3 equivalents of aryl bromide **49** in alkaline dry acetonitrile afforded sensor **39** in 29 % yield (19 % over the two steps).

II-5 Synthesis of Sensor 111

II-5.1 Introduction

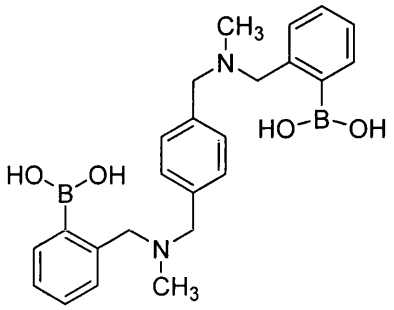

111

Sensor **111** has a similar structure to the *para* series of sensors **43-45**. The spacer is identical (para diaminomethyl-benzyl) but the Flu-CH_2 group have been replaced by methyl groups. Therefore, compound **111** is an ideal reference compound to use in the study of the interactions between sensors **43-48** and saccharides. Data collected could provide information on the effect of a bulky fluorophore.

II-5.2 Synthesis

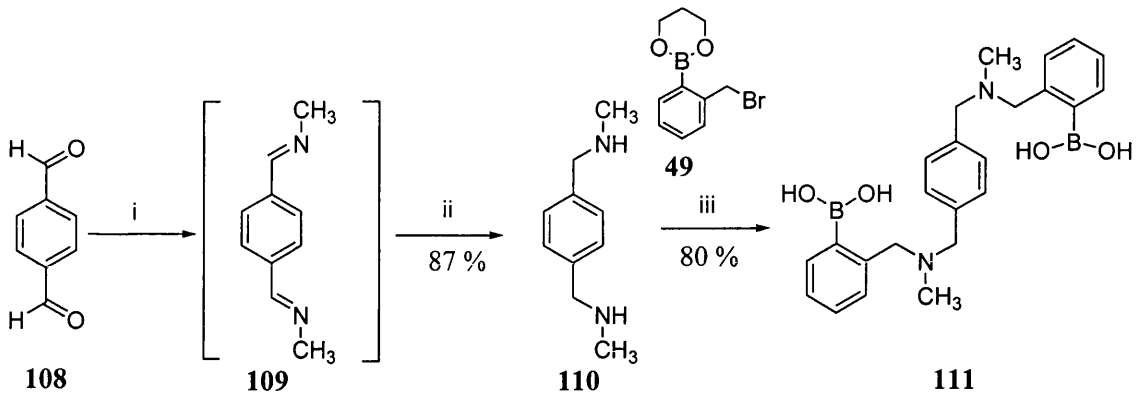

Reagents and conditions: i) CH_3NH_2/ methanol, rt; ii) $NaBH_4$/ methanol, rt; iii) Bromide **49**, K_2CO_3/ dry CH_3CN, Δ.

Scheme 2.22 - Synthesis of Sensor **111**.

Sensor **111** was synthesised in a similar manner to sensor **39**. 1,4-Dibenzaldehyde **108** was treated with a solution of methylamine in methanol (6 equivalents at room temperature) to give the intermediate imine **109** which was not isolated. The imine **109** was then reduced *in situ* with sodium borohydride (5 equivalents) in methanol at room temperature to form the diamine **110** in 87 % yield. Treatment of diamine **110** with 3 equivalents of aryl bromide **49** in alkaline dry acetonitrile afforded sensor **111** in 80 % yield (70 % over two steps).

II-6 Summary of the Synthetic Work

An unique synthesis, rapid (three step procedure) and using mild conditions, was developed and allowed the synthesis of two series of 3 sensors each (**43-45** *para* series and **46-48** *meta* series), Figure II-5 (a). The interactions of these 6 sensors with 4 different saccharides has been evaluated and compared with sensor **39**, the first PET sensor selective for glucose (Part II-7). The synthesis of **39** was achieved using a different starting material than the one used by James,[80] Figure II-5 (b). Compound **111** was synthesised in a similar manner to sensor **39**, Figure II-5 (c).

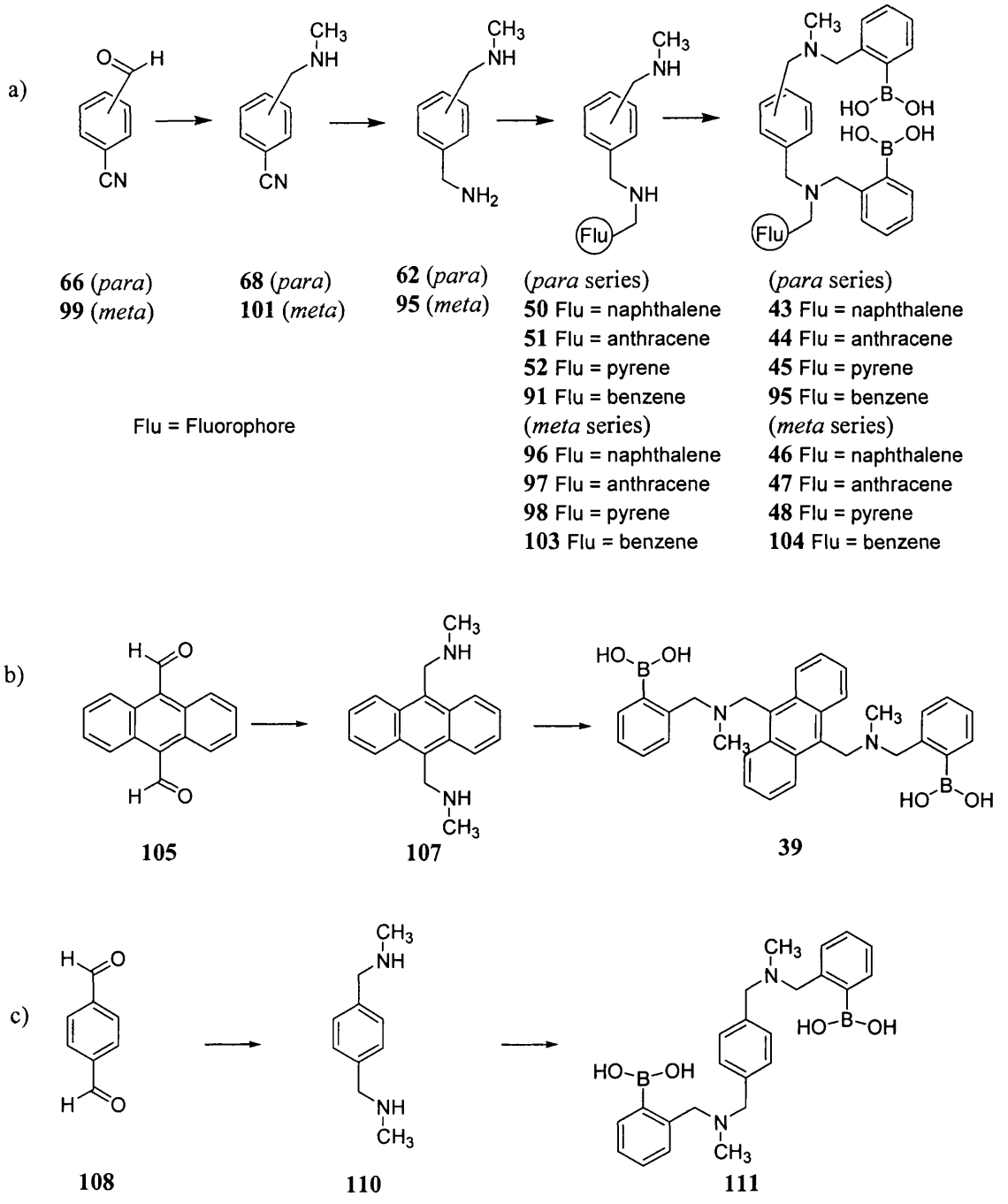

Figure II-5. Summary of the Synthesis of Sensors **43-48** (a), **39** (b) and **111** (c).

II-7 Evaluation of Sensors 43-48 with Saccharides

II-7.1 Introduction

Studies have been carried out on the 9 systems **43**, **44**, **45**, **46**, **47**, **48**, **95**, **104** and **111** and on the glucose selective fluorescent sensor **39** in order to evaluate the interactions of the sensors with saccharides. For these studies, 4 different saccharides were used- D-glucose **112**, D-galactose **113**, D-mannose **114** and D-fructose **115**. The structures of the saccharides are given below in Figure II-6.

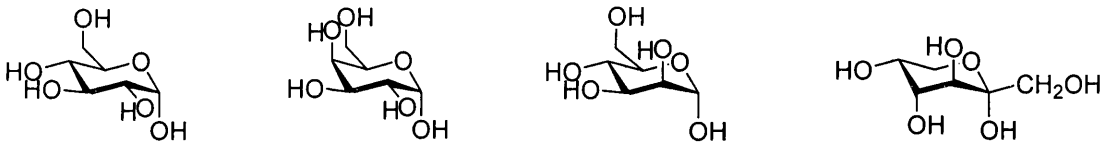

112 **113** **114** **115**

Figure II-6. Structures of D-glucose **112**, D-galactose **113**, D-mannose **114** and D-fructose **115**.

As the particular interest for D-glucose has already been mentioned in the Introduction (p 4), the 3 other saccharides were chosen because of their low cost, commercial availability and their common presence in nature. The structures of D-galactose and D-glucose differ only in the orientation of the 4-hydroxy group. D-Glucose and D-mannose differ in the orientation of the 2-hydroxy group. In D-mannose, the 2-OH is in an axial position, compared to D-glucose, in which the 2-hydroxy group is in an equatorial position. Finally, D-fructose in its pyranose form seems to offer the biggest structural differences.

Fluorescence experiments were carried out initialy in order to determine the stability constants *K* of the complex formed between the sensors and the saccharide, and then

CD (Circular Dichroism) spectroscopy provided information on the structure of the complexes.

II-7.2 Fluorescence Measurements

II-7.2.1 Florescence Titrations

The intensity of the fluorescence emission (I_F) of sensors **39**, **43**, **44**, **45**, **46**, **47** and **48** was measured at different concentrations of D-glucose **112**, D-galactose **113**, D-mannose **114** and D-fructose **115** and are reported in Figures II-7 – II-13. Unfortunately, the fluorescence of compounds **95**, **104** and **111** was too weak to measure and the calculation of the stability constant *K* of the complexes formed between the sensors and the saccharides was not possible.

All the experiments were carried out in a 52.1 % (w/w) methanol-water buffer solution at pH 8.21.[99]

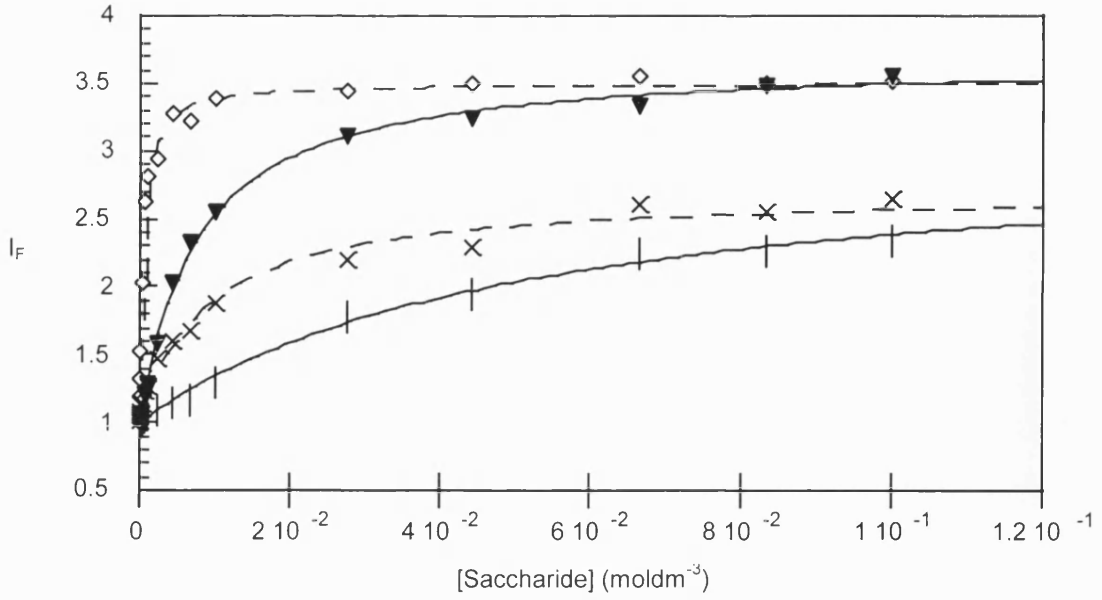

Figure II-7. Fluorescence Intensity (I_F) of Sensor **39** (1×10^{-7} moldm^{-3}) *versus* [D-glucose **112**] (—◇—), [D-galactose **113**] (—✕—), [D-mannose **114**] (—|—) and [D-fructose **115**] (—▼—) at 25 °C at pH 8.21 in 52.1 % (w/w) methanol/ water solution; λ_{ex} = 370 nm, λ_{em} = 422 nm.

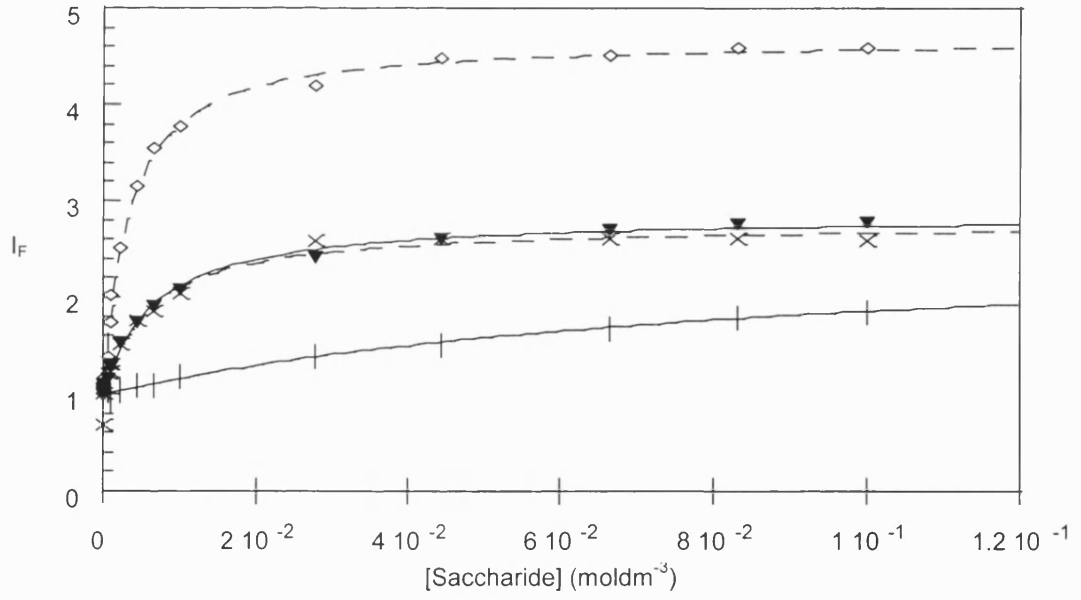

Figure II-8. Fluorescence Intensity (I_F) of Sensor **43** (5×10^{-6} moldm^{-3}) *versus* [D-glucose **112**] (—◇—), [D-galactose **113**] (—✕—), [D-mannose **114**] (—|—) and [D-fructose **115**] (—▼—) at 25 °C at pH 8.21 in 52.1 % (w/w) methanol/ water solution; λ_{ex} = 271 nm, λ_{em} = 339 nm.

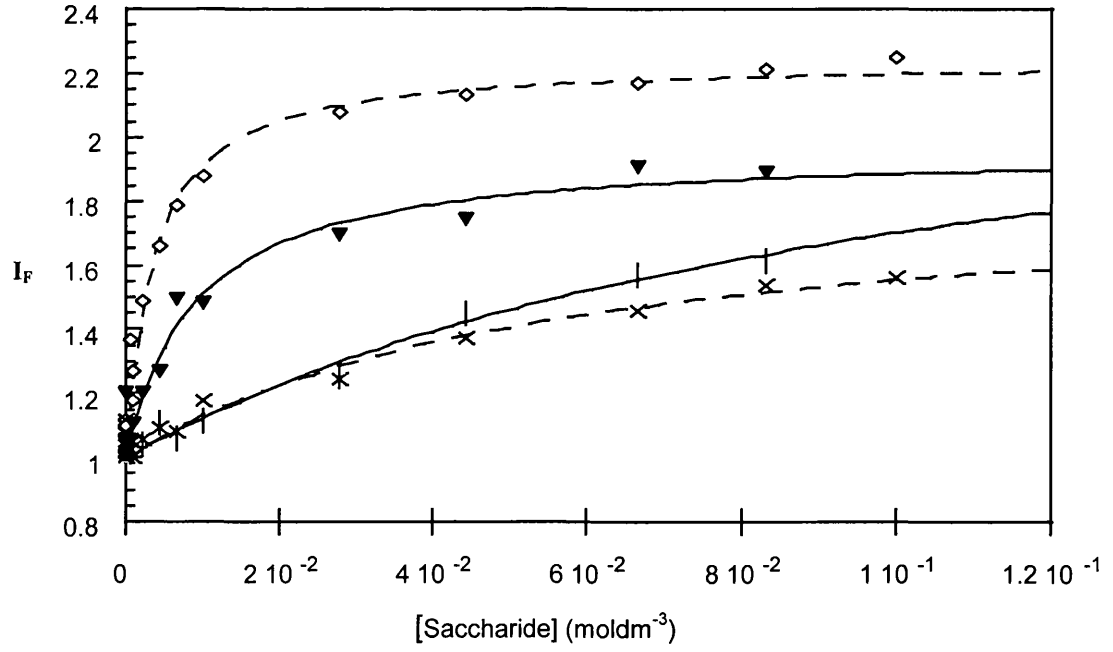

Figure II-9. Fluorescence Intensity (I_F) of Sensor **44** (1×10^{-7} moldm^{-3}) *versus* [D-glucose **112**] (—◇—), [D-galactose **113**] (—×—), [D-mannose **114**] (—|—) and [D-fructose **115**] (—▼—) at 25 °C at pH 8.21 in 52.1 % (w/w) methanol/ water solution; λ_{ex} = 370 nm, λ_{em} = 416 nm.

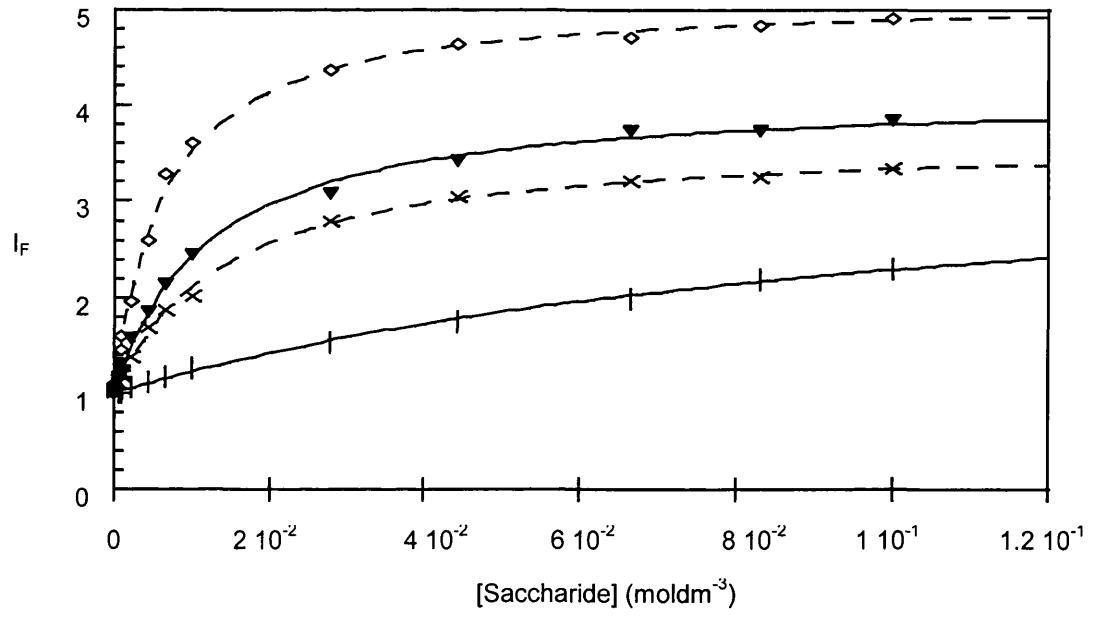

Figure II-10. Fluorescence Intensity (I_F) of Sensor **45** (1×10^{-7} moldm^{-3}) *versus* [D-glucose **112**] (—◇—), [D-galactose **113**] (—×—), [D-mannose **114**] (—|—) and [D-fructose **115**] (—▼—) at 25 °C at pH 8.21 in 52.1 % (w/w) methanol/ water solution; λ_{ex} = 343 nm, λ_{em} = 397 nm.

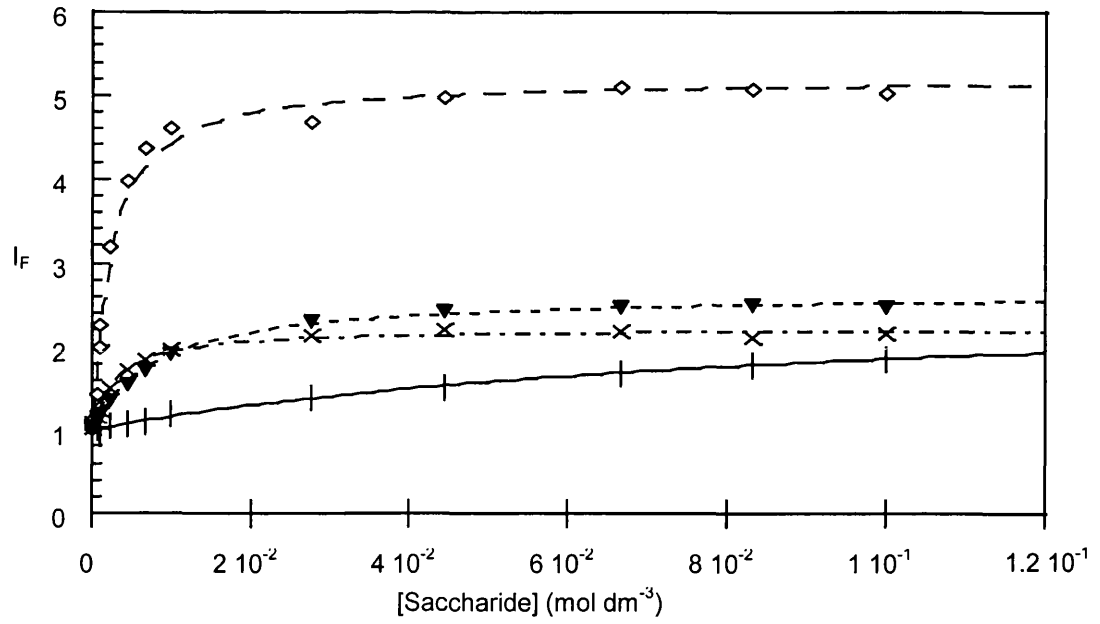

Figure II-11. Fluorescence Intensity (I_F) of Sensor **46** (5×10^{-6} mol dm^{-3}) *versus* [D-glucose **112**] (—◇—), [D-galactose **113**] (—×—), [D-mannose **114**] (—|—) and [D-fructose **115**] (—▼—) at 25 °C at pH 8.21 in 52.1 % (w/w) methanol/ water solution; λ_{ex} = 271 nm, λ_{em} = 343 nm.

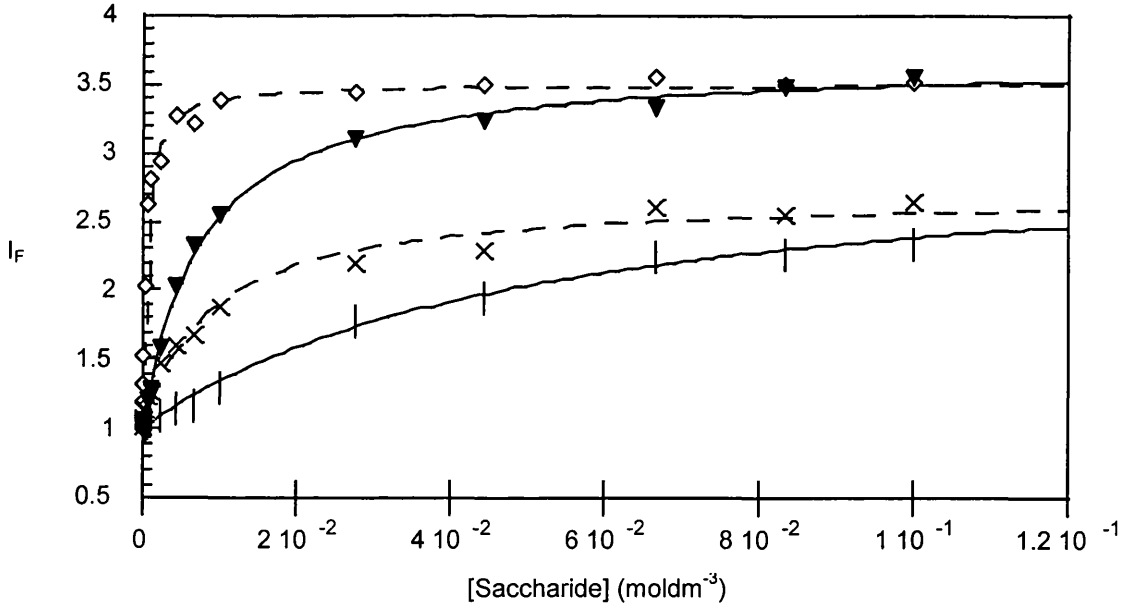

Figure II-12. Fluorescence Intensity (I_F) of Sensor **47** (1×10^{-7} moldm^{-3}) *versus* [D-glucose **112**] (—◇—), [D-galactose **113**] (—×—), [D-mannose **114**] (—|—) and [D-fructose **115**] (—▼—) at 25 °C at pH 8.21 in 52.1 % (w/w) methanol/ water solution; λ_{ex} = 370 nm, λ_{em} = 417 nm.

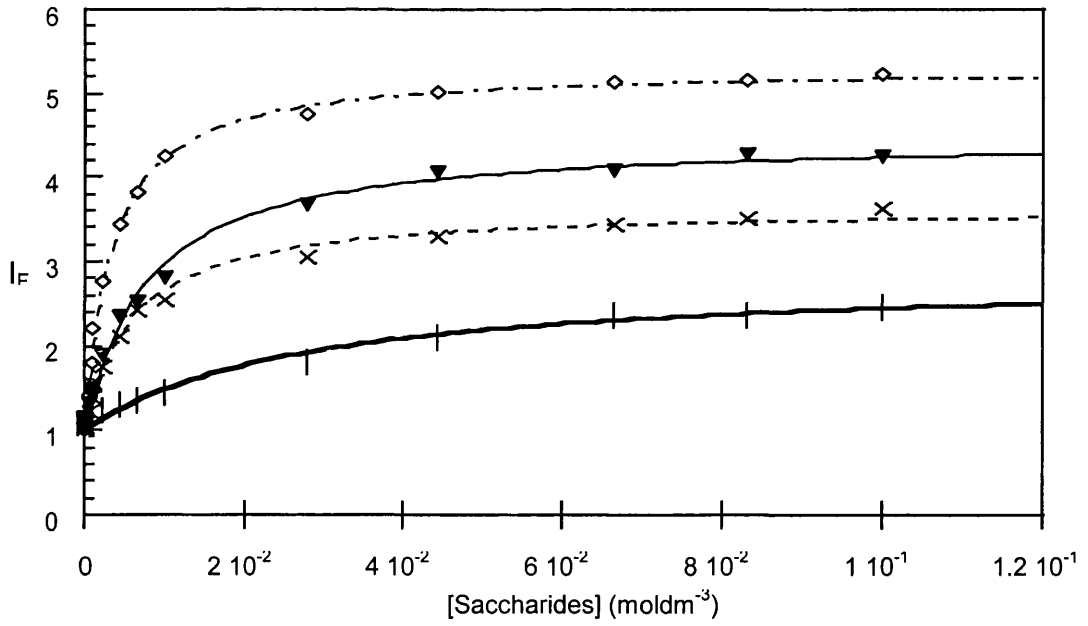

Figure II-13. Fluorescence Intensity (I_F) of Sensor **48** (1×10^{-7} moldm^{-3}) *versus* [D-glucose **112**] (—◇—), [D-galactose **113**] (—×—), [D-mannose **114**] (—+—) and [D-fructose **115**] (—▼—) at 25 °C at pH 8.21 in 52.1 % (w/w) methanol/ water solution; λ_{ex} = 343 nm, λ_{em} = 397 nm.

It was immediately obvious from Figure II-7 – II-13 that the 6 sensors undergo an enhancement of fluorescence when saccharides are added.

The stability constants K of the complexes formed between the sensors and the saccharides were initially analysed using equation (13) below.[100] However, the precision of the value of the stability constant K depends on the accuracy of I_{Fmax}, which is difficult to obtain experimentally. The calculation of K was therefore carried out using equation (12). Plots of fluorescence intensity (I_F) *versus* concentration of saccharide ([saccharide]) gave the calculated stability constant (K) and the final fluorescence intensity (I_{Fmax}). Curve fitting was performed using KaleidaGraph software.[101]

$$I_F = (I_{Fmin} + I_{Fmax} \times K \times [\text{saccharide}])/(1 + K \times [\text{saccharide}]) \quad (12)$$

$$\text{Log}[\text{saccharide}] = \log[(I_F - I_{Fmin})/(I_{Fmax} - I_F)] - \log K \quad (13)$$

I_{Fmin} is the initial (minimum) fluorescence intensity; I_{Fmax} is the final (maximum) fluorescence intensity; I_F is the fluorescence intensity for a particular [saccharide]; K is the stability constant of the sensor with the saccharide.

The stability constants of sensors **39**, **43**, **44**, **45**, **46**, **47** and **48** are shown in Table 2.2 and a graphical representation is given in Figure II-15.

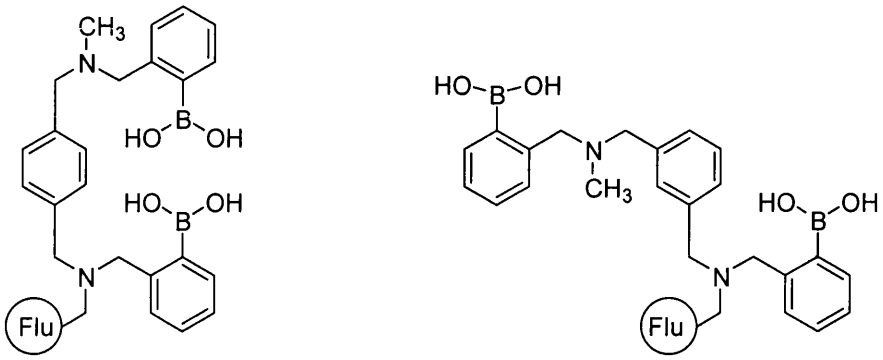

43 Flu = naphthalene
44 Flu = anthracene
45 Flu = pyrene

46 Flu = naphthalene
47 Flu = anthracene
48 Flu = pyrene

Figure II-14. *Para* Series **43-45** and *Meta* Series **46-48** of Sensors.

Table 2.2. Stability constants K (dm^3mol^{-1}) of sensors **43**, **44**, **45**, **46**, **47**, **48** and **39**.

Sensors		D-glucose K (dm^3mol^{-1})	D-galactose K (dm^3mol^{-1})	D-fructose K (dm^3mol^{-1})	D-mannose K (dm^3mol^{-1})
para	**43**	300 ± 20	160 ± 22	149 ± 10	16 ± 4
	44	228 ± 22	21 ± 9	81 ± 13	8 ± 2
	45	160 ± 5	80 ± 6	83 ± 4	9 ± 1
meta	**46**	452 ± 38	330 ± 26	124 ± 5	35 ± 4
	47	415 ± 63	274 ± 34	100 ± 15	24 ± 4
	48	307 ± 15	204 ± 18	133 ± 9	32 ± 5
	39	1950 ± 184	112 ± 14	132 ± 7	14 ± 3

Calculated K values assume a 1:1 complex

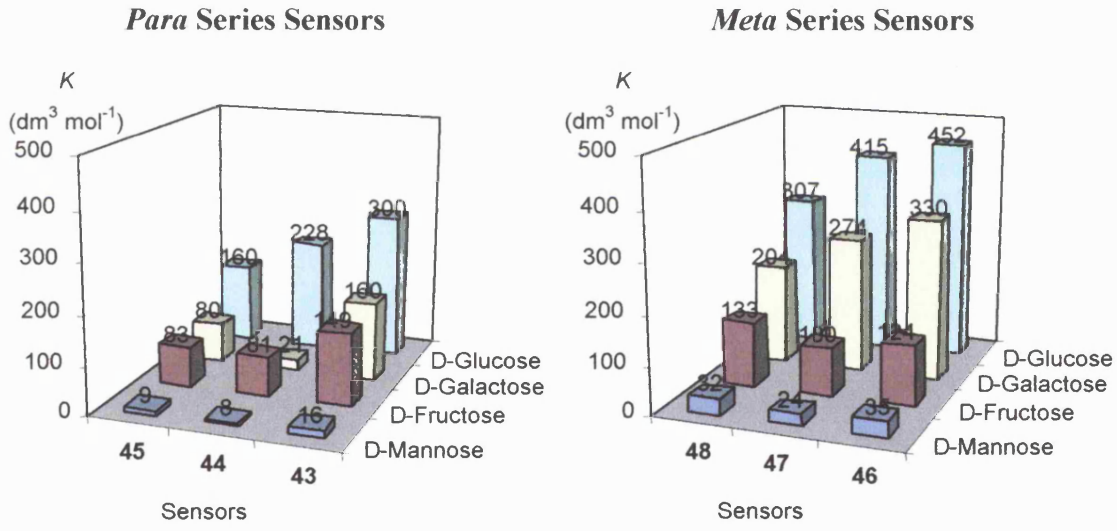

Figure II-15. Stability Constants K (dm^3mol^{-1}) of Sensors **43**, **44**, **45**, **46**, **47** and **48**.

II-7.2.2 Discussion

The two graphs in Figure II-15 show that the stability constants are highest in the *meta* series of sensors (**46**, **47**, **48**) than in the *para* series (**43**, **44**, **45**). Comparing two sensors carrying the same fluorophore (**43** with **46**, **44** with **47** and **45** with **48**), for a given saccharide, the value of the stability constant of the *para* sensor is always smaller

than for the *meta* series sensor. The only apparent difference between the two series of sensors is in the nature of the spacer. The spacer controls the distance between the two nitrogen atoms. The series of sensors with the two boronic acids in the *para* position have a longer spacer (6 carbon atoms between the two nitrogens) than the *meta* series with 5 carbon atoms. The above results (Table 2.2 and Figure II-15) show that in the case of the two series of sensors, a smaller spacer favours complexation with saccharides. Dr. Susumi Arimori[102] has also studied the effect of the distance between the two nitrogen groups with a different system. He synthesised compounds **116$_n$** (n = 3-8), Figure II-16, and calculated the stability constants *K* of the complexes formed between these compounds and D-glucose **112**, D-galactose **113**, D-mannose **114** and D-fructose **115**, Figure II-17.

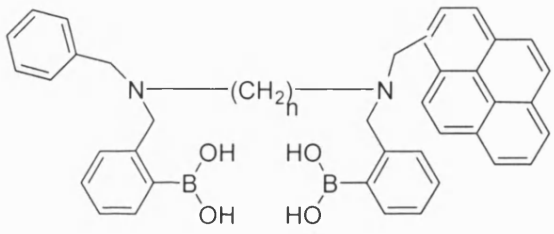

Figure II-16. Compound **116$_n$** (n = 3 - 8).

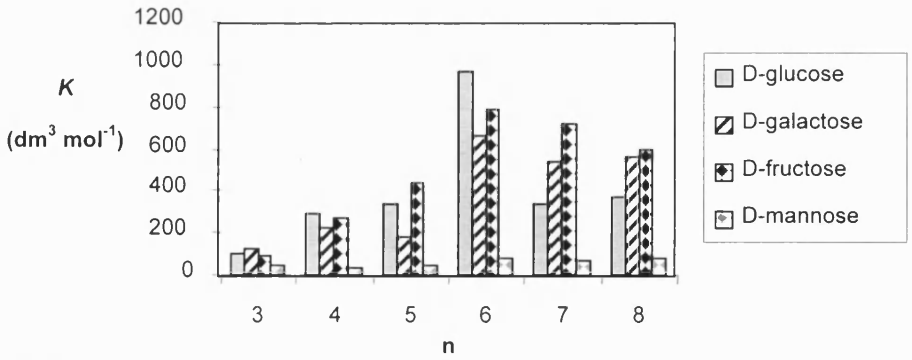

Figure II-17. Relative stability constants of sensors **116$_n$** (n = 3 - 8).

It can be seen from Figure II-17 that the stability constants *K* are maximum for D-glucose **112**, D-galactose **113**, D-mannose **114** and D-fructose **115** when n = 6 (**116$_6$**).

Therefore, a sensor with a spacer composed of 6 carbon atoms seems more favorable for selective saccharide binding than the one with a spacer composed of 5 carbon atom.[102] These results do not seem to agree with previous results where sensors with a 5 carbon atom spacer had stronger stability constants than the one with a 6 carbon atoms spacer. It should be noted that the distance between the two nitrogen atoms in compounds **116$_5$** and **116$_6$** is not exactly identical to the inter nitrogen distances of sensors **46**, **47**, **48** (*meta* series) and sensors **43**, **44** and **45** (*para* series). The spacer of compounds **116$_5$** and **116$_6$** are respectively composed of 6 and 7 single C-C bonds, whereas the spacers of the two series are formed of 4 single C-C bonds and 2 double C=C bonds for the meta series and 4 single C-C bonds and 3 double C=C bonds for the *para* series. However, the distance between the two nitrogen atoms in compound **116$_5$** is still close to that for the *meta* series, and similarly for compound **116$_6$** and the *para* series. By only considering the length of the spacer of these two different systems, the data from the study of Dr Arimori would therefore give a different conclusion concerning the effect of this distance on the selectivity of diboronic acid sensors. However, the nature of the spacer of Arimori's system is different from that for the *meta* and para *series*. Because of this structural difference, other factors need to be taken in account. Arimori's system is, for example, much more flexible than the *meta* and *para* series of sensors which have a more rigid geometry. Arimori's system can rearrange easily upon saccharide binding while the rigidity of the *meta* and *para* systems determine the directional orientation of the two boronic acid groups.

The value of the stability constant (K) calculated by T. D. James from compound **39** can also be compared with the K value of compound **44**.[80]

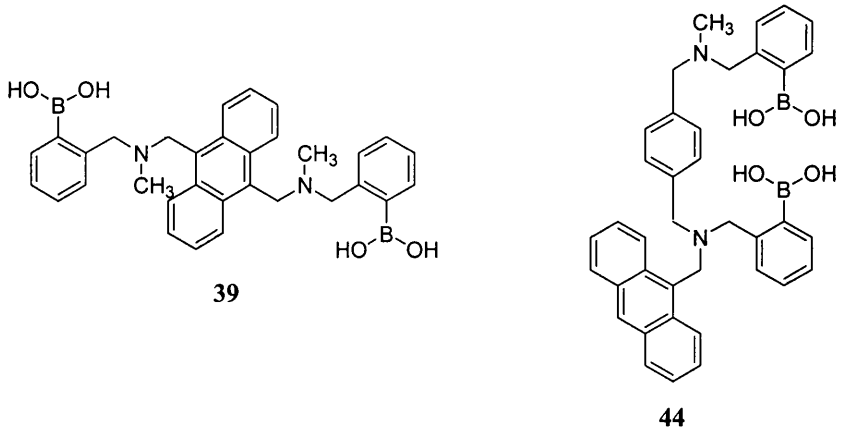

Figure II-18. Similarities of Structure for Sensors **39** and **44**.

Sensors **39** and **44** appear structurally similar, Figure II-18. The distance between the two nitrogen atoms are similar since the distance corresponds to a 1,4-dimethyl benzyl unit. The two sensors also contain the same fluorophore (an anthracene unit). However, the stability constants of the complexes formed between **39** or **44** with D-glucose are very different. The stability constant for **39** is $K = 1950$ and for **44**, $K = 228$ $dm^3\ mol^{-1}$. This result clearly demonstrates that the length of the spacer is not the only factor in determining the selectivity of a diboronic acid sensors (*cf.* differences observed in compounds $\mathbf{116_n}$ and differences observed between the *meta* and the *para* series), obviously other structural factors also need to be taken in account in the design of selective diboronic acid fluorescent sensors. In this case, the difference in the value of the stability constant must be due to steric effects. There is more steric strain on one of the nitrogen atoms in compound **44** (carrying an anthracene unit) than the equivalent nitrogen in sensor **39**, which carries a methyl unit. The greater steric strain in compound **44** decreases the flexibility and therefore the ability of the two boronic acid groups to bind with saccharides.

The following section describes the investigation of the affinity of each sensor of the two series for the 4 different saccharides (D-glucose **112**, D-galactose **113**, D-mannose **114** and D-fructose **115**).

The two graphs in Figure II-15 (p 87) clearly show that the 6 sensors **43-48** are glucose selective with the highest stability constant value (*K*). These 6 sensors also present a similar behaviour concerning their interaction with D-mannose and D-fructose. D-mannose gives the weakest stability constant *K* with the 6 sensors, with *K* = 8-16 dm^3 mol^{-1} for the *para* series and *K* = 24-35 dm^3 mol^{-1} for the *meta* series. The stability constant *K* for the 6 sensors **43**, **44**, **45**, **46**, **47** and **48** is relatively uniform for D-fructose with variation between *K* = 81 and *K* = 149 dm^3 mol^{-1} (*K* = 149, 81, 83, 124, 100 and 133 dm^3 mol^{-1} respectively). However, with D-galactose the stability constants vary considerably from one series of sensors to the second series. The stability *K* increases dramatically for the *meta* series of sensors. The variation of the stability constants of two sensors carrying the same fluorophore when bound to D-glucose and D-galactose is emphasised in Table 2.3.

Table 2.3 Comparison of Stability Constants *K* of Sensors **43** and **46**, **44** and **47** and **45** and **48** toward to D-glucose or D-galactose.

	Sensors	**D-glucose** *K* (dm^3 mol^{-1})	**D-galactose** *K* (dm^3 mol^{-1})
Flu = naphtalene	**43** (*para* series)	300	160
	46 (*meta* series)	452	330
Flu = anthracene	**44** (*para* series)	228	21
	47 (*meta* series)	415	274
Flu = pyrene	**45** (*para* series)	160	80
	48 (*meta* series)	307	204

Sensors composed of a naphthalene (**43**, **46**), an anthracene (**44**, **47**) and a pyrene (**45**, **48**) unit show an increase of respectively 1.5, 1.8 and 1.9 of their stability constants in the case of D-glucose in going from the *para* to the *meta* series. It has been shown previously in the 2 graphs in Figure II-15 (p87) that sensors of the *meta* series have a much higher stability constant than sensors of the *para* series. In the case of D-galactose, the stability constants (*K*) of diboronic acid sensors **46**, **47** and **48** (*meta* series) are respectively 2, 13 and 2.55 times stronger than *para* diboric acid sensors **43**, **44** and **45**. The high value of the stability constant observed for sensor **47** and particularly **46** with D-galactose shows that the fluorophore unit also plays a role in the stability of the complex formed between the saccharide and the sensors. If all the fluorophores would play a similar role in the stability constant of a sensor, the variation of the nature of the fluorophore among a series of sensors should not modify the value of the stability constant and, in this particular example, sensor **46** should have the same stability constant for D-galactose as sensors **47** and **48**. The modification of the fluorophore among a series of sensors was not expected to cause such a variation in the stability constant of the complex as the whole structure of the sensor did not seem to vary significantly when the fluorophore is varied.

In this section, fluorescence experiments have revealed that the 6 sensors of the two series (*meta* and *para*) are selective for D-glucose and that the *meta* position seems to favour the complexation of the sensors with saccharides. It has also been shown that the stability constants of sensors **46** and **47** are particularly strong with D-galactose. The various observations made for each fluorophore shows how difficult it is to predict the behaviour of sensors.

With CD experiments, it will be possible to gain information about the structure of the sensor:saccharide complexes.

II-7.3 CD (Circular Dichroism) Experiments

II-7.3.1 Introduction

Circular Dichroism (CD) is observed when optically active matter absorbs left and right hand circular polarized light slightly differently. If it is the case they are said to be CD active. Figure II-19 (a) shows a circularly polarized light with its right and left components (R and L). When the light passes through a CD active sample with a different absorbance A for the 2 components, the amplitude of the stronger absorbed component will be smaller than that of the less absorbed component. The consequence is that a projection of the resulting amplitude now yields an ellipse instead of the usual line (Figure II-19 (b)). The occurrence of ellipticity is called Circular Dichroism.

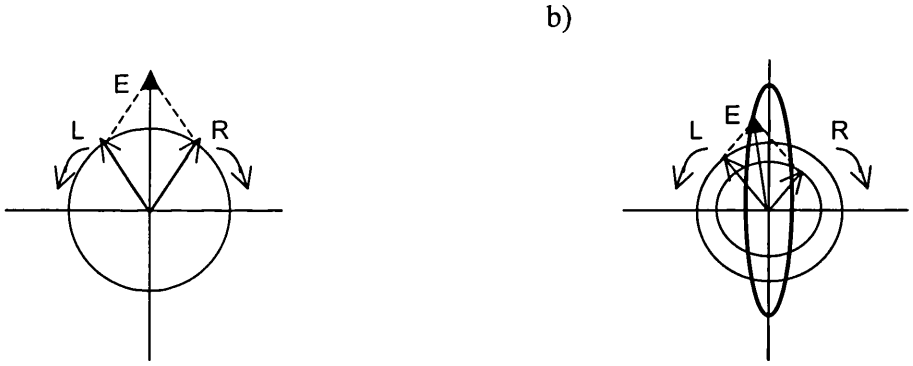

Figure II-19. a) Circular Polarised Light, b) Circular Dichroism.

The two main conditions for a molecule to be CD active is to absorb in the UV spectrum and to be chiral. Some compounds can become CD active when they form "specific" complexes. The complexation between an achiral, chromophoric compound and a chiral non-chromophoric substance results in most cases in a CD active complex. This CD activity can be detected by CD spectropolarimeters, which measure the difference in absorbance of right-and left- circular polarized light as a function of

wavelength. CD thus represents a very powerful tool to determine the structure of complexes.

CD spectroscopy was used with diboronic acid sensors to show the formation of an 1:1 complex with certain saccharides. This was, for example the case with compound **39**,[80] which forms a 1:1 complex with D-glucose Figure II-20.

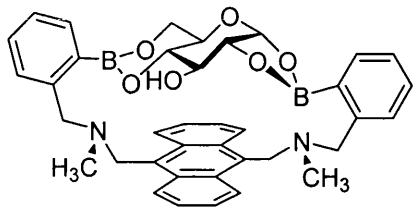

Figure II-20. 1:1 Complex Formed between D-Glucose and Sensor **39**.

The formation of the 1:1 cyclic complex between compound **39** and D-Glucose **112** gives a rigid structure and freezes the molecular motion of the chromophoric anthracene unit in **39**. This situation is favourable for the appearance of a CD signal. The chirality of D-glucose and L-glucose induces the orientation of this rigid structure. The CD signal observed for the complex formed between compound **39** and D-glucose gives an opposite symmetrical signal than the one formed with L-glucose.

II-7.3.2 CD measurements

The CD spectroscopy measurements performed on sensors **43-48** are reported in Table 2.4 and 2.5. This should provide information on the structure of the complex formed between sensors **43-48** and D-glucose **112**, D-galactose **113**, D-mannose **114** and D-fructose **115**.

Table 2.4 Absorption and CD maximum of **43, 44, 45** (*para* series) and its saccharides complexes.

Sensor (*para* series)	**Saccharides**	**Absorption Maximum** (nm)	**CD maximum** Wavelength (λ)/ ellipticity (θ) (nm/ deg cm^2 $dmol^{-1}$)
43	D-glucose	275	289/ - 452
	L-glucose	275	289/ + 390
	D-galactose	274	silent
	D-fructose	273	silent
44	D-glucose	380	393/ + 713
	L-glucose	380	393/ - 944
	D-galactose	378	silent
	D-fructose	379	silent
45	D-glucose	349	356/ - 329
	L-glucose	349	356/ + 352
	D-galactose	345	silent
	D-fructose	345	silent

Table 2.5. Absorption and CD maximum of **46, 47, 48** (meta series) and their saccharides complexes.

Sensors (*meta* series)	**Saccharides**	**Absorption Maximum** (nm)	**CD maximum** Wavelength (λ)/ ellipticity (θ) (nm/ deg cm^2 $dmol^{-1}$)
46	D-glucose	273	289/ + 905
	L-glucose	273	290/ -967
	D-galactose	273	290/ -1052
	D-fructose	275	silent
47	D-glucose	384	395/ - 948
	L-glucose	384	395/ + 806
	D-galactose	383	394/ + 824
	D-fructose	384	silent
48	D-glucose	349	357/ - 934
	L-glucose	349	357/ + 496
	D-galactose	344	silent
	D-fructose	349	silent

Ellipticity (θ in degrees) is the unit of circular dichroism and is defined as the tangent of the ratio of the minor to major elliptical axis. The unit ellipticity persists despite the fact that CD is now measured as the difference in absorption of right- and left- circular components. To compare the data, the ellipticity is usually converted to Molar Ellipticity (deg cm^2 $dmol^{-1}$).

From Tables 2.4 and 2.5, we can see that the six sensors are CD-active with D-glucose **112**, but CD-silent with D-fructose **115**. It is then expected that all the 6 sensors form a 1:1 complex with D-glucose and a 1:2 complex with D-fructose. However, D-galactose **113** gave different results depending on the diboronic acid sensors. Sensors **43**, **44**, **45** and **48** form 1:2 CD-silent complexes with D-galactose **113**, while sensors **46** and **47** form a 1:1 CD-active complex with D-galactose **113**. The explanation is compatible with the fact that sensors **46** and **47** gave higher *K* values with D-galactose than sensors **43**, **44**, **45** and **48** (Table 2.3 p 91, *K* values are still valid for the 1:2 complex – as the fluorophore interacts with only one boronic acid, the complex can be treated as a 1:1 complex). As it has been observed for sensor **39**,[80] it can also be concluded that the ability to form a cyclic structure is thus responsible for a higher stability constant. The structures of sensors **46** and **47** are ideally suited to form a 1:1 complex with D-glucose and D-galactose. However, sensor **48** has the same structure as sensors **46** and **47** and the fact that it does not form the same complex is surprising. This could perhaps be due to the bulk of the fluorophore (pyrene unit), which could make the rotation of the C-N bonds difficult. The lack of flexibility may make it difficult for the two boronic acid groups to rearrange easily and form a cyclic complex.

Figure II-21 shows the CD spectra of **47** in presence of D-glucose and L-glucose and Figure II-22 represents the CD activity of **47** in presence of D-galactose. The CD-active graphs of other sensors are represented in Appendix 5, 10, 15, 20, 21, 26, 27 and 32.

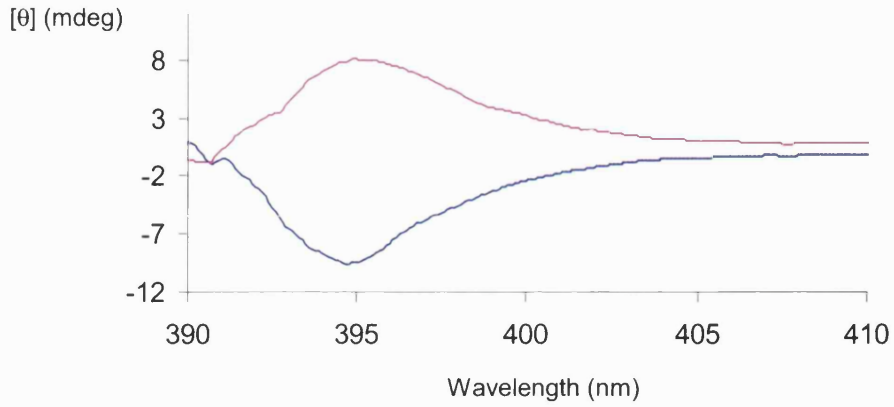

Figure II-21. CD Spectra of **47** (1×10^{-3} moldm^{-3}) in presence of —— D-glucose and —— L-glucose, 25°C.

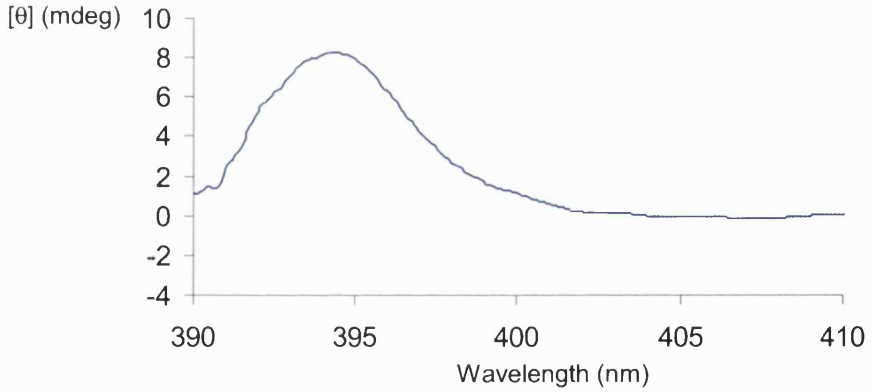

Figure II-22. CD Spectra of **47** (1×10^{-3} moldm^{-3}) in presence of ——D-galactose, 25°C.

II-8 Summary of Analytical Work

As expected, the 6 diboronic acid sensors showed fluorescence enhancement after saccharide addition. Fluorescence titration of sensors **43-48** with various concentrations of D-glucose **112**, D-galactose **113**, D-mannose **114** and D-fructose **115** allowed the calculation of the stability constant *K* of the complexes formed between the sensors and the saccharides. It was apparent that sensors belonging to the *meta* series (**46-48**) have higher stability constants *K* with the 4 saccharides than sensors of the *para* series (**43-45**). It was also shown that all 6 sensors are glucose selective with the highest stability constant *K* observed in presence of D-glucose. However, sensors **46** and **47** also have an unusually high stability constant with D-galactose compared to the other sensors.

CD (Circular Dichroism) spectroscopy permitted the determination of the structure of the complex formed between the sensors and the saccharides. Diboronic acid sensors can form two different complexes with saccharides. Binding of two hydroxy groups of two different saccharide molecules results in a 1:2 complex, whereas binding of four hydroxy groups of the same saccharide molecule results in a cyclic 1:1 complex. 1:2 Complexes are CD-silent whereas 1:1 complexes are CD-active. CD measurements showed that the 6 sensors **43-48** were forming a cyclic 1:1 complex with D-glucose and a 1:2 complex with D-fructose. The mode of binding of D-galactose varied between sensors. Sensors **43**, **44**, **45** and **48** form a CD-silent 1:2 complex with D-galactose while sensors **46** and **48** form a cyclic 1:1 complex. The fluorescence measurements, combined with the CD experiments, confirmed the fact that the selectivity of a sensor for a saccharide depends on the formation of this cyclic 1:1 complex.

III Conclusions

This research has shown that it is possible to synthesise modular PET fluorescent saccharide sensors using quick, easy and mild reaction conditions. Two series of 3 sensors (*para* series **43-45** and *meta* series **46-48**) were synthesised. The 6 sensors (**43-48**), varying in the nature of the fluorophore (naphthalene, anthracene or pyrene) and/or the distance between the two boronic acids units (spacer), allowed the study of the effect of the fluorophore and the spacer on the selectivity of the sensors. Previous research[80] has shown that the selectivity of a sensor toward one particular saccharide can be explained by the formation of a 1:1 cyclic complex between the sensor and the saccharide. This was previously the case for the 1:1 complex formed between sensor **39** and D-glucose. The 6 sensors (**43-48**) shows particular selectivity towards glucose and form cyclic 1:1 complexes with glucose. Two sensors (**46** and **47**) also showed strong affinity for D-galactose. This may suggest that the spacer used in the *meta* series of sensors was favourable for interactions with D-galactose. However, *meta* sensor **48** did not seem to form a 1:1 complex with D-galactose. Therefore the choice of the spacer is important for the selectivity of the sensor. Some structural factors can handicap the formation of the cyclic complex, for example the presence of stericly bulky groups.

It has also been shown that there is a great variation in the value of the stability constant *K*. Sensors **39** and **43-48** are all glucose selective. However, they all have very different stability constant values. The highest stability constant is seen for sensor **39** with K = 1950 dm^3mol^{-1} followed by the *meta* series of sensors **46-48** with K varying between 307 dm^3mol^{-1} (**48**) and 452 dm^3mol^{-1} (**46**). The para series of sensors have the lowest stability constant values varying between 160 (**45**) and 300 $dm^3\ mol^{-1}$ (**43**).

The results discussed in this chapter have confirmed the fact that PET diboronic acid sensors represent a powerful tool for the detection of saccharides. These results could form the basis of further research. For example, sensors **46** and **47** can be used as models for the design of D-galactose selective fluorescent sensors and for the basis of further studies. It is possible that this work could lead to the development of sensors attached to polymer resins bound to fibre-optic devices, for example, to allow continuous monitoring of glucose *in vivo* for a variety of industrial and medicinal applications.

IV Experimental

IV-1 General methods and materials

NMR spectroscopy: NMR spectra were recorded on a Bruker AC-300 or AM-300, a Varian Gemini 500, a Jeol 270-EX or a Jeol 400-EX spectrometer. All chemical shift (δ) are described in parts per million relative to tetramethylsilane as the internal standard. The multiplicities of the spectroscopic data are presented in the following manner: s = singlet; d = doublet; t = triplet; m = multiplet and the values of the coupling constants *J* are given in Hz.

Mass spectrometry: Mass spectra and accurate mass were recorded on a Kratos Profile or VG ProSpec for Electron Impact (E.I.), a VG ProSpec for Chemical Ionisation (C.I.), a VG ZabSpec for Fast Atom Bombardment (F.A.B.), a micromass LCT for Electrospray Ionisation (E.I.) or a Micromass Autospec spectrometer with E.I., C.I., F.A.B. and Electrospray sources. Electrospray samples were prepared in a CH_3OH/ H_2O 1:1 solution and F.A.B. spectra were recorded using *m*-nitrobenzyl alcohol or glycerol as a matrix.

Infrared spectra: Infrared Spectra were recorded on a Perkin-Elmer Paragon 1000 FT-IR or a Perkin-Elmer 1600 FT-IR spectrometer. The samples were prepared as Nujol mulls, solutions in chloroform or as neat samples. The frequencies (υ) as absorption maxima are given in wavenumbers (cm^{-1}).

Elemental analyses were performed at the University of North London, the University of Birmingham and the University of Bath.

Melting points were determined using a Gallenkamp melting point apparatus and are reported uncorrected.

Thin Layer Chromatography (TLC): Precoated aluminium-backed silica plates were supplied by Fluka Chemie, (Silica gel with fluorescent indicator 254 nm, thickness 0.2 mm). Ultraviolet light was employed for visualisation.

Column Chromatography: Column Chromatography was performed using silica gel 60 (0.063-0.200 mm), (E. Merck, 64 271 Darstadt, Germany) and the column fractions were collected and monitored by TLC.

Fluorescence experiments: Fluorescence measurements were recorded on a Perkin Elmer LS 50 B Fluorimeter using quartz cuvets with 10 mm path length.

IV-2 Characterisation

4-Methylaminomethyl-benzonitrile (68)

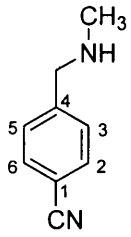

Methylamine (45.7 cm^3 of a 2.0 $moldm^{-3}$ solution in methanol, 91.4 mmol) was added under argon atmosphere to 4-cyanobenzaldehyde (2.00 g, 15.25 mmol) in a stirred round-bottomed flask at room temperature. The reaction was left stirring overnight. A solution of sodium borohydride (5.64 g, 152.50 mmol) in dry methanol (100 cm^3) was added in one portion to the reaction mixture and the reaction mixture was stirred for 4 hours and then concentrated under reduced pressure. Then water (50 cm^3) was added to the solution and the aqueous layer was extracted with dichloromethane (3 x 50 cm^3). The combined organic extracts were dried ($MgSO_4$), filtered and concentrated under reduced pressure to give the amine **68** as a yellow oil (1.88 g, 84.4 %), (Found: M^+, 146.0835. $C_9H_{10}N_2$ requires 146.0843); υ_{max} (Neat)/cm^{-1} 2229 (CN nitrile). δ_H(300 MHz; C^2HCl_3) 2.29 (3H, s, CH_3), 3.67 (2H, s, CH_2), 7.30 (2H, d, $J_{2,3}$ 8.1 Hz, 2-Ar*CH* and 6-Ar*CH*), 7.45 (2H, d, $J_{3,2}$ 8.1 Hz, 3-Ar*CH* and 5-Ar*CH*); δ_C(75 MHz; C^2HCl_3) 36.05 (CH_3), 55.43 (CH_2), 110.52 (4-Ar*C*), 119.09 (CN), 128.66 (2-Ar*C*H and 6-Ar*C*H), 132.13 (3-Ar*C*H and 5-Ar*C*H) and 145.17 (1-Ar*C*); *m/z* (EI^+) 146 (66 %, M^+) and 44 (100, $[CH_3NHCH_2]^+$).

4-(5,5-Dimethyl-1,3-dioxan-2-yl)benzenecarbonitrile (73)

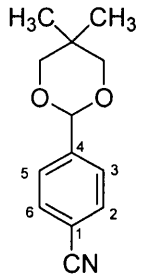

To a stirred solution of 4-cyanobenzaldehyde **66** (1.35 g, 10.30 mmol) in toluene (20 cm^3) was added 2,2-dimethyl 1,3-propanediol (1.40 g, 13.40 mmol), followed by TsOH (0.13 g, 0.75 mmol). The mixture was stirred and refluxed for 2 hours. Water formed during the reaction was removed under Dean and Stark conditions. After 2 hours all the starting material had been converted to the protected aldehyde. The solution was concentrated under reduced pressure and hexane was used to remove the remaining toluene. The carbonitrile **73** was obtained as a white solid (2.20 g, 99.3 %), mp 97-99 °C, (Found: C, 71.8; H, 6.9; N, 6.4. Calc. For $C_{13}H_{15}NO_2$: C, 71.9; H, 6.9; N, 6.4 %); υ_{max} (Nujol)/cm^{-1} 2228 (CN nitrile). δ_H(300 MHz; C^2HCl_3) 0.80 and 1.26 (3H, s, CH_3-axial and 3H, s, CH_3-equatorial), 3.65 and 3.77 (2H, d, $J_{Haxial\text{-}Hequatorial}$ 10.3 Hz, 2 × CH-axial and 2H, d, $J_{Hequatorial\text{-}Haxial}$ 9.9 Hz, 2 × CH-equatorial), 5.41 (1H, s, CH), 7.61 (2H, d, $J_{3,2}$ 8.3 Hz, 3-ArC*H* and 5-ArC*H*) and 7.66 (2H, d, $J_{2,3}$ 8.3 Hz, 2-ArC*H* and 6-ArC*H*); δ_C(75 MHz; C^2HCl_3) 21.84 and 22.99 (2 × CH_3), 30.30 and 30.96 (2 × CH_2), 56.34 (*C*$(CH_3)_2$), 100.25 (CH), 112.60 (1-Ar*C*), 118.73 (CN), 127.05 (3-Ar*C*H and 5-Ar*C*H), 132.15 (2-Ar*C*H and 6-Ar*C*H) and 143.21 (4-Ar*C*); *m/z* (EI^+) 217 (63%, M^+) and 56 (100, $[(CH_3)_2CCH_2]^+$).

4-(5,5-Dimethyl-1,3-dioxan-2-yl)benzenaldehyde (74)

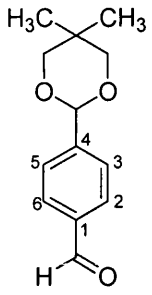

A 1.0 moldm^{-3} solution of DIBAL-H in THF (8.75 cm^3, 8.75 mmol) was added slowly to a cool (0 °C) solution of the protected 4-cyanobenzaldehyde **73** (1.52 g, 7.00 mmol) in dry benzene (30 cm^3). The reaction mixture was allowed to stir overnight, and then 1.0 moldm^{-3} HCl (30 cm^3) was added to dissolve the precipitate. The aqueous fraction was extracted with ethyl acetate (3 x 50 cm^3), dried ($MgSO_4$) and concentrated under reduced pressure to yield crude **74** as a yellow oil. Purification by column chromatography on silca gel (1:9 ethyl acetate/ hexane) afforded pure **74** as a yellow (0.46 g, 29.8 %), (Found: C, 70.2; H, 7.5. Calc. For $C_{13}H_{16}O_3$: C, 70.5; H, 7.3 %); υ_{max} (Nujol)/cm^{-1} 1703 (C=O aldehyde). δ_H(300 MHz; C^2HCl_3) 0.79 and 1.27 (3H, s, CH_3-axial and 3H, s, CH_3-equatorial), 3.65 and 3.77 (2H, d, $J_{Haxial\text{-}Hequatorial}$ 10.3 Hz, 2 × CH-axial and 2H, d, $J_{Hequatorial\text{-}Haxial}$ 9.9 Hz, 2 × CH-equatorial), 5.42 (1H, s, CH), 7.65 (2H, d, $J_{3,2}$ 8.4 Hz, 3-ArC*H* and 5-ArC*H*), 7.87 (2H, d, $J_{2,3}$ 8.4 Hz, 2-ArC*H* and 6-ArC*H*) and 10.0 (1H, s, CHO); δ_C(75 MHz; C^2HCl_3) 31.6 (2 × CH_3), 56.80 (2 × CH_2), 100.33 (CH), 112.60 (1-Ar*C*), 127.11 (3-Ar*C*H and 5-Ar*C*H) and 132.24 (2-Ar*C*H and 6-Ar*C*H); *m/z* (EI$^+$) 220 (58 %, M$^+$) and 56 (100, $[(CH_3)_2CCH_2]^+$).

{[4-(5,5-Dimethyl-1,3-dioxan-2-yl)phenyl]methyl}methylamine (75)

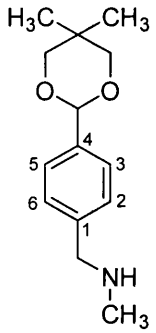

Method 1: Methylamine (4.5 cm^3 of a 2.0 $moldm^{-3}$ solution in methanol, 9.00 mmol) was added under argon atmosphere to the aldehyde **74** (0.30 g, 1.36 mmol) in a round-bottomed flask at room temperature with stirring. After 5 hours' stirring, the formation of the imine was complete. A solution of sodium borohydride (1.67 g, 45.00 mmol) in dry methanol (40 cm^3) was added in one portion and the reaction mixture was stirred for 4 hours and then concentrated under reduced pressure. Water (50 cm^3) was then added to the solution and the aqueous layer was extracted with dichloromethane (3 x 50 cm^3). The combined organic extracts were dried ($MgSO_4$), filtered, and concentrated under reduced pressure to give the amine **75** as a yellow oil (0.28 g, 87.6 %).

Method 2: To a solution of amide **77** (1.25 g, 5.00 mmol) in dry THF (40 cm^3) was added $LiAlH_4$ (25 cm^3 of a 1.0 $moldm^{-3}$ solution in dry THF, 25.00 mmol) at 0 °C and the resulting mixture was heated under reflux for 3 hours. After cooling, the solvent was removed under reduced pressure, and water (50 cm^3) was added dropwise. The aqueous layer was extracted with dichloromethane (3 × 50 cm^3) and the combined extracts were dried ($MgSO_4$), filtered, and concentrated under reduced pressure, affording the amine **75** as a yellow oil (0.53 g, 45.1 %).

(Found: C, 71.3; H, 9.1; N, 6.0. Calc. For $C_{14}H_{21}NO_2$: C, 71.4; H, 9.0; N, 6.0 %). δ_H(300 MHz; C^2HCl_3) 0.79 and 1.29 (3H, s, CH_3-axial and 3H, s, CH_3-equatorial), 2.41 (3H, s, NCH_3), 3.64 and 3.76 (2H, d, $J_{Haxial\text{-}Hequatorial}$ 11.0 Hz, 2 × CH-axial and 2H, d,

$J_{Hequatorial\text{-}Haxial}$ 11.0 Hz, 2 × CH-equatorial), 3.74 (2H, s, NCH_2), 5.37 (1H, s, OCHO), 7.31 (2H, d, $J_{2,3}$ 8.4 Hz, 2-ArC*H* and 6-ArC*H*) and 7.46 (2H, d, $J_{3,2}$ 8.4 Hz, 3-ArC*H* and 5-ArC*H*); δ_C(75 MHz; C^2HCl_3) 21.9 and 23.0 ((CH_3)$_2$C), 30.2 (2 × OCH_2), 35.8 (CH_3NH), 55.7 (CH_2NH), 60.6 (*C*(CH_3)$_2$), 101.7 (OCHO), 126.2 (2-Ar*C*H, 6-Ar*C*H), 128.1 (3-Ar*C*H, 5-Ar*C*H), 137.3 (1-Ar*C*) and 140.8 (4-Ar*C*); *m/z* (EI^+) 234 (72 %, $[M - H]^+$) and 120 (100, $[C_6H_4CH_2NHCH_3]^+$).

4-(5,5-Dimethyl-[1,3] dioxan-2-yl)-benzoic acid methyl ester (76)

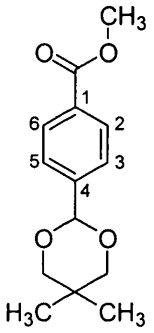

To a stirred solution of methyl 4-formylbenzoate **69** (4.00 g, 24.30 mmol) in 70 cm^3 of toluene was added 2,2-dimethyl 1,3-propanediol (3.00 g, 29.10 mmol), followed by TsOH (0.50 g, 0.92 mmol). The mixture was stirred and heated under Dean Stark conditions for 2 hours. After cooling, the solvent was removed under reduced pressure and the resulting residue was triturated with methanol, affording the ester **76** as a white powder (4.27 g, 70.2 %), mp 108-109 °C, (Found: C, 66.9; H, 7.2. Calc. For $C_{14}H_{18}O_4$: C, 67.1; H, 7.2 %), υ_{max} (nujol)/ cm^{-1} 1731 (C=O). δ_H(300 MHz; C^2HCl_3) 0.79 and 1.28 (3H, s, CH_3-axial and 3H, s, CH_3-equatorial), 3.64 and 3.77 (2H, d, $J_{Haxial\text{-}Hequatorial}$ 10.6 Hz, 2 × CH-axial and 2H, d, $J_{Hequatorial\text{-}Haxial}$ 10.0 Hz, 2 × CH-equatorial), 3.90 (3H, s, CH_3O), 5.41 (1H, s, CH), 7.54 (2H, d, *J* 8.4 Hz, 3-ArC*H* and 5-ArC*H*) and 8.03 (2H, d, *J* 8.4 Hz, 2-ArC*H* and 6-ArC*H*); δ_C(75 MHz; C^2HCl_3) 21.89 and 23.05 ((CH_3)$_2$C), 30.30 (2 × OCH_2), 52.15 (OCH_3), 100.99 (CH), 126.26 (3-Ar*C*H and 5-Ar*C*H), 129.64

(2-ArCH and 6-ArCH), 130.50 (4-ArC), 143.05 (1-ArC) and 167.01 (CO); *m/z* (EI^+) 249 (69 %, $[M - H]^+$) and 165 (100, $[HC(O)C_6H_4C(O)OCH_3 + H]^+$).

4-(5,5-Dimethyl-[1,3] dioxan-2-yl)-*N*-methyl-benzamide (77)

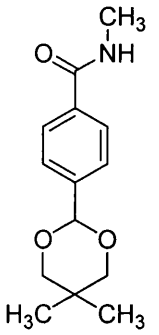

To a solution of the ester **76** (2.50 g, 10.00 mmol) in methanol (50 cm^3) was added methylamine (50 cm^3 of a 2.0 $moldm^{-3}$ solution in methanol, 100 mmol) under argon atmosphere. After 2 days stirring, the reaction was not complete (by TLC) and more methylamine (25 cm^3) was added. After stirring for 10 days, the reaction was complete and the solvent was removed under reduced pressure to give the pure amide **77** as a white powder (2.47 g, 99.1 %), mp 138-139 °C, (Found: C, 67.5; H, 7.8; N, 5.5. Calc. For $C_{14}H_{19}NO_3$: C, 67.5; H, 7.7; N, 5.6 %); υ_{max} (nujol)/ cm^{-1} 1633 (C=O amide). δ_H(300 MHz; C^2HCl_3) 0.80 and 1.28 (3H, s, CH_3-axial and 3H, s, CH_3-equatorial), 2.99 (3H, s, CH_3NH), 3.64 and 3.77 (2H, d, $J_{Haxial\text{-}Hequatorial}$ 10.6 Hz, 2 × CH-axial and 2H, d, $J_{Hequatorial\text{-}Haxial}$ 10.0 Hz, 2 × CH-equatorial), 5.41 (1H, s, CH), 6.19 (1H, s, NH), 7.55 (2H, d, *J* 8.1 Hz, 3-ArCH and 5-ArCH) and 7.76 (2H, d, *J* 8.4 Hz, 2-ArCH and 6-ArCH); δ_C(75 MHz; C^2HCl_3) 21.79 and 22.97 ($(CH_3)_2C$), 26.75 (CH_3NH), 30.20 (2 × CH_2O), 100.94 (CH), 126.33 (3-ArCH and 5-ArCH), 126.80 (2-ArCH and 6-ArCH), 134.86 (4-ArC), 141.45 (1-ArC) and 167.83 (CO); *m/z* (EI^+) 248 (41 %, $[M - H]^+$), 219 (9, $[M - CH_3NH]$) and 164 (100, $[HC(O)C_6H_4C(O)NHCH_3 + H]^+$).

4-Methylaminomethyl-benzaldehyde (61)

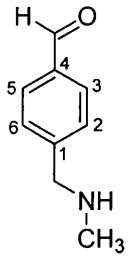

The amine **75** (0.047g, 0.20 mmol) was added to 6 cm^3 of formic acid and the reaction mixture was warmed to 50 °C and stirred for 3 hours. After cooling, the concentration mixture was concentrated under reduced pressure to give the crude aldehyde **61** as a yellow oil. It was not possible to purify this compound further (yield 15 % from NMR). δ_H(300 MHz; C^2HCl_3) 2.64 (3H, s, CH_3), 4.18 (2H, s, CH_2), 7.59 (2H, d, $J_{2,3}$ 8.1 Hz, 2-ArC*H* and 6-ArC*H*), 7.88 (2H, d, $J_{3,2}$ 8.1 Hz, 3-ArC*H* and 5-ArC*H*) and 9.99 (1H, s, CHO); *m/z* (EI^+) 149 (10 %, M^+) and 44 (100, $[CH_3NHCH_2]^+$).

4-(*tert*-Butoxycarbonylaminomethyl)-benzoic acid (86)

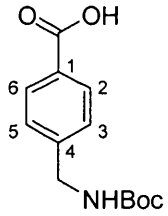

To a stirred solution of 4-(aminomethyl)benzoic acid **85** (7.55 g, 50.00 mmol) in propan-2-ol (45 cm^3) was added an aqueous solution of NaOH (1.0 $moldm^{-3}$, 70 cm^3). The mixture was cooled to 0 °C and a solution of Boc_2O (12.00 g, 55.00 mmol) in propan-2-ol (45 cm^3) was added. The resulting mixture was left to stir for 4 hours at room temperature, then concentrated under reduced pressure. The resulting aqueous layer was washed with diethyl ether (3 × 50 cm^3), then acidified to pH 1 (2 M HCl). The aqueous phase was extracted with ethyl acetate (4 × 50 cm^3) and dried ($MgSO_4$). The solvent was removed under reduced pressure to afford the pure benzoic acid **86** as a

white solid (11.55 g, 92.0 %), mp 163-164 °C, (Found: C, 62.1; H, 6.7; N, 5.6. Calc. For $C_{13}H_{17}NO_4$: C, 62.1; H, 6.8; N, 5.6 %); υ_{max} (nujol)/ cm^{-1} 1682 and 1698 (C=O carboxylic acid and C=O urethane). δ_H(300 MHz; C^2HCl_3) 1.46 (9H, s, 3 × CH_3), 4.39 (2H, d, *J* 5.8 Hz, CH_2NH), 4.95 (1H, m, NH), 7.37 (2H, d, *J* 8.1 Hz, 3-ArC*H* and 5-ArC*H*) and 8.06 (2H, d, *J* 8.1 Hz, 2-ArC*H* and 6-ArC*H*); δ_C(75 MHz; C^2HCl_3) 29.37 (3 × CH_3), 45.37 ($C(CH_3)_3$), 80.98 (CH_2), 128.60 (3-Ar*C*H and 5-Ar*C*H), 131.23 (4-Ar*C*), 131.54 (2-Ar*C*H and 6-Ar*C*H), 147.08 (1-Ar*C*), 159.40 (CO-urethane) and 170.35 (CO-carboxylic acid); *m/z* (EI^+) 252 (14 %, $[M + H]^+$) and 196 (100, $[M - C(CH_3)_3 + 2H]^+$).

(4-Methylcarbamoyl-benzyl)-carbamic acid *tert*-butylester (87)

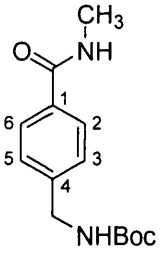

87

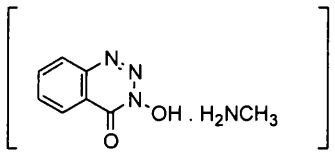

89

Reagent 3-hydroxy-1,2,3-benzotriazin-4(3*H*)-one methylammonium salt (CH_3NH_2 . HOOBt) **89** was previously prepared following this general procedure. HOOBt (9.79 g, 60.00 mmol) was dissolved in methanol (100 cm^3) and the methanolic solution was neutralized by a 1 $moldm^{-3}$ solution of CH_3NH_2 in MeOH, and the solution was concentrated to half of the original volume. The precipitated yellow, crystalline salts was filtrated, dried and used in the next step as a reagent without further purification (8.64 g, 98.6 %). 4-(*tert*-Butoxycarbonylaminomethyl)-benzoic acid **86** (6.27 g, 25.00 mmol) and the reagent CH_3NH_2 . HOOBt **89** (4.85 g, 25.00 mmol) were dissolved in DMF (60 cm^3) and cooled to 0 °C in an ice bath. To this solution was added DCC (6.00 g, 27.50 mmol) with stirring, and the mixture stirred at 0 °C for 1 hour, then for another

3 hours at room temperature. The mixture was then concentrated under reduced pressure and ethyl acetate (60 cm^3) added to the residue. The resultant precipitate of DCU was removed by filtration and the filtrate was washed with water (50 cm^3), saturated $NaHCO_3$ solution (50 cm^3), water (50 cm^3) and then dried ($MgSO_4$). The solvent was removed under reduced pressure and the crude product was crystallized from EtOAc/ hexane to give the pure amide **87** (3.04 g, 46.0 %) as a white solid, mp 177-179 °C (decomp.), (Found: C, 63.6; H, 7.6; N, 10.7. Calc. For $C_{14}H_{20}N_2O_3$: C, 63.6; H, 7.6; N, 10.6 %); υ_{max} (Neat)/ cm^{-1} 1631 (C=O amide) and 1681 (C=O urethane). δ_H(300 MHz; C^2HCl_3) 1.43 (9H, s, $(CH_3)_3C$), 2.97 (3H, d, *J* 4.8 Hz, CH_3NH), 3.31 (2H, d, *J* 5.9 Hz, CH_2NH), 4.96 and 6.24 (1H, m, NHC(O)O and 1H, m, $NHC(O)C_6H_4$), 7.29 (2H, d, *J* 8.1 Hz, 3-ArCH and 5-ArCH) and 7.69 (2H, d, *J* 8.1 Hz, 2-ArCH and 6-ArCH); δ_C(75 MHz; C^2HCl_3) 26.67 (CH_3NH), 28.22 ($(CH_3)_3C$), 44.11 ($C(CH_3)_3$), 79.61 (CH_2NH), 126.99 (3-ArCH and 5-ArCH), 127.21 (2-ArCH and 6-ArCH), 133.44 (4-ArC), 142.38 (1-ArC) and 155.49 and 167.74 (CO-amide and CO-urethane); *m/z* (EI^+) 265 (2 %, $[M + H]^+$), 234 (9, $[M - CH_3NH]^+$) and 208 (100, $[M - C(CH_3)_3 + H]^+$).

4-Aminomethyl-*N*-methyl-benzamide hydrochloride (88)

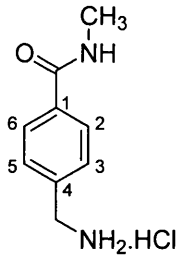

The protected amide **87** (2.88 g, 10.90 mmol) was dissolved in a 32 % concentrated solution of HCl (8.00 g) in EtOAc (75 cm^3). After 30 minutes the solution was concentrated under reduced pressure and the resulting mixture was triturated with diethyl ether, filtered, and dried. The hydrochloride salt **88** was obtained as a white

solid (2.16 g, 99.1 %), mp 270-272 °C, (Found: C, 53.3; H, 6.5; N, 13.7. Calc. For $C_9H_{13}N_2OCl$: C, 53.7; H, 6.5; N, 13.9 %); υ_{max} (nujol)/ cm^{-1} 1618 (C=O amide). δ_H(300 MHz; $C^2H_3O^2H$) 2.91 (3H, s, CH_3), 4.18 (2H, s, CH_2), 7.55 (2H, d, *J* 8.8 Hz, 3-ArC*H* and 5-ArC*H*) and 7.88 (2H, d, *J* 8.5 Hz, 2-ArC*H* and 6-ArC*H*); δ_C(75 MHz; $C^2H_3O^2H$) 27.58 (CH_3), 44.45 (CH_2), 129.60 (3-Ar*C*H and 5-Ar*C*H), 130.78 (2-Ar*C*H and 6-Ar*C*H), 136.81 (4-Ar*C*), 138.42 (1-Ar*C*) and 170.43 (CO); *m/z* (EI^+) 163 (28 %, $[M - H - HCl]^+$), 134 (85, $[M - HCl - CH_3NH]^+$) and 106 (100, $[M - HCl - C(O)NHCH_3]^+$).

4-Methylaminomethyl-benzylamine (62)

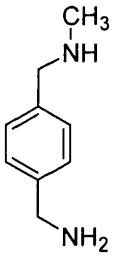

Method 1: To a solution of the amine hydrochloride **88** (0.50 g, 2.50 mmol) in dry THF (10 cm^3) at 0 °C, was added $LiAlH_4$ (12.5 cm^3 of a 1.0 $moldm^{-3}$ solution in dry THF, 12.50 mmol) and the resultant reaction mixture heated under reflux for 3 hours. After cooling, the solvent was removed under reduced pressure, and water (50 cm^3) was added drop wise. The aqueous layer was extracted with DCM (3 × 50 cm^3) and the combined organic extracts dried ($MgSO_4$), filtered and concentrated under reduced pressure to afford the amine **62** as a yellow oil (0.13 g, 34.6 %).

Method 2: To a solution of 4-methylaminomethyl-benzonitrile **68** (1.22 g, 8.35 mmol) in dry THF (30 cm^3) at 0 °C was added $LiAlH_4$ (40 cm^3 of a 1.0 $moldm^{-3}$ solution in dry diethylether, 40.00 mmol) and the resultant reaction mixture heated under reflux for 3 hours. After cooling, the solvent was removed under reduced pressure and water (50

cm^3) was added drop wise. The organic phase was extracted with DCM (3 × 50 cm^3) and dried ($MgSO_4$). The solvent was removed under reduced pressure to afford the amine **62** as a yellow oil (1.04 g, 83.0 %).

(Found: M^+, 150.1148. $C_9H_{14}N_2$ requires 150.1156). δ_H(300 MHz; C^2HCl_3) 36.05 (3H, s, CH_3), 3.71 and 3.82 (4H, 2 × s, $CH_2C_6H_4CH_2$) and 7.20-7.30 (4H, m, 4 × Ar-C*H*); δ_C(75 MHz; C^2HCl_3) 36.05 (CH_3), 46.22 and 55.79 (CH_2), 127.17 and 128.41 (Ar-*C*H), 138.72 and 142.07 (Ar-*C*); *m/z* (EI^+) 149 (28 %, $[M - H]^+$), 133 (20, $[M - NH_3]^+$) and 120 (100, $[M - CH_3NH]^+$).

4-(Benzylamino-methyl)-*N*-methyl-benzamide (90)

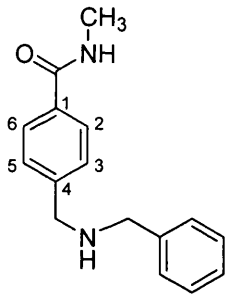

To a solution of amine hydrochloride **88** (0.15 g, 0.75 mmol) and triethylamine (0.76 g, 0.75 mmol) in methanol (25 cm^3) was added benzaldehyde (0.80 g, 0.75 mmol) under an argon atmosphere. After 5 hours stirring, a solution of $NaBH_4$ (0.14 g, 3.75 mmol) in methanol (20 cm^3) was added. The reaction mixture was stirred for 4 hours at room temperature and then the solution was concentrated. Water (50 cm^3) was added carefully and the organic phase was extracted with DCM (3 × 50 cm^3) and dried ($MgSO_4$). The solvent was removed under reduced pressure to afford the amide **90** as a yellow oil (0.10 g, 52.5 %). δ_H(300 MHz; C^2HCl_3) 2.87 (3H, d, *J* 4.7 Hz, CH_3), 3.71 and 3.74 (4H, 2 × s, 2 × Ar-CH_2), 7.16-7.34 (7H, m, Ar-C*H*) and 7.73 (2H, d, *J* 8.1 Hz, 2-ArC*H* and 6-ArC*H*); δ_C(75 MHz; C^2HCl_3) 26.72 (CH_3), 52.57 and 53.05 (2 × CH_2),

126.96, 127.06, 127.99, 128.05 and 128.35 (Ar-*C*H), 133.14, 139.13 and 143.69 (Ar-*C*) and 168.26 (CO); *m/z* (EI^+) 255 (100 %, $[M + H]^+$), 225 (10, $[M - CH_3NH + H]^+$), 163 (35, $[M - C_6H_4CH_2 - H]^+$) and 148 (30, $[M - C_6H_4CH_2NH - H]^+$).

[4-(Benzylamino-methyl)-benzyl]-methyl-amine (91)

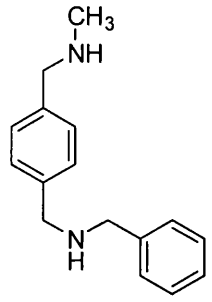

Method 1: To a solution of amide **90** (0.10 g, 0.39 mmol) in dry THF (10 cm^3) at 0 °C was added $LiAlH_4$ (1.95 cm^3 of a 1.0 $moldm^{-3}$ solution in dry THF, 1.95 mmol) and the solution heated under reflux for 3 hours. After cooling, the mixture was concentrated under reduced pressure, and then water (30 cm^3) was added dropwise. The aqueous layer was extracted with DCM (3 × 30 cm^3) and the combined organic layers dried ($MgSO_4$), filtered and concentrated under reduced pressure to afford the amine **91** as a yellow oil (0.03 g, 32.1 %).

Method 2: To a stirred solution of amine **62** (0.45 g, 3.00 mmol) in methanol (50 cm^3) was added benzaldehyde (0.32 g, 3.00 mmol). After 5 hours stirring, a solution of $NaBH_4$ (0.56 g, 15.00 mmol) in methanol (20 cm^3) was then added and the reaction mixture stirred for 4 hours, then concentrated under reduced pressure. Water (50 cm^3) was added carefully and the aqueous phase was extracted with DCM (3 × 50 cm^3). The combined DCM extracts were dried ($MgSO_4$), filtered and concentrated under reduced pressure to afford the diamine **91** as a yellow oil (0.67 g, 93.4 %)

(Found: $[M + H]^+$, 241.1702. $C_{16}H_{21}N_2$ requires 241.1704). δ_H(300 MHz; C^2HCl_3) 2.43 (3H, s, CH_3), 3.71, 3.78 and 3.79 (6H, 3 × s, ArCH_2NH$CH_2C_6H_4CH_2$) and 7.22-7.33 (9H, m, Ar-C*H*); δ_C(75 MHz; C^2HCl_3) 26.72 (CH_3), 52.75, 53.02 and 55.61 (CH_2), 126.82, 127.04, 128.05, 128.11 and 128.27 (Ar-*C*H) and 138.55, 138.92 and 140.17 (Ar-*C*); *m/z* (ES^+) 241 (100 %, $[M + H]^+$) and 210 (10, $[M - CH_3NH]^+$).

(4-Methylaminomethyl-benzyl)-naphthalen-2-ylmethyl-amine (50)

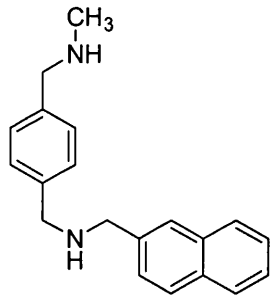

To a solution of the amine **62** (0.92 g, 6.10 mmol) in methanol (50 cm^3) was added 2-naphthaldehyde **63** (0.95 g, 6.10 mmol). After 5 hours stirring at room temperature, a solution of $NaBH_4$ (1.11 g, 30.00 mmol) in methanol (20 cm^3) was added and the reaction mixture was stirred for 4 hours and then concentrated under reduced pressure. Water (50 cm^3) was added carefully and the organic phase was extracted with DCM (3 × 50 cm^3) and dried ($MgSO_4$). The solvent was removed under reduced pressure to afford the diamine **50** as a yellow oil (1.30 g, 73.5 %), (Found: M^+, 290.1780. $C_{20}H_{22}N_2$ requires 290.1782). δ_H(300 MHz; C^2HCl_3) 2.43 (3H, s, CH_3), 3.72 and 3.81 (4H, 2 × s, $CH_2C_6H_4CH_2$), 3.94 (2H, s, Naph-CH_2) and 7.29-7.76 (11H, m, 11 × Ar-C*H*); δ_C(75 MHz; C^2HCl_3) 36.05 (CH_3), 52.96, 53.29 and 55.82 (CH_2), 125.56, 125.94, 126.02, 126.54, 126.67, 127.34, 127.43, 127.72, 127.94, 128.16 and 129.13 (Ar-*C*H) and 132.74, 133.61, 137.86, 138.78 and 139.08 (Ar-*C*); *m/z* (EI^+) 289 (36 %, $[M - H]^+$), 260 (9, $[M - (CH_3NH)]^+$), 170 (10, $[NaphCH_2NHCH_2]^+$) and 141 (100, $[NaphCH_2]^+$).

(4-{[(Anthracen-9-ylmethyl)-amino]-methyl}-benzyl)-methyl-amine (51)

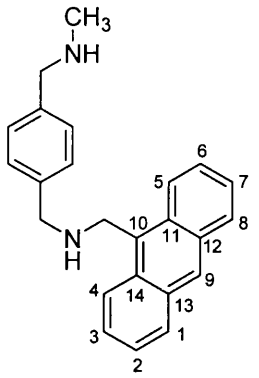

To a solution of amine **62** (0.65 g, 4.30 mmol) in methanol (50 cm^3) was added 9-anthraldehyde (0.89 g, 4.30 mmol). After 5 hours stirring, a solution of $NaBH_4$ (0.75 g, 20.00 mmol) in methanol (20 cm^3) was added. The reaction mixture was stirred for 4 hours at room temperature and then concentrated under reduced pressure. Water (50 cm^3) was added carefully and the aqueous layer was extracted with DCM (3 × 50 cm^3). The combined organic layers were dried ($MgSO_4$), filtered and concentrated under reduced pressure to afford the diamine **51** as a yellow-orange oil (0.86 g, 58.8 %), (Found: M^+, 340.1995. $C_{24}H_{24}N_2$ requires 340.1992). δ_H(300 MHz; C^2HCl_3) 2.47 (3H, s, CH_3), 3.77 and 4.02 (4H, 2 × s, $CH_2C_6H_4CH_2$), 4.68 (2H, s, Anth-CH_2), 7.25-7.51 (8H, m, 8 × Ar-C*H*), 7.99 (2H, d, *J* 7.5 Hz, 1-AnthC*H* and 8-AnthC*H*), 8.21 (2H, d, *J* 7.5 Hz, 4-AnthC*H* and 5-AnthC*H*), and 8.39 (1H, s, 1 × 9-AnthC*H*); δ_C(75 MHz; C^2HCl_3) 35.97 (CH_3), 44.92, 54.06 and 55.80 (CH_2), 124.18, 124.91, 126.01, 127.19, 127.82, 128.32, 128.42, 128.61, 129.11 and 129.25 (Ar-*C*H), 130.33, 131.54, 131.66, 138.88 and 139.12 (Ar-*C*); *m/z* (ES^+) 363 (100 %, $[M + Na]^+$), 341 (49, $[M + H]^+$) and 310 (47, $[M - CH_3NH]^+$).

(4-Methylaminomethyl-benzyl)-pyren-1-ylmethyl-amine (52)

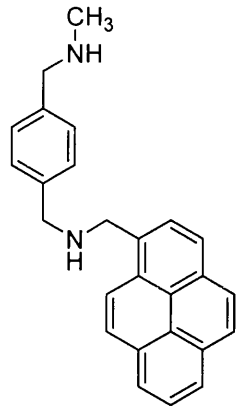

To a stirred solution of amine **62** (0.72 g, 4.80 mmol) in methanol (50 cm^3) was added 1- pyrenecarboxaldehyde (1.10 g, 4.80 mmol). After 5 hours stirring, a solution of $NaBH_4$ (0.94 g, 25.00 mmol) in methanol (20 cm^3) was added, and the reaction mixture was stirred for 4 hours at room temperature. The reaction mixture was concentrated under reduced pressure and water (50 cm^3) was added carefully. The aqueous phase was extracted with DCM (3 × 50 cm^3) and the combined DCM extracts were dried ($MgSO_4$), filtered and concentrated under reduced pressure to afford the diamine **52** as a yellow oil (1.57 g, 89.8 %), (Found: $[M+H]^+$, 365.1999. $C_{26}H_{25}N_2$ requires 365.2017). δ_H(300 MHz; C^2HCl_3) 2.44 (3H, s, CH_3), 3.73 and 3.91 (4H, 2 × s, $CH_2C_6H_4CH_2$), 4.44 (2H, s, Py-CH_2) and 7.23-8.09 (13H, m, 13 × Ar-C*H*); δ_C(75 MHz; C^2HCl_3) 36.07 (CH_3), 51.08, 53.51 and 55.85 (CH_2), 123.32, 124.69, 125.02, 125.09, 125.90, 127.09 and 128.34 (Ar-*C*H), 128.49, 129.16, 130.69, 130.86, 131.32, 133.86, 138.90 and 139.10 (Ar-*C*); *m/z* (ES^+) 365 (100 %, $[M+H]^+$) and 334 (43, $[M - CH_3NH]^+$).

2-*o*-Tolyl-[1,3,2] dioxaborinane (117)

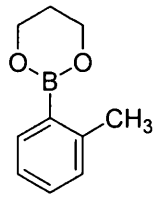

To a stirred solution of *o*-tolylboronic acid (2.50 g, 18.40 mmol) in toluene (70 cm^3) was added 1,3-propanediol (2.80 g, 36.80 mmol). The mixture was heated and stirred under Dean and Stark conditions for 1 hour. After cooling, the reaction mixture was washed with water (50 cm^3) and dried ($MgSO_4$). The solvent was removed under reduced pressure affording 2-*o*-tolyl-[1,3,2] dioxaborinane **117** as a dark yellow oil (2.97 g, 91.7 %). δ_H(400 MHz; C^2HCl_3) 2.04-2.05 (2H, m, $OCH_2CH_2CH_2O$), 2.55 (3H, s, CH_3), 4.19 (4H, t, *J* 5.4 Hz, $OCH_2CH_2CH_2O$), 7.16-7.20 (2H, m, 2 × Ar-C*H*), 7.29-7.31 (1H, m, 1 × Ar-C*H*) and 7.32-7.77 (1H, m, 1 × Ar-C*H*); δ_C(100MHz; C^2HCl_3) 22.45 (CH_3), 27.46 ($OCH_2CH_2CH_2O$), 61.85 ($OCH_2CH_2CH_2O$), 124.45, 129.79 and 134.58 (Ar-*C*H) and 143.72 (Ar-*C*); *m/z* (EI^+) 176 (100 %, M^+).

2-(2-Bromomethyl-phenyl)-[1,3,2] dioxaborinane (49)

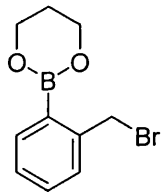

To a stirred solution of 2-*o*-tolyl-[1,3,2] dioxaborinane **117** (2.94 g, 16.70 mmol) in benzene (60 cm^3) was added *N*-bromosuccinimide (3.10 g, 17.60 mmol) and AIBN (0.30 g). The mixture was heated and stirred under reflux for 2 hours. The resulting mixture was then cooled on an ice-water-bath and the precipitate was removed by filtration. The filtrate solvent was removed under reduced pressure and the crude product was purified by silica gel chromatography eluting with n-hexane:chloroform

(1:5) to afford the dioxaborinane **49** as a yellow oil (2.55 g, 60.1 %), (Found: C, 47.1; H, 4.6. Calc. For $C_{10}H_{12}BBrO_2$: C, 47.1; H, 4.7 %). δ_H(400 MHz; C^2HCl_3) 2.06-2.52 (2H, m, $OCH_2CH_2CH_2O$), 4.19 (4H, t, *J* 5.4 Hz, $OCH_2CH_2CH_2O$), 4.92 (2H, s, CH_2Br), 7.25-7.92 (4H, m, 4 × Ar-C*H*); δ_C(100 MHz; C^2HCl_3) 27.27 (CH_2Br), 27.45 ($OCH_2CH_2CH_2O$), 62.08 ($OCH_2CH_2CH_2O$), 127.37, 129.98, 130.23 and 135.18 (Ar-*C*H) and 143.16 (Ar-*C*); *m/z* (EI^+) 253 (1.8 %, $[M - H]^+$ and 175 (96, $[M - Br]^+$).

*Note: All diboronic acid compounds (**39**, **43-48**, **95**, **104** and **111**) were submitted for elemental analysis. However, except for sensor **45** compounds gave much lower CHN compositions than expected. Boronic acids have long been known to give poor correlations between calculated and found compositions[103] which is probably due to the formation of incombustible residues. Accurate Mass measurements were also attempted but the lack of a molecular ion in the mass spectra due to the formation of adducts (H_2O, CH_3OH, protecting group) in solution also made this technique unsuitable.*

(4-{[Benzyl-(2-boronobenzyl)-amino]-methyl}-benzyl)-(2-boronobenzyl)-methyl-amine (95)

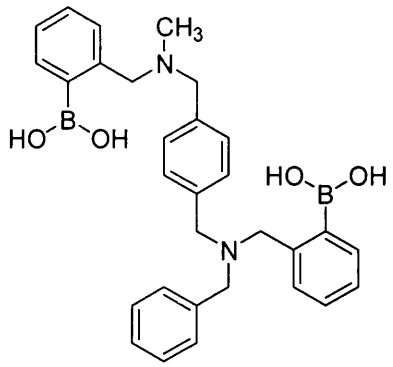

To a stirred solution of amine **91** (0.16 g, 0.67 mmol) in dry acetonitrile (30 cm^3) was added 2-(2-bromomethyl-phenyl)-[1,3,2]dioxaborinane **49** (0.51 g, 2.00 mmol), followed by K_2CO_3 (0.73 g, 5.33 mmol). The reaction mixture was then stirred and heated under reflux for 5 hours. After cooling, the acetonitrile was then removed under reduced pressure and water (50 cm^3) was added. The aqueous phase was extracted with DCM (3 × 50 cm^3) and the combined organic extracts were dried ($MgSO_4$). After filtration, the filtrate was concentrated until dryness to afford the crude product as a dark yellow solid. Recrystalisation from chloroform/hexane afforded the diamine **95** as a pale yellow powder (0.30 g, 88.1 %), mp 97-99 °C (decomp.). δ_H(300 MHz; C^2HCl_3/ $C^2H_3O^2H$ 1:1) 2.34 (3H, s, CH_3), 3.67, 3.68, 3.96, 4.00 (4H, s, 2 × Ar-C*H*$_2$ and 6H, 3 × s, 3 × Ar-C*H*$_2$) and 7.11-7.59 (17H, m, Ar-C*H*); δ_C(75 MHz; C_2HCl_3/ $C^2H_3O^2H$ 1:1) 42.29 (CH_3), 54.46, 58.37 and 63.17 (CH_2), 128.89, 129.01, 129.27, 129.32, 129.87, 129.99, 130.08, 130.11, 130.13, 130.25, 130.34, 130.97, 131.03, 131.62 and 131.76 (Ar-*C*H), 137.47, 137.67 and 143.14 (Ar-*C*); *m/z* (ES^+) 695 (100 %, [M - 2 × H_2O + 2 × $HO(CH_2)_3OH$ + CH_3OH + $K]^+$).

(2-Boronobenzyl)-(4-{[(2-boronobenzyl)-methyl amino] methyl}-benzyl)-naphthalen-2-ylmethyl-amine (43)

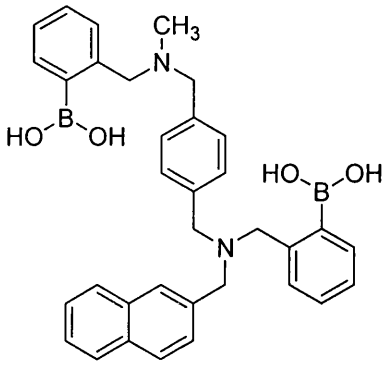

To a stirred solution of diamine **50** (0.58 g, 2.00 mmol) in 50 cm^3 of dry acetonitrile was added 2-(2-bromomethyl-phenyl)-[1,3,2]dioxaborinane **49** (1.52 g, 6.00 mmol), followed by K_2CO_3 (1.10 g, 8.00 mmol). The reaction mixture was heated and stirred under reflux for 5 hours. The acetonitrile was then removed under reduced pressure and water (50 cm^3) was added. The aqueous phase was extracted with DCM (3 × 50 cm^3) and the combined organic extracts were dried ($MgSO_4$). After filtration, the solvent was removed under reduced pressure to afford the crude product as a dark yellow solid. Recrystallisatiom from $CHCl_3$/ hexane afforded the boronic acid diamine **43** as a pale yellow powder (0.92 g, 82.4 %), mp 134-136 °C (decomp.). δ_H(300 MHz; C^2HCl_3/ $C^2H_3O^2H$ 1:1) 2.13 (3H, s, CH_3), 3.42, 3.47, 3.49 and 3.52 (8H, 4 × s, 4 × $C_6H_4CH_2$), 3.60 (2H, s, Naph-CH_2) and 7.06-7.60 (19H, m, 19 × Ar-C*H*); δ_C(75 MHz; C^2HCl_3/ $C^2H_3O^2H$ 1:1) 39.56 (CH_3), 56.60, 56.82, 57.92, 58.19 and 65.69 (CH_2), 125.51, 125.59, 126.45, 126.81, 127.07, 127.13, 127.25, 127.56, 127.85, 128.33, 128.97, 129.58, 130.50, 132.45, 132.49 and 132.85 (Ar-*C*H) and 138.78, 141.03 and 142.94 (Ar-*C*); *m/z* (ES^+) 633 (40 %, $[M - 3 \times H_2O + 4 \times CH_3OH + H]^+$ and 619 (100, $[M - 2 \times H_2O + 3 \times CH_3OH + H]^+$).

Anthracen-9-ylmethyl-(2-boronobenzyl)-(4-{[(2-boronobenzyl)methyl-amino] methyl} -benzyl)-amine (44)

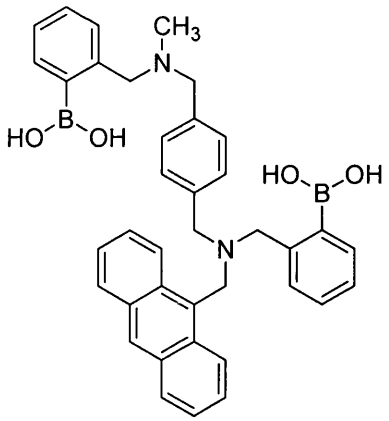

To a stirred solution of diamine **51** (0.34 g, 1.00 mmol) in dry acetonitrile (40 cm^3) was added 2-(2-bromomethyl-phenyl)-[1,3,2]dioxaborinane **49** (0.76 g, 3.00 mmol), followed by K_2CO_3 (0.55 g, 4.00 mmol). The reaction mixture was then heated and stirred under reflux for 5 hours. The acetonitrile was removed under reduced pressure and water (50 cm^3) was added. The aqueous phase was extracted with DCM (3 × 50 cm^3) and the combined organic extracts were dried ($MgSO_4$), filtered and removed under reduced pressure to afford the crude product as a yellow-orange solid. Recrystalisation from chloroform/hexane afforded the boronic acid diamine **44** as a pale yellow powder (0.49 g, 80.5 %), mp 154-155 °C (decomp.). δ_H(300 MHz; C^2HCl_3/ $C^2H_3O^2H$ 1:1) 2.06 (3H, s, CH_3), 3.49, 3.58 and 3.74 (4H, 2 × s, 2 × $C_6H_4CH_2$ and 4H, s, 2 × $C_6H_4CH_2$), 4.47 (2H, s, Anth-CH_2) and 7.05-8.37 (21H, m, 21 × Ar-C*H*); δ_C(125 MHz; C^2HCl_3/ $C^2H_3O^2H$ 1:1) 40.21 (CH_3), 59.18, 59.44 and 59,77 (CH_2), 124.55, 124.68, 124.82, 124.93 (Ar-*C*H) and 131.21 and 131.49 (Ar-*C*); *m/z* (ES^+) 727 (46 %, $[M - 4 \times H_2O + 2 \times HO(CH_2)_3OH + K]^+$) and 799 (92 %, $[M + 2 \times HO(CH_2)_3OH + K]^+$).

(2-Boronobenzyl)-(4-{[(2-boronobenzyl)-methyl-amino]-methyl}-benzyl)-pyren-1-ylmethyl-amine (45)

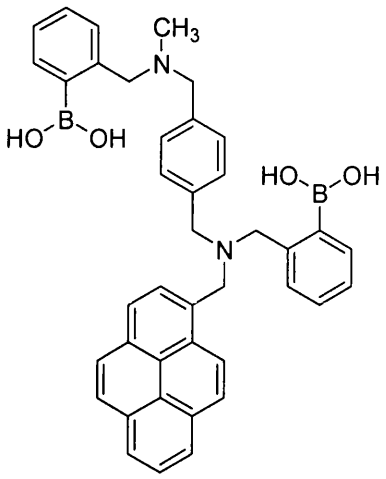

45

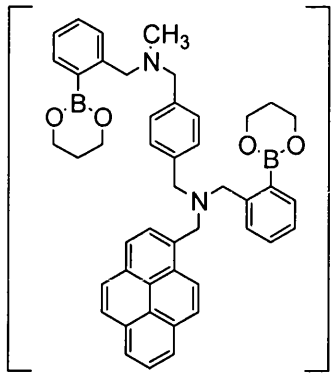

45a

To a stirred solution of diamine **52** (0.72 g, 2.00 mmol) in dry acetonitrile (40 cm^3) was added 2-(2-bromomethyl-phenyl)-[1,3,2]dioxaborinane **49** (1.52 g, 6.00 mmol) , followed by K_2CO_3 (1.10 g, 8.00 mmol). The reaction mixture was then stirred and heated under reflux for 5 hours. The acetonitrile was removed under reduced pressure and water (50 cm^3) was added. The aqueous phase was extracted with DCM (3 × 50 cm^3) and the combined organic extracts were dried ($MgSO_4$). After filtration, the filtrate were concentrated under reduced pressure to afford the crude product as a dark yellow solid. Recrystalisation from chloroform/hexane afforded the boronic acid diamine **45** as a pale yellow powder (1.04 g, 82.3 %), mp 174-175 °C (decomp.), (Found: C, 77.3; H, 6.2; N, 3.9. Calc. For $C_{46}H_{46}B_2N_2O_4$ (protected compound **45a**): C, 77.5; H, 6.5; N, 3.9 %). δ_H(300 MHz; C^2HCl_3/ $C^2H_3O^2H$ 1:1) 1.79 (3H, s, CH_3), 3.25, 3.46 and 3.63 (4H, 2 × s, $CH_2C_6H_4CH_2$ and 4H, s, 2 × $C_6H_4CH_2$), 4.05 (2H, s, Py-CH_2) and 6.74-7.93 (21H, m, 21 × Ar-C*H*); δ_C(125 MHz; C^2HCl_3/ $C^2H_3O^2H$ 1:1) 40.19 (CH_3), 52.95, 54.89, 57.86, 57.99 and 59.49 (CH_2), 123.14, 124.25, 124.72, 125.07,

125.78, 127.21 and 127.28 (Ar-*C*H) and 130.57, 131.05 and 131.13 (Ar-*C*); *m/z* (ES^+) 711 (100 %, $[M - 4 \times H_2O + 4 \times CH_3OH + Na]^+$).

3-Methylaminomethyl-benzonitrile (102)

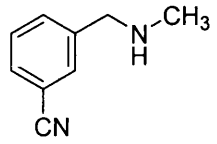

Methylamine (60 cm^3 of a 2.0 $moldm^{-3}$ solution in CH_3OH, 120 mmol) was added under an argon atmosphere to a solution of 3-cyanobenzaldehyde **100** (2.62 g, 20.00 mmol) in methanol CH_3OH (30 cm^3). After 5 hours stirring at room temperature, the reaction was complete as judged by TLC. A solution of $NaBH_4$ (3.78 g, 100 mmol) in methanol (30 cm^3) was then added in one portion, the reaction mixture stirred for 4 hours at room temperature and then concentrated under reduced pressure. Water (50 cm^3) was then added and the aqueous layer was extracted with DCM (3 × 50 cm^3). The combined organic extracts were dried ($MgSO_4$), filtered and concentrated under reduced pressure to afford the amine **102** as a yellow oil (2.69 g, 92.1 %), (Found: M^+, 146.0837. $C_9H_{10}N_2$ requires 146.0843); υ_{max} ($CHCl_3$)/cm^{-1} 2232 (CN nitrile). δ_H(270 MHz; C^2HCl_3) 2.38 (3H, s, CH_3), 3.72 (2H, s, CH_2) and 7.34-7.57 (4H, m, 4 × Ar-C*H*); δ_C(67.5 MHz; C^2HCl_3) 35.86 (CH_3), 55.92 (CH_2), 112.03 (*C*-CN), 118.64 (Ar-*C*), 128.81, 130.30, 131.24 and 132.26 (Ar-*C*H) and 141.50 (CN); *m/z* (EI^+) 145 (77 %, $[M - H]^+$), 116 (49, $[M - CH_3NH]^+$) and 44 (100, $[CH_3NHCH_2]^+$).

3-Methylaminomethyl-benzylamine (96)

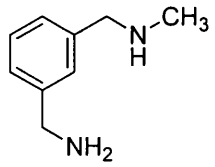

To a solution of 3-methylaminomethyl-benzonitrile **100** (0.73 g, 5.00 mmol) in dry THF (30 cm^3) at 0 °C was added $LiAlH_4$ (25.0 cm^3 of a 1.0 $moldm^{-3}$ solution in dry diethylether, 25.00 mmol) and the resultant reaction mixture heated under reflux for 3 hours. After cooling, the solvent was removed under reduced pressure and water (50 cm^3) was added drop wise. The aqueous phase was extracted with DCM (3 × 50 cm^3) and dried ($MgSO_4$). The solvent was removed under reduced pressure, to afford the amine **96** as a yellow oil (0.59 g, 79.0 %), (Found: M^+, 150.1147. $C_9H_{14}N_2$ requires 150.1156). δ_H(270 MHz; C^2HCl_3) 2.45 (3H, s, CH_3), 3.74 and 3.85 (2H, s, CH_2NH and 2H, s, CH_2NH_2) and 7.18-7.38 (4H, m, 4 × Ar-C*H*); δ_C(100 MHz; C^2HCl_3) 36.00 (CH_3), 46.35 and 55.92 (CH_2), 125.54, 126.45, 126.69 and 128.35 (Ar-*C*H), 140.06 and 143.15 (Ar-*C*); *m/z* (EI^+) 149 (34 %, $[M - H]^+$), 133 (90, $[M - NH_3]^+$) and 120 (100, $[M - CH_3NH]^+$).

[3-Benzylamino]-methyl)-benzyl]-methyl-amine (103)

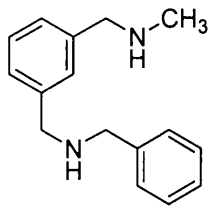

To a stirred solution of amine **96** (0.45 g, 3.00 mmol) in methanol (30 cm^3) was added benzaldehyde (0.32 g, 3.00 mmol). After 5 hours stirring, a solution of $NaBH_4$ (0.56 g, 15.00 mmol) in methanol (20 cm^3) was then added and the reaction mixture was stirred for 4 hours, then concentrated under reduced pressure. Water (50 cm^3) was added carefully and the aqueous phase extracted with DCM (3 × 50 cm^3). The combined DCM extracts were dried ($MgSO_4$), filtered and concentrated under reduced pressure to afford the diamine **103** as a yellow oil (0.51 g, 70.8 %), (Found: $[M + H]^+$, 241.1709. $C_{16}H_{21}N_2$ requires 241.1704). δ_H(300 MHz; C^2HCl_3) 2.45 (3H, s, CH_3), 3.73, 3.79 and 3.80 (6H, 3 × s, $ArCH_2NHCH_2C_6H_4CH_2$) and 7.18-7.33 (9H, m, 9 × Ar-C*H*); δ_C(75 MHz; C^2HCl_3) 36.45 (CH_3), 53.55, 53.67 and 56.41 (CH_2), 120.72, 126.83, 127.85, 128.08, 128.29 and 128.32 (Ar-C*H*), 140.63, 140.68 and 140.86 (Ar-*C*); *m/z* (ES^+) 241 (76 %, $[M + H]^+$) and 210 (100, $[M - CH_3NH]^+$)

Methyl-(3-{[(naphthalene-2ylmethyl)amino]-methyl}-benzyl)-amine (97)

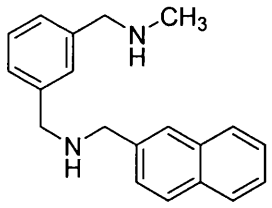

To a stirred solution of amine **96** (0.45 g, 3.00 mmol) in methanol (50 cm^3) was added 2-naphthaldehyde (0.47 g, 3.00 mmol) **63**. After 5 hours stirring, a solution of $NaBH_4$ (0.56 g, 15.00 mmol) in methanol (20 cm^3) was then added and the reaction mixture stirred for 4 hours, then concentrated under reduced pressure. Water (50 cm^3) was added carefully and the aqueous phase was extracted with DCM (3 × 50 cm^3). The combined DCM extracts were dried ($MgSO_4$), filtered and concentrated under reduced pressure to afford the diamine **97** as a yellow oil (0.75 g, 85.9 %), (Found: $[M + H]^+$, 291.1863. $C_{20}H_{23}N_2$ requires 291.1861). δ_H(270 MHz; C^2HCl_3) 2.40 (3H, s, CH_3), 3.69 and 3.79 (4H, 2 × s, 2 × $C_6H_4CH_2$), 3.92 (2H, s, Naph-CH_2) and 7.14-7.79 (11H, m, 11 × Ar-C*H*); δ_C(100 MHz; C^2HCl_3) 36.34 (CH_3), 53.52, 53.72 and 56.26 (CH_2), 125.75, 126.19, 126.72, 126.82, 127.11, 127.14, 127.85, 127.89, 128.25, 128.26 and 128.69 (Ar-*C*H), 132.87, 133.64, 137.93, 140.21, and 140.63 (Ar-*C*); *m/z* (ES^+) 291 (100 %, $[M + H]^+$).

(3-{[(Anthracen-9-ylmethyl)-amino]-methyl}-benzyl)-methyl-amine (98)

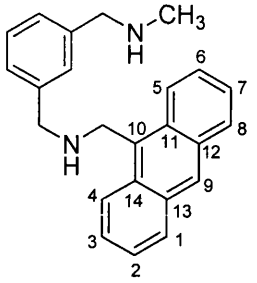

To a stirred solution of amine **96** (0.45 g, 3.00 mmol) in methanol (50 cm^3) was added 9-anthraldehyde (0.61 g, 3.00 mmol) **64**. After 5 hours stirring, a solution of $NaBH_4$ (0.56 g, 15.00 mmol) in methanol (20 cm^3) was added and the reaction mixture was stirred for 4 hours and then concentrated under reduced pressure. Water (50 cm^3) was added carefully and the aqueous phase was extracted with DCM (3 × 50 cm^3). The combined DCM extracts were dried ($MgSO_4$), filtered and concentrated under reduced pressure to afford the diamine **98** as a yellow-orange oil (0.94 g, 92.2 %), (Found: $[M + H]^+$, 341.2010. $C_{24}H_{25}N_2$ requires 341.2017). δ_H(400 MHz; C^2HCl_3) 2.46 (3H, s, CH_3), 3.77 and 4.02 (4H, 2 × s, 2 × $C_6H_4CH_2$), 4.69 (2H, s, AnthCH_2), 7.33-7.51 (8H, m, 8 × Ar-C*H*), 7.99 (2H, d, *J* 8.0 Hz, 1-AnthC*H* and 8-AnthC*H*), 8.22 (2H, d, *J* 8.0 Hz, 4-AnthC*H* and 5-AnthC*H*) and 8.39 (1H, s, 9-AnthC*H*); δ_C(100 MHz; C^2HCl_3) 36.04 (CH_3), 45.00, 54.28 and 56.00 (CH_2), 124.06, 124.76, 125.87, 126.86, 126.92, 127.06, 128.02, 128.37 and 128.97 (Ar-*C*H), 130.18, 131.39, 131.48, 140.02, and 140.37 (Ar-*C*); *m/z* (ES^+) 341 (100 %, $[M + H]^+$).

Methyl-(3-{[(pyren-1-ylmethyl)-amino]-methyl}-benzyl)-amine (99)

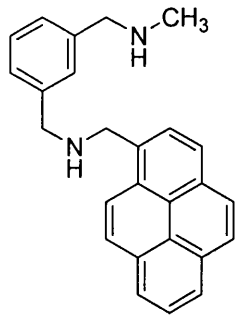

To a stirred solution of amine **96** (0.45 g, 3.00 mmol) in methanol (50 cm^3) was added 1- pyrenecarboxaldehyde (0.69 g, 3.00 mmol) **65**. After 5 hours stirring, a solution of $NaBH_4$ (0.55 g, 15.00 mmol) in methanol (20 cm^3) was added. The reaction mixture was stirred for 4 hours and then concentrated under reduced pressure. Water (50 cm^3) was added carefully and the aqueous phase was extracted with DCM (3 × 50 cm^3). The combined DCM extracts were dried ($MgSO_4$), filtered and concentrated under reduced pressure to afford the diamine **99** as a yellow oil (0.85 g, 77.8 %), (Found: $[M + H]^+$, 365.2008. $C_{26}H_{25}N_2$ requires 365.2017). δ_H(400 MHz; C^2HCl_3) 2.46 (3H, s, CH_3), 3.76 and 3.96 (4H, 2 × s, 2 × $CH_2C_6H_4CH_2$), 4.47 (2H, s, Py-CH_2) and 7.20-8.31 (13H, m, 13 × Ar-C*H*); δ_C(100 MHz; C^2HCl_3) 35.91 (CH_3), 51.07, 53.67 and 55.85 (CH_2), 123.08, 124.47, 124.78, 124.86, 125.67, 126.77, 126.83, 126.86, 127.25, 127.33, 127.93 and 128.31 (Ar-*C*H), 128.93, 130.46, 130.63, 131.10, 133.58, 139.76 and 140.31 (Ar-*C*); *m/z* (ES^+) 365 (100 %, $[M + H]^+$) and 334 (43, $[M - CH_3NH]^+$).

(3-{[Boronobenzyl)-amino]-methyl}-benzyl)-(2-boronobenzyl)- methyl-amine (104)

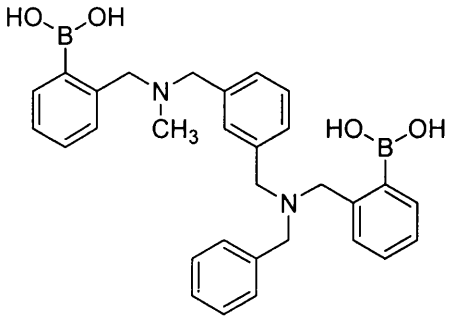

To a stirred solution of diamine **103** (0.20 g, 0.83 mmol) in dry acetonitrile (30 cm^3) was added 2-(2-bromomethyl-phenyl)-[1,3,2]dioxaborinane **49** (0.51 g, 2.00 mmol), followed by K_2CO_3 (0.73 g, 5.33 mmol). The reaction mixture was stirred and heated under reflux for 5 hours. After cooling, the acetonitrile was removed under reduced pressure and water (50 cm^3) was added. The aqueous phase was extracted with DCM (3 × 50 cm^3) and the combined organic extracts were dried ($MgSO_4$), filtered, and concentrated until dryness to afford the crude product as a dark yellow oil. Recrystalisation from chloroform/hexane afforded the diamine **104** as a pale yellow powder (0.27 g, 64.0 %), mp 139-140 °C (decomp.). δ_H(300 MHz; C^2HCl_3/ $C^2H_3O^2H$ 1:1) 2.13 (3H, s, CH_3), 3.61, 3.62, 3.63 and 3.65 (6H, 3 × s, 3 × ArCH_2 and 4H, s, 2 × ArCH_2) and 6.67-7.79 (17H, m, 17 × Ar-C*H*); δ_C(75 MHz; C^2HCl_3/ $C^2H_3O^2H$ 1:1) 36.11 (CH_3), 61.64, 68.99 and 74.73 (CH_2), 129.39, 129.50, 129.99 and 130.10 (Ar-*C*H) and 140.32 (Ar-*C*); *m/z* (ES^+) 605 (100 %, $[M - 3 \times H_2O + 2 \times HO(CH_2)_3OH - H]^+$).

(2-Boronobenzyl)-(3-{[(2-boronobenzyl)naphthalen-2-ylmethyl-amino]-methyl}-benzyl)-methyl-amine (46)

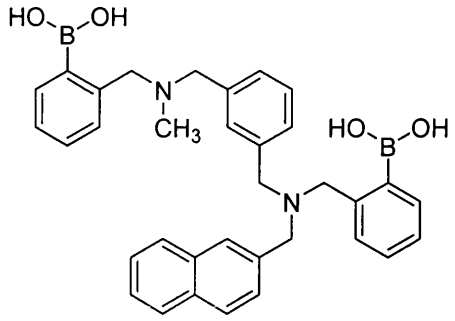

To a stirred solution of diamine **97** (0.58 g, 2.00 mmol) in dry acetonitrile (40 cm^3) was added 2-(2-bromomethyl-phenyl)-[1,3,2]dioxaborinane **49** (1.52 g, 6.00 mmol), followed by K_2CO_3 (1.10 g, 8.00 mmol). The reaction mixture was then stirred and heated under reflux for 5 hours. After cooling, the acetonitrile was removed under reduced pressure and water (50 cm^3) was added. The aqueous phase was extracted with DCM (3 × 50 cm^3) and the combined organic extracts were dried ($MgSO_4$). After filtration, they were concentrated until dryness to afford the crude product as a dark yellow solid. Recrystalisation from chloroform/hexane afforded the diamine **46** as a pale yellow powder (0.95 g, 85.1 %), mp 147-150 °C (decomp.). δ_H(300 MHz; C^2HCl_3/ $C^2H_3O^2H$ 1:1) 2.28 (3H, s, CH_3), 3.80, 3.83, 3.87 and 3.92 (8H, 4 × s, 4 × $C_6H_4CH_2$), 4.56 (2H, s, Naph-CH_2), and 7.06-7.81 (19H, m, 19 × Ar-C*H*); δ_C(75 MHz; C^2HCl_3/ $C^2H_3O^2H$ 1:1) 40.61 (CH_3), 57.13, 58.11, 60.63 and 66.44 (CH_2), 124.57, 125.08, 125.24, 126.04, 126.15, 126.31, 126.66, 126.84, 126.96, 127.03, 127.26, 127.37, 127.97, 128.10, 128.42 and 132.22 (Ar-*C*H) and 136.50 and 137.40 (Ar-*C*); *m/z* (ES^+) 615 (30 %, $[M - 4 \times H_2O + 4 \times CH_3OH + H]^+$) and 777 (100 %, $[M - 2 \times H_2O + 2 \times HO(CH_2)_3OH + 2 \times CH_3OH + K]^+$).

(3-{[Anthracen-9-ylmethyl-(2-boronobenzyl)-amino]-methyl}-benzyl)-(2-borono benzyl)-methyl-amine (47)

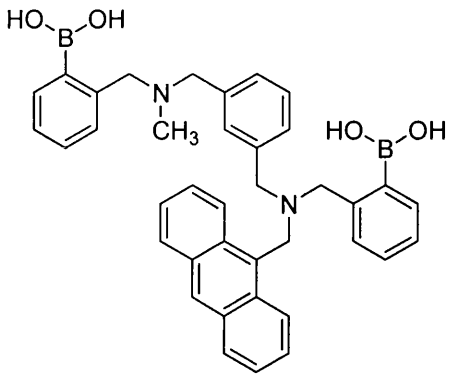

To a stirred solution of diamine **98** (0.68 g, 2.00 mmol) in dry acetonitrile (40 cm^3) was added 2-(2-bromomethyl-phenyl)-[1,3,2]dioxaborinane **49** (1.52 g, 6.00 mmol) , followed by K_2CO_3 (1.10 g, 8.00 mmol). The reaction mixture was then stirred and heated under reflux for 5 hours. After cooling, the acetonitrile was removed under reduced pressure and water (50 cm^3) was added. The aqueous phase was extracted with DCM (3 × 50 cm^3) and the combined organic extracts were dried ($MgSO_4$). After filtration, the filtrate was concentrated until dryness to afford the crude product as a dark yellow solid. Recrystalisation from chloroform/hexane afforded the diamine boronic acid **47** as a pale yellow powder (1.11 g, 91.3 %), mp 179-180 °C (decomp.). δ_H(300 MHz; C^2HCl_3/ $C^2H_3O^2H$ 1:1) 2.21 (3H, s, CH_3), 3.66, 3.68, 3.70 and 3.73 (8H, 4 × s, 4 × $C_6H_4CH_2$), 4.57 (2H, s, Anth-CH_2) and 6.99-8.38 (21H, m, 21 × Ar-C*H*); *m/z* (ES^+) 665 (50 %, $[M - 4 \times H_2O + 4 \times CH_3OH + H]^+$).

(2-Boronobenzyl)-(3-{[(2-boronobenzyl)-pyren-1-yl methyl-amino]-methyl}-benzyl) -methyl-amine (48)

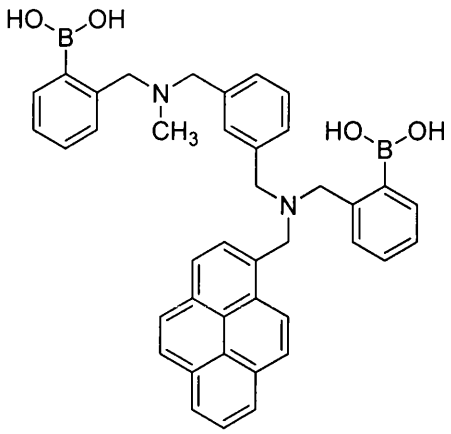

To a stirred solution of diamine **99** (0.72 g, 2.00 mmol) in dry acetonitrile (40 cm^3) was added 2-(2-bromomethyl-phenyl)-[1,3,2]dioxaborinane **49** (1.52 g, 6.00 mmol), followed by K_2CO_3 (1.10 g, 8.00 mmol). The reaction mixture was then stirred and heated under reflux for 5 hours. After cooling, the acetonitrile was removed under reduced pressure and water (50 cm^3) was added. The aqueous phase was extracted with DCM (3 × 50 cm^3) and the combined organic extracts were dried ($MgSO_4$). After filtration, the filtrate was concentrated until dryness to afford the crude product as a dark yellow solid. Recrystalisation from chloroform/hexane afforded the diamine boronic acid **48** as a pale yellow powder (0.99 g, 78.3 %), mp 173-174 °C (decomp.). δ_H(300 MHz; C^2HCl_3/ $C^2H_3O^2H$ 1:1) 2.18 (3H, s, CH_3), 3.69, 3.72, 3.82 and 3.85 (8H, 4 × s, 4 × $C_6H_4CH_2$), 4.30 (2H, s, Py-CH_2) and 6.70-8.30 (21H, m, 21 × Ar-C*H*); *m/z* (ES^+) 837 (90 %, $[M - H_2O + 2 \times HO(CH_2)_3OH + CH_3OH + K]^+$) and 851 (100 %, $[M - 2 \times H_2O + 2 \times HO(CH_2)_3OH + 2 \times CH_3OH + K]^+$).

9,10-Bis[(methylamino)methyl]anthracene (107)

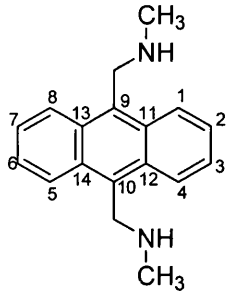

Methylamine (7.5 cm^3 of a 2.0 $moldm^{-3}$ solution in methanol, 15.00 mmol) was added under argon atmosphere to a solution of 9,10-dialdehyde anthracene **105** (1.17 g, 5.00 mmol) in methanol (20 cm^3) a stirred round-bottomed flask at room temperature. After stirring overnight, a solution of sodium borohydride (0.93 g, 25.00 mmol) in dry methanol (10 cm^3) was added in one portion and the reaction mixture was stirred for 4 hours before being poured onto 50 cm^3 of water. The aqueous layer was extracted with dichloromethane (3 x 50 cm^3). The combined organic extracts were dried ($MgSO_4$), filtered, and concentrated under reduced pressure to give the diamine **107** as a yellow-orange powder (1.10 g, 83.2 %), mp 139-140°C. δ_H(300 MHz, C^2HCl_3) 2.58 (6H, s, 2 × CH_3), 4.70 (4H, s, 2 × CH_2), 7.59 (4H, dd, $J_{2,1}$ 6.9 Hz, $J_{2,4}$ 3.3 Hz, 2-Anth*CH*, 3-Anth*CH*, 6-Anth*CH*, 7-Anth*CH*) and 8.41 (4H, dd, $J_{1,2}$ 6.9 Hz, $J_{1,3}$ 3.3 Hz, 1-Anth*CH*, 4-Anth*CH*, 5-Anth*CH*, 8-Anth*CH*); δ_C(75 MHz, C^2HCl_3) 37.20 (2 × CH_3), 48.05 (2 × CH_2), 124.87 (2-Anth*C*H, 3-Anth*C*H, 6-Anth*C*H, 7-Anth*C*H), 125.72 (1-Anth*C*H, 4-Anth*C*H, 5-Anth*C*H, 8-Anth*C*H), 130.17 and 131.97 (11-Anth*C*, 12-Anth*C*, 13-Anth*C*, 14-Anth*C* and 9-Anth*C*, 10-Anth*C*); *m/z* (FAB^+) 265 (32 %, $[M + H]^+$) and 234 (100, $[M - CH_3NH]^+$).

9,10-Bis[[*N*-methyl-*N*-(o-boronobenzyl)amino]methyl]anthracene (39)

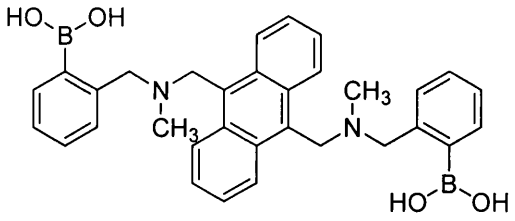

To a stirred solution of diamine **107** (0.53 g, 2.00 mmol) in 50 cm^3 of dry acetonitrile was added the benzyl bromide **49** (1.52 g, 6.00 mmol), followed by K_2CO_3 (1.10 g, 8.00 mmol). The reaction mixture was then allowed to stir under reflux overnight. The acetonitrile was removed under reduced pressure and water (50 cm^3) was added. The aqueous layer was then extracted with dichloromethane (3 x 50 cm^3) and the organic layers were combined, dried ($MgSO_4$) and then concentrated under reduced pressure to afford crude **39**. The crude material was purified by trituration with ethyl acetate to give **39** as a yellow orange powder (0.30 g, 28.2 %), mp 188-190°C (decomp.). δ_H(300 MHz; C^2HCl_3/ $C^2H_3O^2H$ 1:1) 2.19 (6H, 2 × s, 2 × NCH_3), 3.90 and 4.46 (2H, s, 2 × Ar-CH_2 and 2H, s, 2 × Anth-CH_2), 7.28-8.38 (16H, m, Ar-C*H*); *m/z* (FAB^+) 645 (24 %, [M – 4 × H_2O + 2 × glycerol + H]$^+$) and 205 (100, [$CH_2AnthCH_2$ + H]$^+$).

Methyl-(4-methylaminomethyl-benzyl)-amine (110)

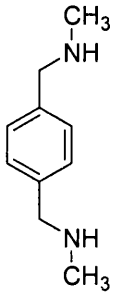

Methylamine (30 cm^3 of a 2.0 $moldm^{-3}$ solution in CH_3OH, 60.00 mmol) was added under an argon atmosphere to a solution of benzene-1,4-dicarbaldehyde **108** (0.67 g, 5.00 mmol) in methanol (10 cm^3). After 5 hours stirring at room temperature, the reaction was complete as deduced by TLC. A solution of $NaBH_4$ (0.94 g, 25.00 mmol) in methanol (30 cm^3) was then added in one portion and the reaction mixture was stirred for 4 hours. The solvent was concentrated under reduced pressure and then water (50 cm^3) was added and the aqueous layer extracted with DCM (3 × 50 cm^3). The combined organic extracts were dried ($MgSO_4$), filtered and concentrated under reduced pressure to afford the amine **110** as a yellow oil (0.71 g, 86.6 %), (Found: M^+, 164.1304. $C_{10}H_{16}N_2$ requires 164.1313). δ_H(270 MHz; C^2HCl_3) 2.42 (6H, s, 2 × CH_3), 3.70 (4H, s, $CH_2C_6H_4CH_2$) and 7.26 (4H, s, 4 × Ar-C*H*); δ_C(67.5 MHz; C^2HCl_3) 35.63 (2 × CH_3), 55.4 (2 × CH_2), 127.80 (4 × Ar-*C*H) and 138.49 (2 × Ar-*C*); *m/z* (EI^+) 164 (79 %, M^+) and 120 (100, $[M - (CH_3NHCH_2)]^+$).

(2-boronobenzyl)-4-{[(2-boronobenzyl)-methylamino]-methyl}-benzyl)-methyl-amine (111)

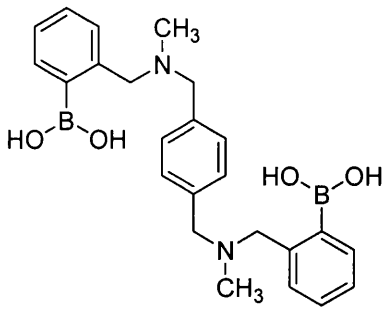

To a stirred solution of diamine **110** (0.32 g, 2.00 mmol) in dry acetonitrile (50 cm^3) was added 2-(2-bromomethyl-phenyl)-[1,3,2]dioxaborinane **49** (1.52 g, 6.00 mmol), followed by K_2CO_3 (1.10 g, 8.00 mmol). The reaction mixture was then stirred and heated under reflux for 5 hours. The acetonitrile was removed under reduced pressure and water (50 cm^3) was added. The aqueous phase was extracted with DCM (3 × 50 cm^3) and the combined organic extracts were dried ($MgSO_4$). After filtration, the filtrate was concentrated until dryness to afford the crude product as a dark yellow solid. Recrystalisation from chloroform/hexane afforded the diamine **111** as a pale yellow powder (0.69 g, 79.8 %), mp 193-194 °C (decomp.). δ_H(300 MHz; C^2HCl_3/ $C^2H_3O^2H$ 1:1) 2.35 (6H, s, 2 × CH_3), 3.90 and 3.99 (4H, s, 2 × $C_6H_4CH_2$ and 4H, s, 2 × $C_6H_4CH_2$) and 7.12-7.62 (12H, s, 12 × Ar-C*H*); δ_C(75 MHz; C^2HCl_3/ $C^2H_3O^2H$ 1:1) 41.92 (CH_3), 60.44 and 63.34 (CH_2), 129.87 and 134.08 (Ar-*C*H); *m/z* (ES^+) 511 (60 %, [M - 4 × H_2O + 4 × CH_3OH + Na]$^+$) and 651 (100 %, [M - 2 × H_2O + 2 × $HO(CH_2)_3OH$ + 2 × CH_3OH + K]$^+$).

IV-3 Fluorescence and CD measurements

IV-3.1 Fluorescence Measurements

The fluorescence spectra of **43** (5×10^{-6} moldm^{-3}), **44** (1×10^{-7} moldm^{-3}), **45** (1×10^{-7} moldm^{-3}), **46** (5×10^{-6} moldm^{-3}), **47** (1×10^{-7} moldm^{-3}) and **48** (1×10^{-7} moldm^{-3}) in a pH 8.21 buffer [0.01000 mol dm^{-3} KCl, 0.002752 mol dm^{-3} KH_2PO_4 and 0.002757 mol dm^{-3} Na_2HPO_4, in 52.1 % methanol- 47.9 % water (w/w)[99] were recorded as increasing amounts of various saccharides (D-glucose **112**, D-galactose **113**, D-mannose **114** and D-fructose **115**) were added to the solution.

IV-3.2 CD Measurements

The CD spectra of **43** (1×10^{-3} moldm^{-3}), **44** (1×10^{-3} moldm^{-3}), **45** (1×10^{-3} moldm^{-3}), **46** (1×10^{-3} moldm^{-3}), **47** (1×10^{-3} moldm^{-3}) and **48** (1×10^{-3} moldm^{-3}) in a 90 % methanol- 10 % water (v/v)] were recorded in presence of D-glucose (1×10^{-2} moldm^{-3}), L-glucose (1×10^{-2} moldm^{-3}), D-mannose (1×10^{-2} moldm^{-3}) and D-fructose (1×10^{-2} moldm^{-3}).

V References

1. Czarnik, A. W. *Fluorescent Chemosensors for Ion and Molecule Recognition*; American Chemical Society: Washington, **1993**.
2. Yasuda, H.; Kurokawa, T.; Fuji, Y.; Yamashita, A.; Ishibashi, S. *Biochim. Biophys. Acta.* **1990,** *1021*, 114.
3. Feodak, R. N.; Gershon, M. D.; Field, M. *Gasteroenterology* **1989,** *96*, 37.
4. Baxter, P.; Goldhill, J.; Hardcastle, P. T.; Taylor, C. J. *Gut.* **1990,** *31*, 817.
5. De Marchi, S.; et al. *J. Nephrol.* **1984,** *4*, 280.
6. Elsaa, L. J.; Rosenberg, L. E. *J. Clinic. Invest.* **1969**, 48.
7. Yamamoto, T.; et al. *Biochem. Biophys. Res. Commun.* **1990,** *170*, 223.
8. D'Auria, S.; Lakowicz, J. R. *Curr. Opin. Biotechnol.* **2001,** *12*, 99.
9. Chang, M. S.; Shih, J. S. *Sens. Actuator B-Chem.* **2000,** *67*, 275.
10. Bridge, K. A.; Higson, S. P. J. *Electroanalysis* **2001,** *13*, 191.
11. Sugawara, K.; Fukushi, H.; Hoshi, S.; Akatsuka, K. *Anal. Sci.* **2000,** *16*, 1139.
12. Davis, A. P.; Wareham, R. S. *Angew. Chem., Int. Ed. Engl.* **1999**, 38.
13. Turner, A. P. F.; Chen, B.; Piletsky, S. A. *Clin. Chem.* **1999,** *45*, 1596.
14. Turner, A. P. F. *Biosensors & Bioelectronics*; Elsevier Science: Oxford, **1998**.
15. Edleman, P. G.; Wang, J. *Overview of Biosensors*; American Chemical Society Publications: Washington, **1992**; pp. 487.
16. Clark, L. C.; Lyons, C. *Ann. N. Y. Acad. Sci.* **1962,** *102*, 29.
17. Lerner, H.; Giner, J.; Soeldner, J. S.; Colton, C. K. *Ann. N. Y. Acad. Sci.* **1984,** *428*, 263.
18. Cass, A. E. G.; Davis, G.; Francis, G. D.; Hill, H. A. O.; Aston, W. J.; Higgins, I. J. *Anal. Chem.* **1984,** *56*, 667.
19. Gunasingham, H.; Tan, C. H. *Anal. Chim. Acta.* **1990,** *234*, 321.

20. Kajiya, Y.; Sugai, H.; Iwakura, C.; Yoneyama, H. *Anal. Chem.* **1991,** *63*, 49.

21. Iwakura, C.; Kajiya, Y.; Yoneyama, H. *J. Chem. Soc., Chem. Commun.* **1988,** 1019.

22. Pravda, M.; Jungar, C. M.; Iwuoha, E. I.; Smyth, M. R.; Vytras, K.; Ivaska, A. *Anal. Chim. Acta.* **1995,** *304*, 127.

23. Amine, A.; Kauffmann, J.-M.; Guilbault, G. G.; Bacha, S. *Anal. Lett.* **1993,** *26*, 1281.

24. Yabuki, S.; Mizutani, F. *Biosens. Biolectron.* **1995,** *10*, 353.

25. Sakslund, H.; Wang, J.; Hammerich, O. *J. Electroanal. Chem.* **1996,** *402*, 149.

26. Danil de Namor, A. F.; Blackett, P. M.; Cabaleiro, M. C.; al Ravi, J. M. A. *J. Chem. Soc. Faraday Trans.* **1994,** *90*, 845.

27. Aoyama, Y.; Tanaka, Y.; Toi, H.; Ogoshi, H. *J. Am. Chem. Soc.* **1988,** *110*, 634.

28. Bonar-Law, R. P.; Davis, A. P.; Murray, B. A. *Angew. Chem., Int. Ed. Engl.* **1990,** *29*, 1407.

29. Bonar-Law, R. P.; Davis, A. P. *Tetrahedron* **1993,** *49*, 9845.

30. Mizutani, T.; Murakami, T.; Matsumi, N.; Kurahashi, T.; Ogoshi, H. *J. Chem. Soc. Chem. Commun.* **1995**, 1257.

31. Mizutani, T.; Kurahashi, T.; Murakami, H.; Matsumi, N.; Ogoshi, H. *J. Am. Chem. Soc.* **1997,** *119*, 8991.

32. Kral, V.; Rusin, O.; Schmidtchen, F. P. *Org. Lett.* **2001,** *3*, 873.

33. Cuntze, J.; Owens, L.; Alcazar, V.; Seiler, P.; Diederich, F. *Helv. Chim. Acta* **1995,** *78*.

34. Huang, C. Y.; Cabell, L. A.; Anslyn, E. V. *J. Am. Chem. Soc.* **1994,** *116*, 2778.

35. Inouye, M.; Miyake, T.; Furusyo, M.; Nakazumi, H. *J. Am. Chem. Soc.* **1995,** *117*, 12416.

36. Das, G.; Hamilton, A. D. *J. Am. Chem. Soc.* **1994,** *116*, 11139.

37. Das, G.; Hamilton, A. D. *Tetrahedron Lett.* **1997,** *38*, 3675.

38. Michaelis, A.; Becker, P. *Ber. Dtsch. Chem. Ges.* **1880,** *13*, 58.

39. Kuivila, H. G.; Keough, A. H.; Soboczenski, E. J. *J. Org. Chem.* **1954,** *19*, 780.

40. Lorand, J. P.; Edwards, J. D. *J. Org. Chem.* **1959,** *24*, 769.

41. Bielecki, M.; Eggert, H.; Norrild, J. C. *J. Chem. Soc., Perkin Trans. 2* **1999,** 449.

42. Wang, W.; Gao, S. H.; Wang, B. H. *Org. Lett.* **1999,** *1*, 1209.

43. Nicolas, M.; Fabre, B.; Simonet, J. *Electrochim. Acta* **2001,** *46*, 1179.

44. Karpa, M. J.; Duggan, P. J.; Griffin, G. J.; Freudigmann, S. J. *Tetrahedron* **1997,** *53*, 3669.

45. Morin, G. T.; Hughes, M. P.; Paugam, M. F.; Smith, B. D. *J. Am. Chem. Soc.* **1994,** *116*, 8895.

46. Bien, J. T.; Shang, M. Y.; Smith, B. D. *J. Org. Chem.* **1995,** *60*, 2147.

47. Wulff, G. *Pure Appl. Chem.* **1982,** *54*, 2093.

48. Sandanayake, K.; Nakashima, K.; Shinkai, S. *J. Chem. Soc. Chem. Commun.* **1994**, 1621.

49. Shiomi, Y.; Saisho, M.; Tsukagoshi, K.; Shinkai, S. *J. Chem. Soc., Perkin Trans. 1* **1993**, 211.

50. Shinmori, H.; Takeuchi, M.; Shinkai, S. *J. Chem. Soc., Perkin Trans. 2* **1996**, 1.

51. Ward, C. J.; Patel, P.; Ashton, P. R.; James, T. D. *Chem. Commun.* **2000**, 229.

52. Rendel, D. *Fluorescence and Phosphorescence Spectroscopy*; John Wiley & Sons: New York, **1987**.

53. Leray, I.; O'Reilly, F.; Jiwan, J. L. H.; Soumillion, J. P.; Valeur, B. *Chem. Commun.* **1999**, 795.

54. Sousa, L. R.; et al. *Fluorescent Chemosensors for Ion and Molecule Recognition*; American Chemical Society: Washington, **1993**.

55. Valeur, B.; Leray, I. *Coord. Chem. Rev.* **2000,** *205*, 3.

56. de Silva, A. P.; Gunaratne, H. Q. N.; Gunnlaugsson, T.; Huxley, A. J. M.; McCoy, C. P.; Rademacher, J. T.; Rice, T. E. *Chem. Rev.* **1997,** *97*, 1515.

57. Valeur, B.; Bourson, J.; Pouget, J. *Fluorescent Chemosensors for Ion and Molecule Recognition*; American Chemical Society: Washington, **1993**.

58. Martin, M. M.; Plaza, P.; Dai Hung, N.; Meyer, Y. H.; Bourson, J.; Valeur, B. *Chem. Phys. Lett.* **1993,** *202*, 425.

59. Martin, M. M.; Plaza, P.; Meyer, Y. H.; Begin, L.; Bourson, J.; Valeur, B. *J. Fluorescence* **1994,** *4*, 271.

60. Martin, M. M.; Plaza, P.; Meyer, Y. H.; Badaoui, F.; Bourson, J.; Lefevre, J. P.; Valeur, B. *J. Phys. Chem.* **1996,** *100*, 6879.

61. Fery-Forgues, S.; Le Bris, M. T.; Mialocq, J. C.; Pouget, J.; Rettig, W.; Valeur, B. *J. Phys. Chem.* **1992,** *96*, 701.

62. Bourson, J.; Borrel, M. N.; Valeur, B. *Anal. Chim. Acta.* **1992,** *257*, 189.

63. Bourson, J.; Pouget, J.; Valeur, B. *J. Phys. Chem.* **1993,** *97*, 4552.

64. Bourson, J.; Badaoui, F.; Valeur, B. *J. Fluorescence* **1994,** *4*, 275.

65. Wang, Y. C.; Morawetz, H. *J. Am. Chem. Soc.* **1976,** *98*, 3611.

66. Selinger, B. K. *Aust. J. Chem.* **1997,** *30*, 2087.

67. de Silva, A. P.; de Silva, S. A. *J. Chem. Soc. Chem. Commun.* **1986,** 1709.

68. de Silva, A. P.; Gunaratne, H. Q. N.; Sandanayake, K. R. A. S. *Tetrahedron Lett.* **1990,** 5193.

69. de Silva, A. P.; Gunaratne, H. Q. N. *J. Chem. Soc. Chem. Commun.* **1990,** 186.

70. Herman, P.; Murtaza, Z.; Lakowicz, J. R. *Anal. Biochem.* **1999,** *272*, 87.

71. de Silva, A. P.; de Silva, S. A.; Dissanayake, A. S.; Sandanayake, K. R. A. S. *Chem. Commun.* **1989**, 1054.

72. Balzani, V.; Ceroni, P.; Gestermann, S.; Kauffmann, C.; Gorka, M.; Vogtle, F. *Chem. Commun.* **2000**, 853.

73. Kijima, H.; Takeuchi, M.; Robertson, A.; Shinkai, S.; Cooper, C.; James, T. D. *Chem. Commun.* **1999**, 2011.

74. de Silva, A. P.; Zavaleta, A.; Baron, D. E.; Allam, O.; Isidor, E. V.; Kashimura, N.; Percarpio, J. M. *Tetrahedron Lett.* **1997,** *38*, 2237.

75. de Silva, A. P.; Gunaratne, H. Q. N.; McCoy, C. P. *Chem. Commun.* **1996**, 2399.

76. Cooper, C. R. *Novel PET Sensors*, Birmingham **2001**.

77. Yoon, J.; Czarnik, A. W. *J. Am. Chem. Soc.* **1992,** *114*, 5874.

78. Nagai, Y.; Kobayashi, K.; Toi, H.; Aoyama, Y. *Bull. Chem. Soc. Jpn.* **1993,** *66*, 2965.

79. James, T. D.; Sandanayake, K.; Shinkai, S. *J. Chem. Soc., Chem. Commun.* **1994**, 477.

80. James, T. D.; Sandanayake, K.; Iguchi, R.; Shinkai, S. *J. Am. Chem. Soc.* **1995,** *117*, 8982.

81. Sandanayake, K.; James, T. D.; Shinkai, S. *Chem. Lett.* **1995**, 503.

82. Linnane, P.; James, T. D.; Imazu, S.; Shinkai, S. *Tetrahedron Lett.* **1995,** *36*, 8833.

83. James, T. D.; Shinmori, H.; Shinkai, S. *Chem. Commun.* **1997**, 71.

84. Levacher, V.; Boussad, N.; Dupas, G.; Bourguignon, J.; Queguiner, G. *Tetrahedron* **1992,** *48*, 831.

85. Higgins, R. W.; Hilton, C. L.; Deodhar, S. D. *J. Org. Chem.* **1951,** *16*, 1275.

86. Guennouni, F.; Szonyi, F.; Cambon, A. *Synth. Commun.* **1998,** *28*, 995.

87. Marshall, J. A.; Andersen, N. H. *J. Org. Chem.* **1970,** *35*, 858.

88. Grieco, P. A.; Yokoyama, Y.; Withers, G. P.; Okuniewicz, F. J.; Wang, C. L. J. *J. Org. Chem.* **1978,** *43*, 4178.

89. Hagiwara, H.; Uda, H. *J. Chem. Soc. Chem. Commun.* **1987**, 1351.

90. Osuka, A.; Nagata, T.; Kobayashi, F.; Maruyama, K. *J. Het. Chem.* **1990,** *27*, 1657.

91. Baumgarten, H. E.; Bower, F. A.; Okamoto, T. T. *J. Am. Chem. Soc.* **1957,** *79*, 3145.

92. Masquelin, T.; Obrecht, D. *Tetrahedron* **1997,** *53*, 641.

93. Bardsley, W. G.; Ashford, J. S.; Hill, C. M. *Biochem. J.* **1971,** *122*, 557.

94. Kao, L.; Barfield, M. *J. Am. Chem. Soc.* **1985,** *107*, 2323.

95. Somlai, C.; Szokan, G.; Balaspiri, L. *Synthesis* **1992,** *3*, 285.

96. Stahl, G.; Walter, R.; Smith, C. W. *J. Org. Chem.* **1978,** *43*, 2285.

97. Schmidt, U.; Lieberknecht, A.; Bokens, H.; Griesser, H. *J. Org. Chem.* **1983,** *48*, 2680.

98. Gutsche, C. D.; Johnson, H. E. *J. Am. Chem. Soc.* **1955,** *77*, 109.

99. Perrin, D. D.; Dempsey, B. *Buffers for pH and Metal Ion Control*; Chapman & Hall, **1974**.

100. Fery-Forgues, S.; Le Bris, M. T.; Guette, J.-P.; Valeur, B. *J. Phys. Chem.* **1988,** *92*, 6233.

101. James, T. D.; Cooper, C. R. *J. Chem. Soc., Perkin Trans. 1* **2000**, 963.

102. Arimori, S.; Bell, M.; Oh, C.; Frimat, K.; James, T. D. *J. Chem. Soc., Perkin Trans. 1* **in press**.

103. Seaman, W.; Johnson, J. R. *J. Am. Chem. Soc.* **1931,** *53*, 711.

VI Appendix

Appendix 1: Fluorescence Intensity (I_F) of Sensor **43** with increasing concentration of D-glucose at pH 8.21.

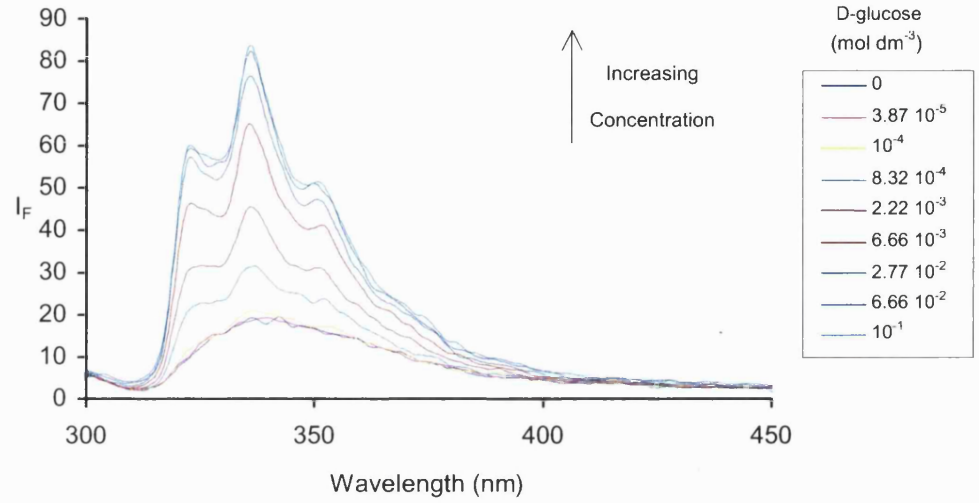

Appendix 2: Fluorescence Intensity (I_F) of Sensor **43** with increasing concentration of D-galactose at pH 8.21.

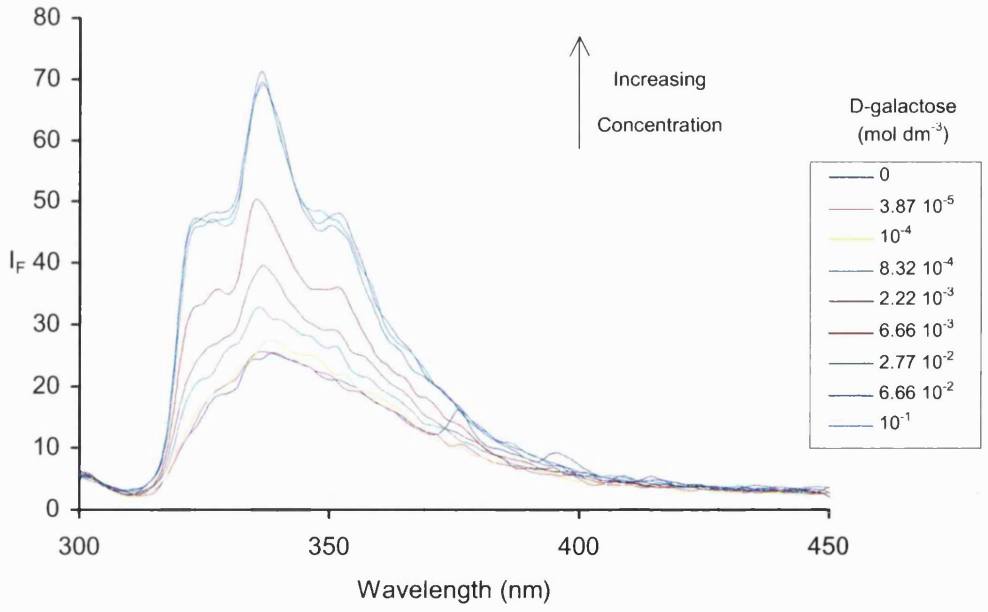

Appendix 3: Fluorescence Intensity (I_F) of Sensor **43** with increasing concentration of D-mannose at pH 8.21.

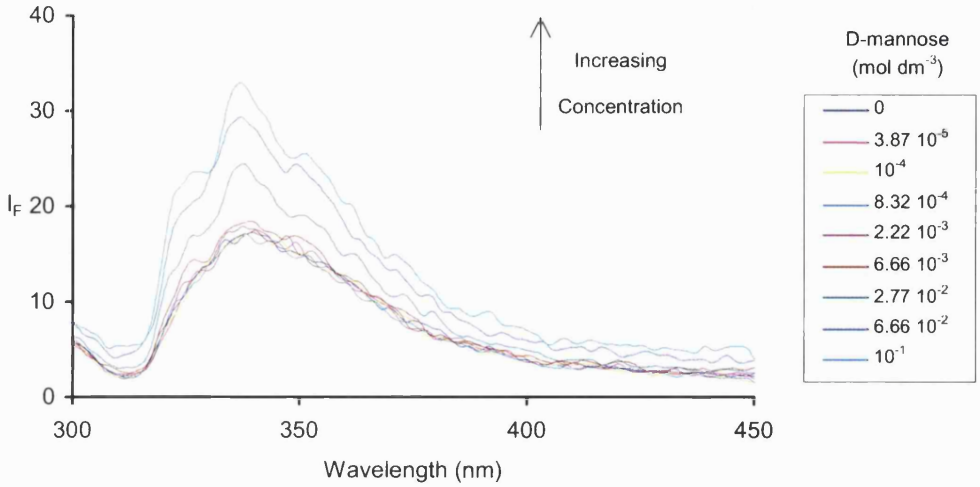

Appendix 4: Fluorescence Intensity (I_F) of Sensor **43** with increasing concentration of D-fructose at pH 8.21.

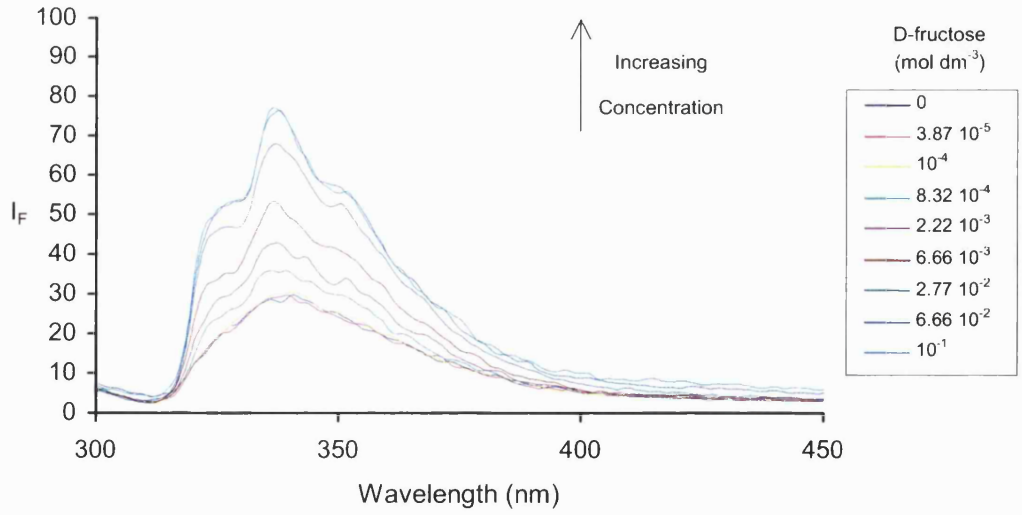

Appendix 5: CD Spectra of Sensor **43** in the presence of L-or D-glucose at pH.

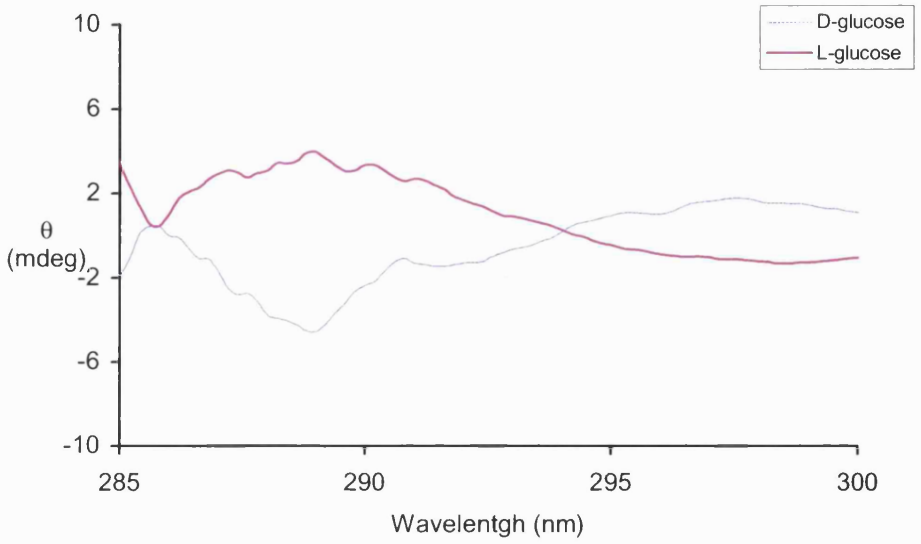

Appendix 6: Fluorescence Intensity (I_F) of Sensor **44** with increasing concentration of D-glucose at pH 8.21.

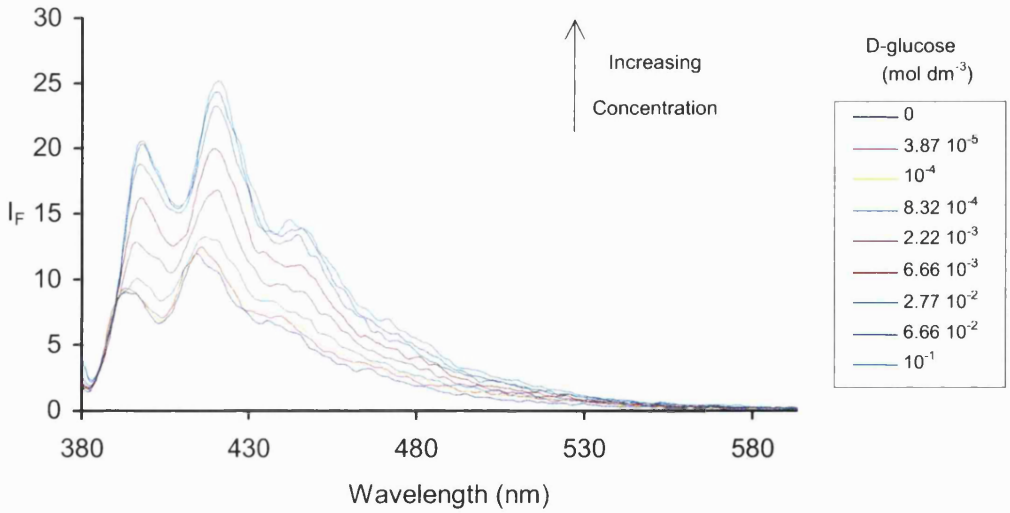

Appendix 7: Fluorescence Intensity (I_F) of Sensor **44** with increasing concentration of D-galactose at pH 8.21.

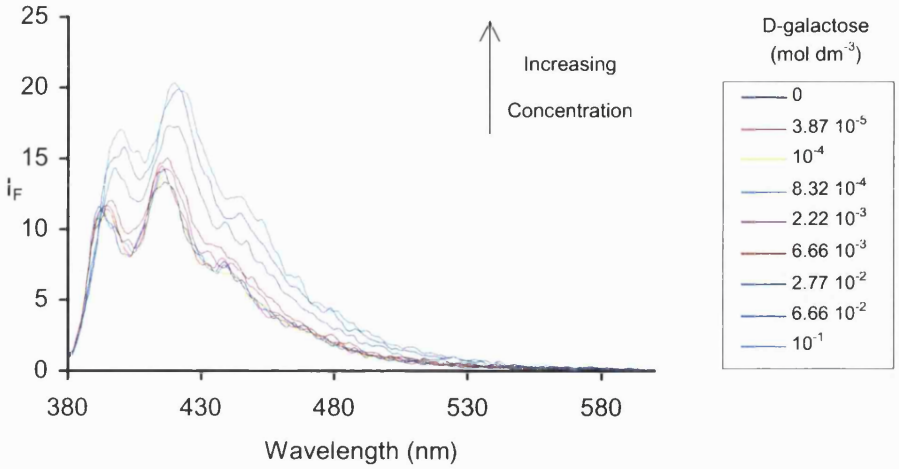

Appendix 8: Fluorescence Intensity (I_F) of Sensor **44** with increasing concentration of D-mannose at pH 8.21.

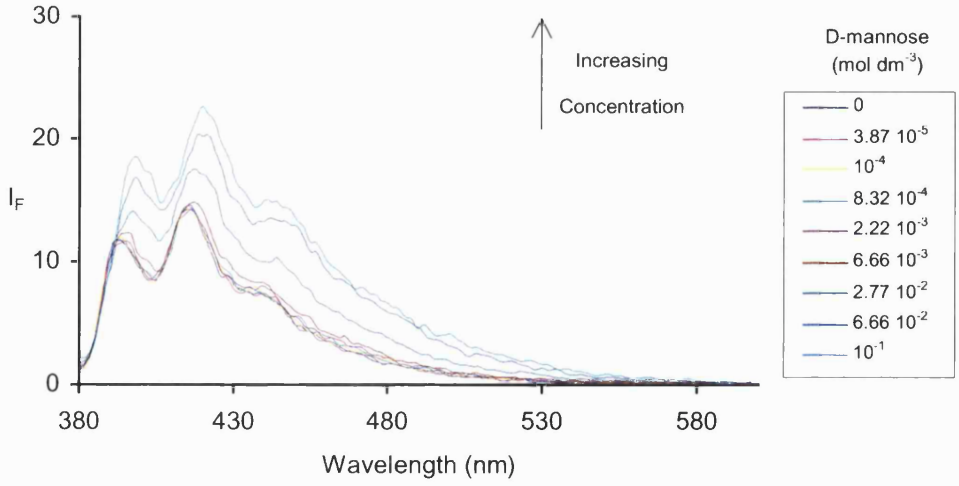

Appendix 9: Fluorescence Intensity (I_F) of Sensor **44** with increasing concentration of D-fructose at pH 8.21.

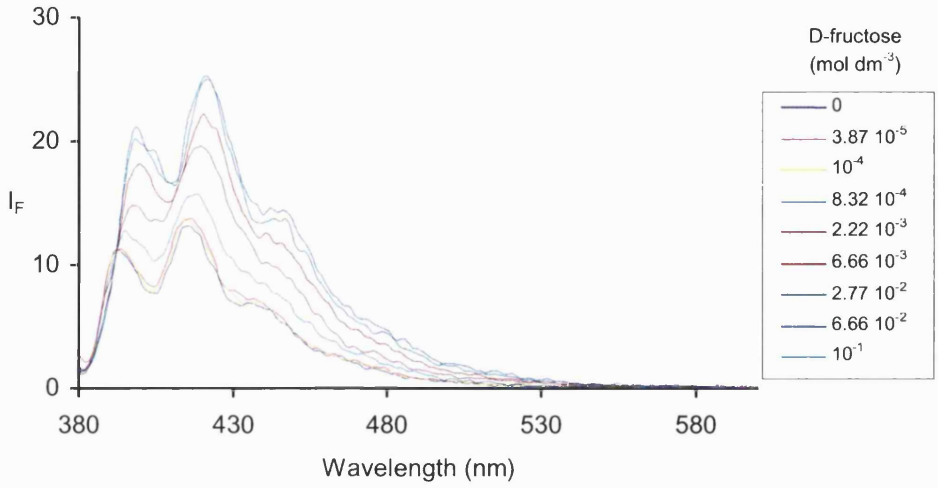

Appendix 10: CD Spectra of Sensor **44** in the presence of L-or D-glucose.

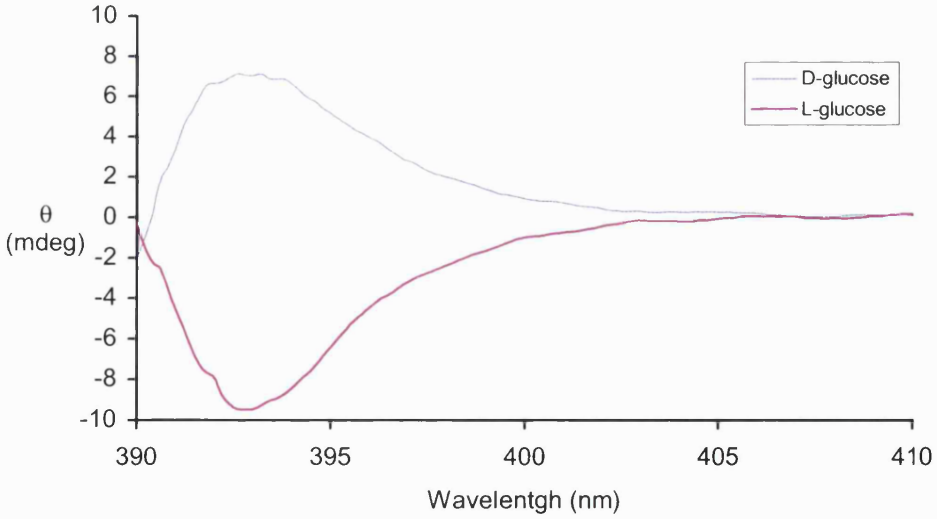

Appendix 11: Fluorescence Intensity (I_F) of Sensor **45** with increasing concentration of D-glucose at pH 8.21.

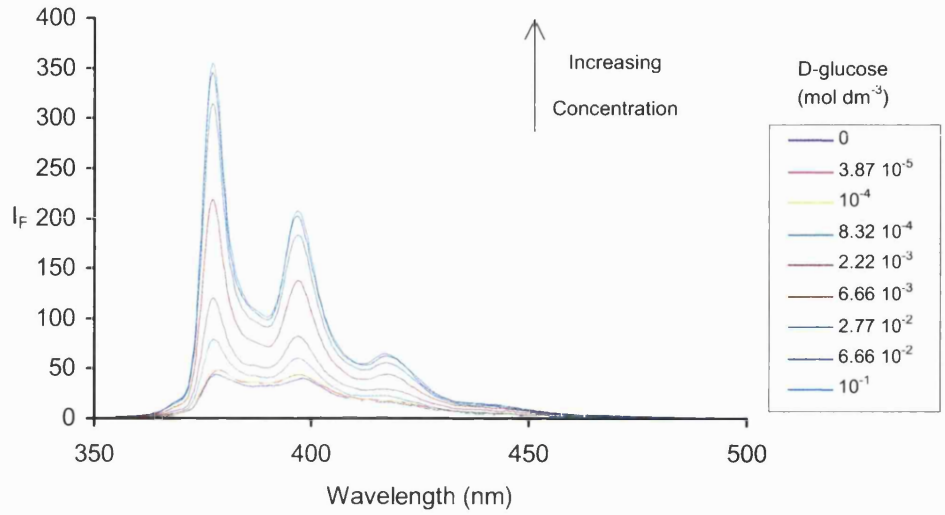

Appendix 12: Fluorescence Intensity (I_F) of Sensor **45** with increasing concentration of D-galactose at pH 8.21.

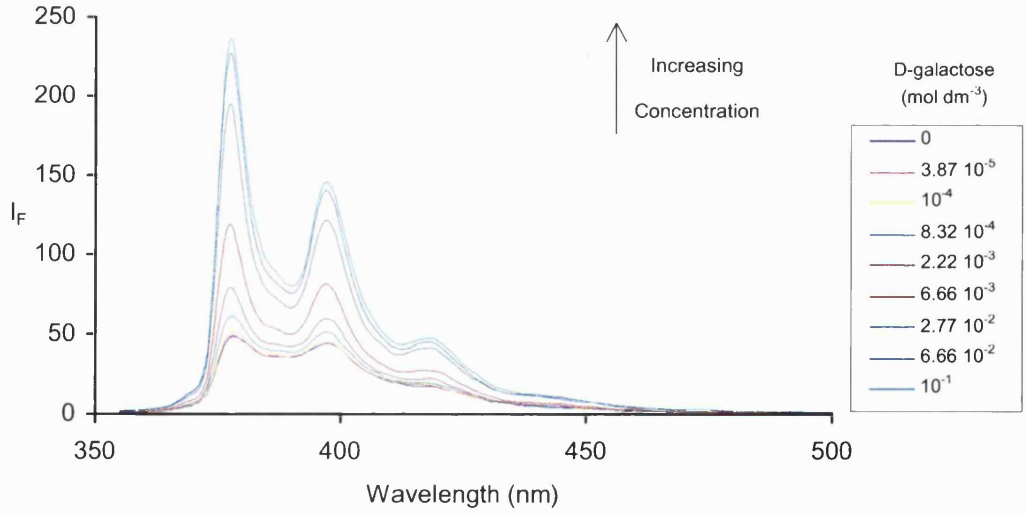

Appendix 13: Fluorescence Intensity (I_F) of Sensor **45** with increasing concentration of D-mannose at pH 8.21.

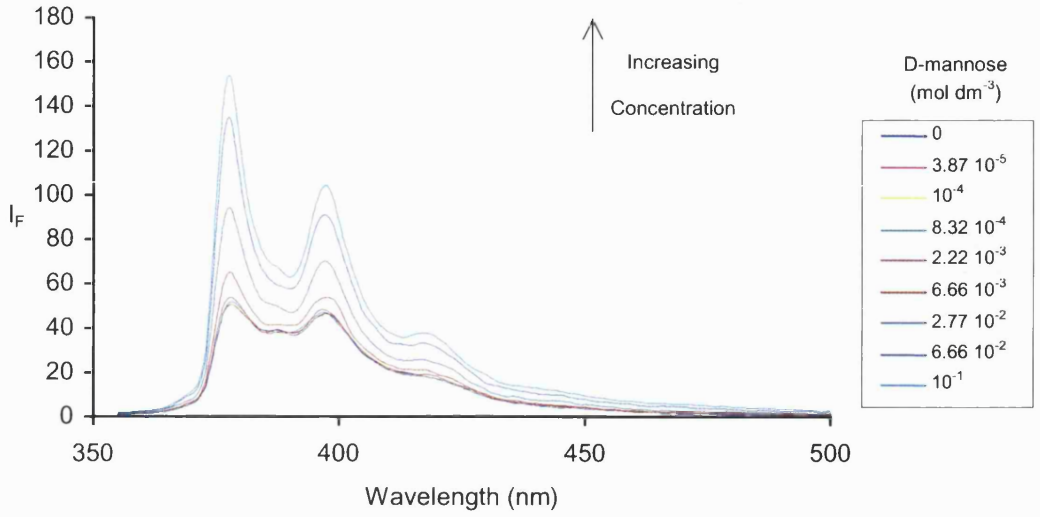

Appendix 14: Fluorescence Intensity (I_F) of Sensor **45** with increasing concentration of D-fructose at pH 8.21.

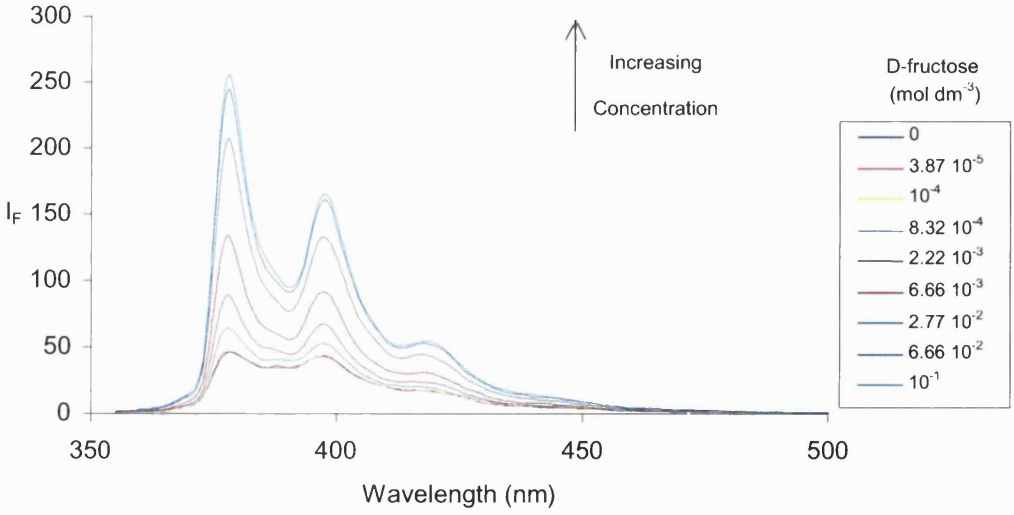

Appendix 15: CD Spectra of Sensor **45** in the presence of L-or D-glucose.

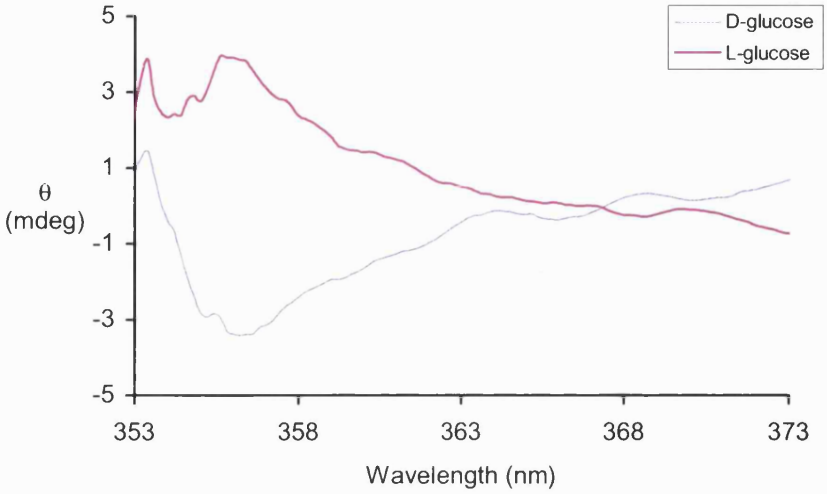

Appendix 16: Fluorescence Intensity (I_F) of Sensor **46** with increasing concentration of D-glucose at pH 8.21.

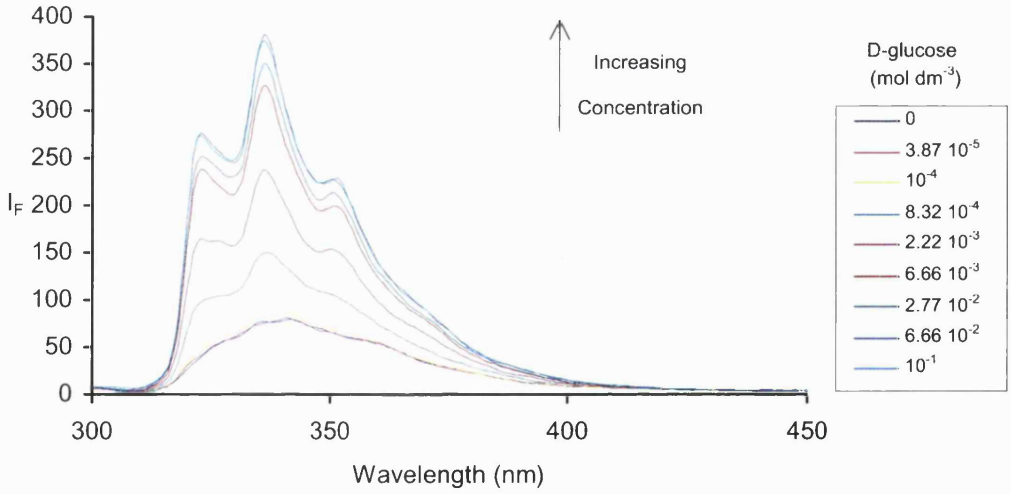

Appendix 17: Fluorescence Intensity (I_F) of Sensor **46** with increasing concentration of D-galactose at pH 8.21.

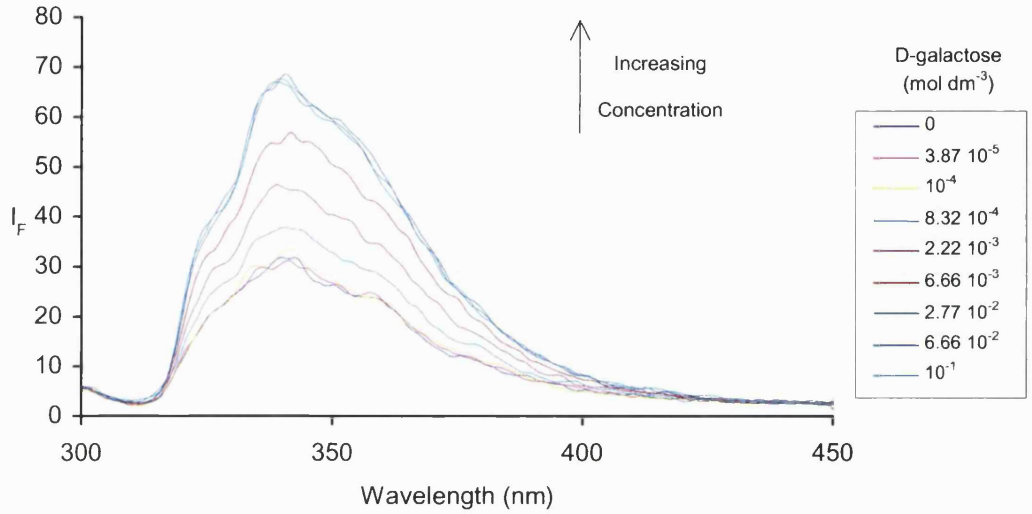

Appendix 18: Fluorescence Intensity (I_F) of Sensor **46** with increasing concentration of D-mannose at pH 8.21.

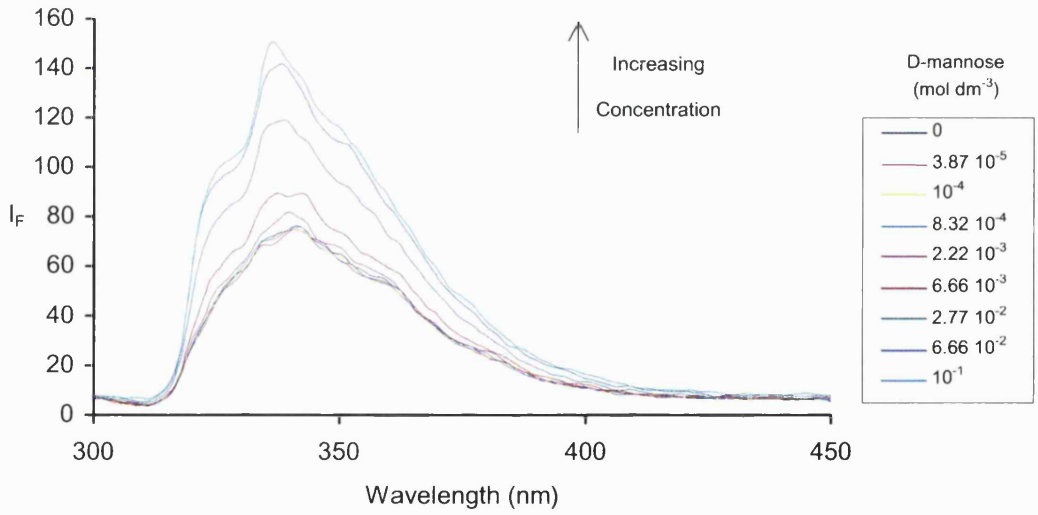

Appendix 19: Fluorescence Intensity (I_F) of Sensor **46** with increasing concentration of D-fructose at pH 8.21.

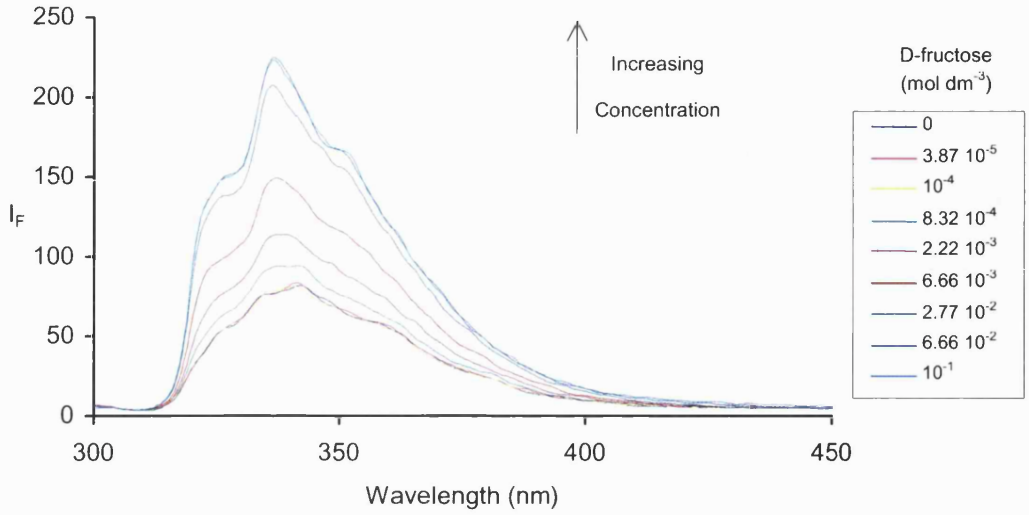

Appendix 20: CD Spectra of Sensor **46** in the presence of L-or D-glucose.

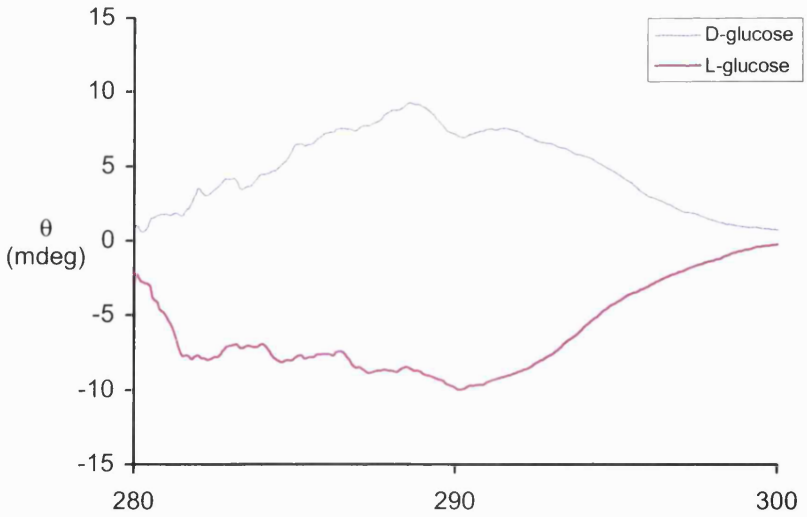

Appendix 21: CD Spectra of Sensor **46** in the presence of D-galactose.

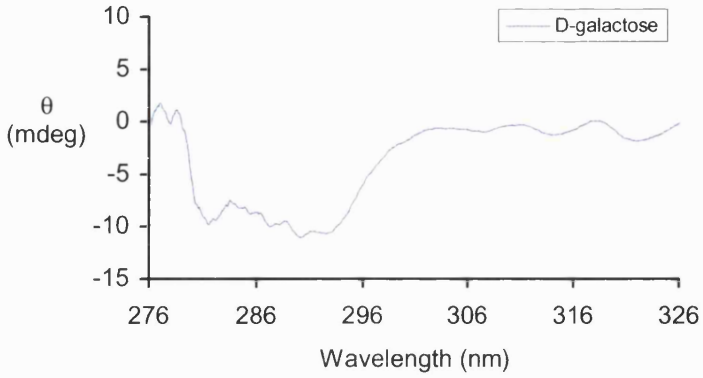

Appendix 22: Fluorescence Intensity (I_F) of Sensor **47** with increasing concentration of D-glucose at pH 8.21.

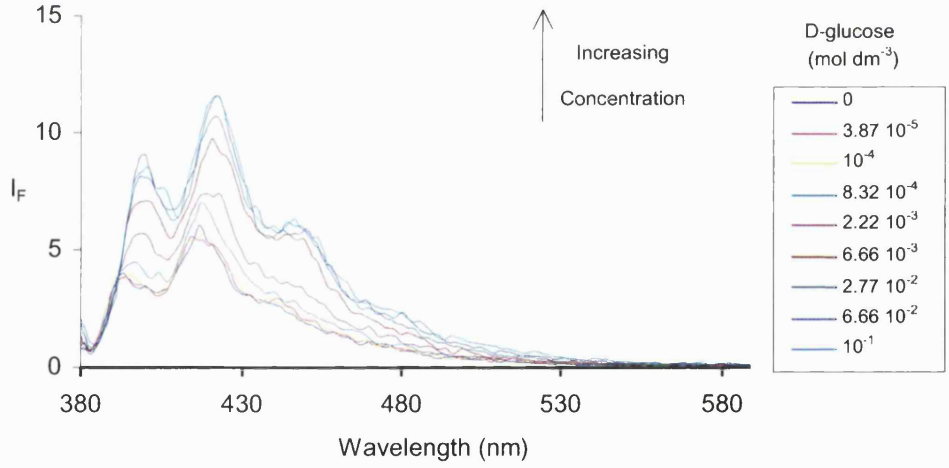

Appendix 23: Fluorescence Intensity (I_F) of Sensor **47** with increasing concentration of D-galactose at pH 8.21.

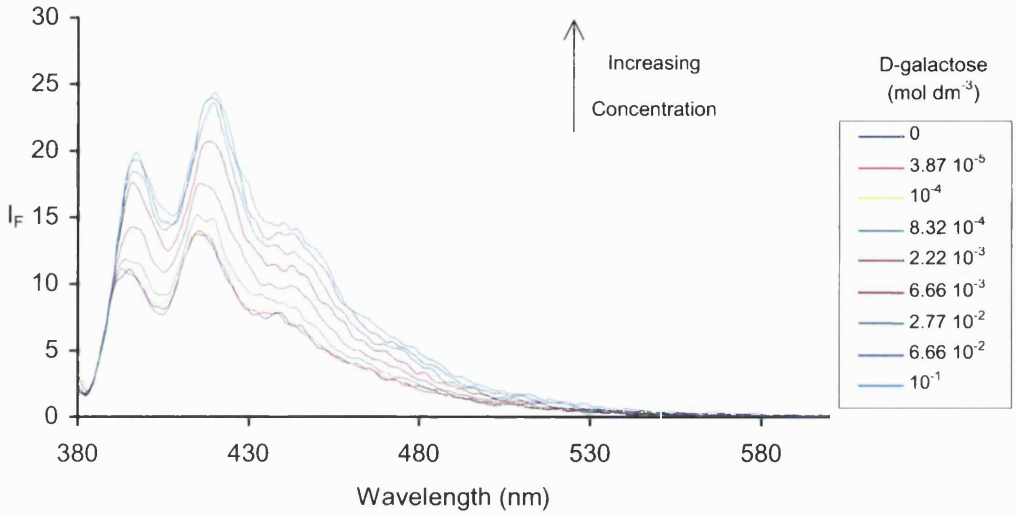

Appendix 24: Fluorescence Intensity (I_F) of Sensor **47** with increasing concentration of D-mannose at pH 8.21.

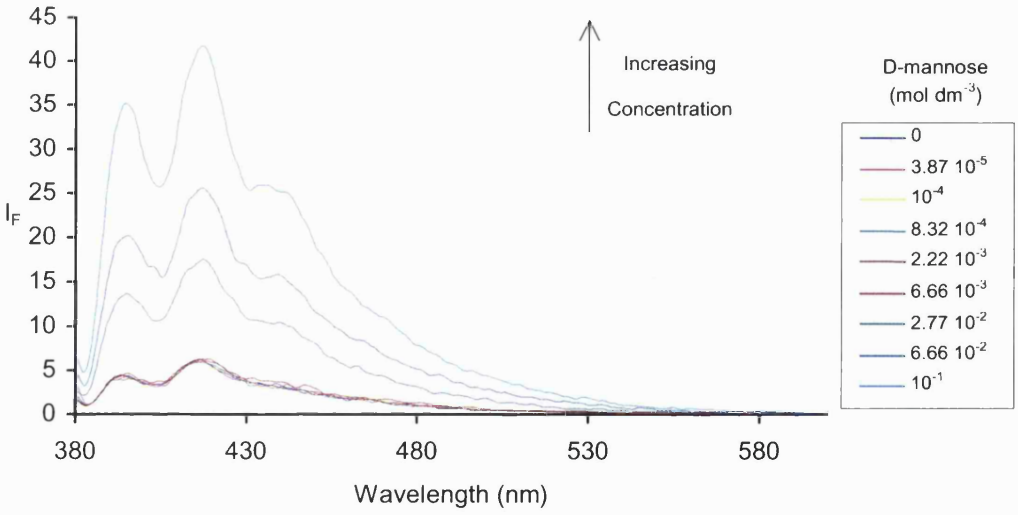

Appendix 25: Fluorescence Intensity (I_F) of Sensor **47** with increasing concentration of D-fructose at pH 8.21.

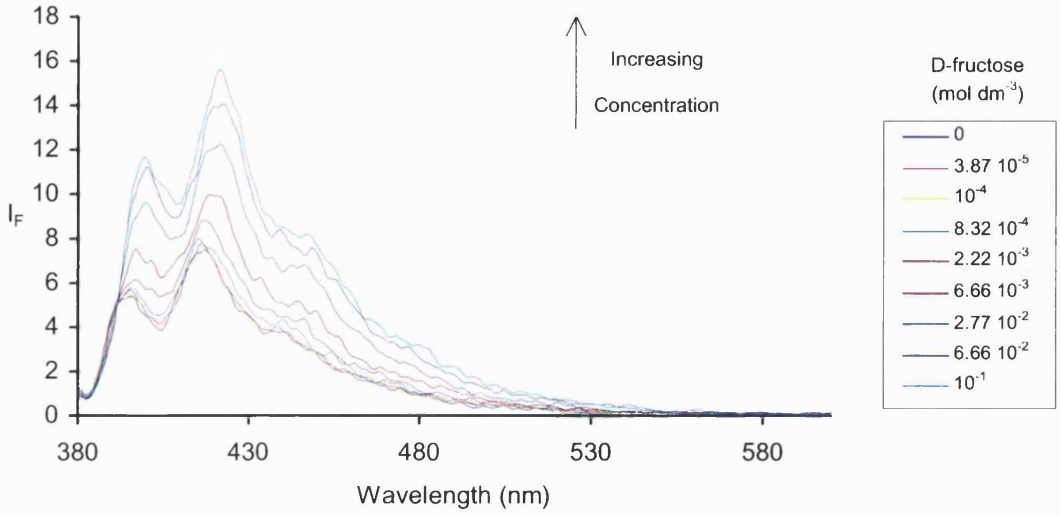

Appendix 26: CD Spectra of Sensor **47** in the presence of D-and L-glucose.

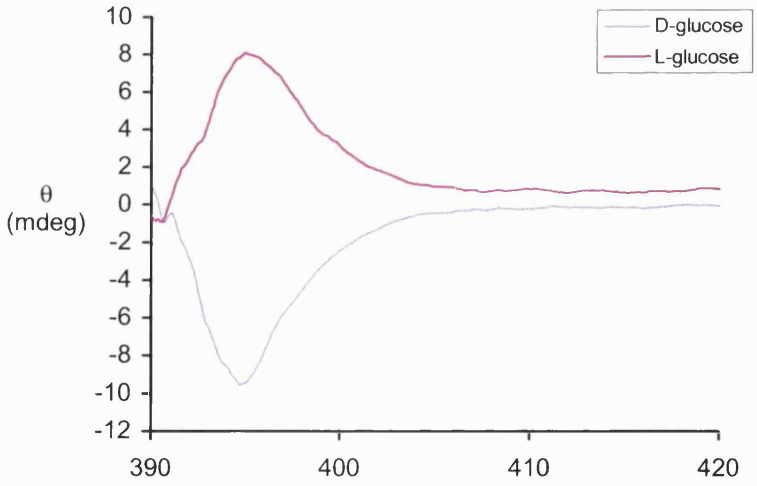

Appendix 27: CD Spectra of Sensor **47** in the presence of D-galactose.

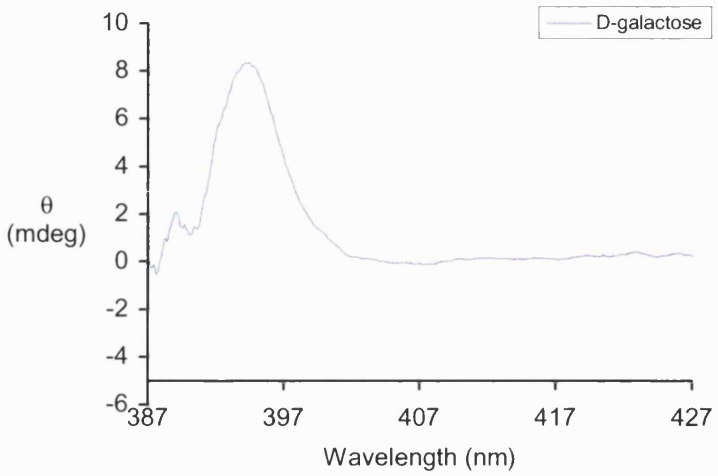

Appendix 28: Fluorescence Intensity (I_F) of Sensor **48** with increasing concentration of D-glucose at pH 8.21.

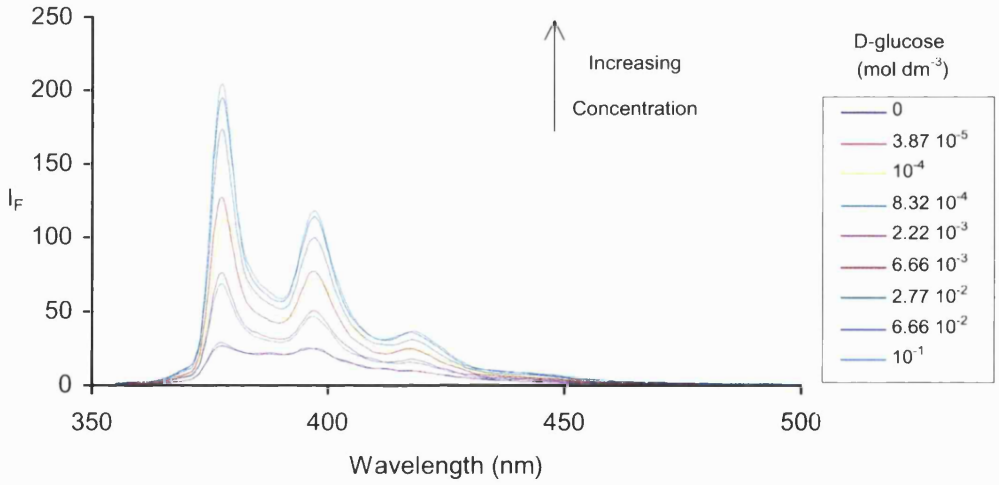

Appendix 29: Fluorescence Intensity (I_F) of Sensor **48** with increasing concentration of D-galactose at pH 8.21.

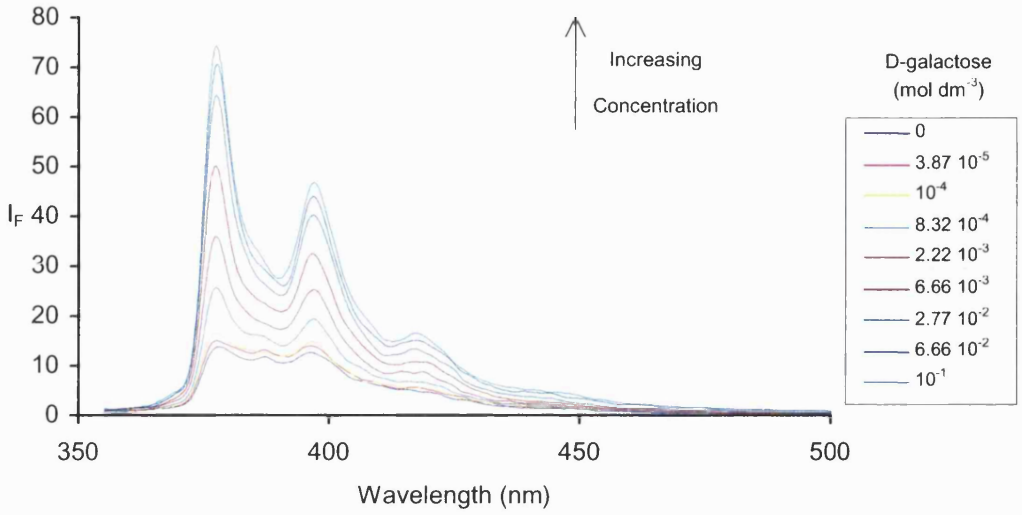

Appendix 30: Fluorescence Intensity (I_F) of Sensor **48** with increasing concentration of D-mannose at pH 8.21.

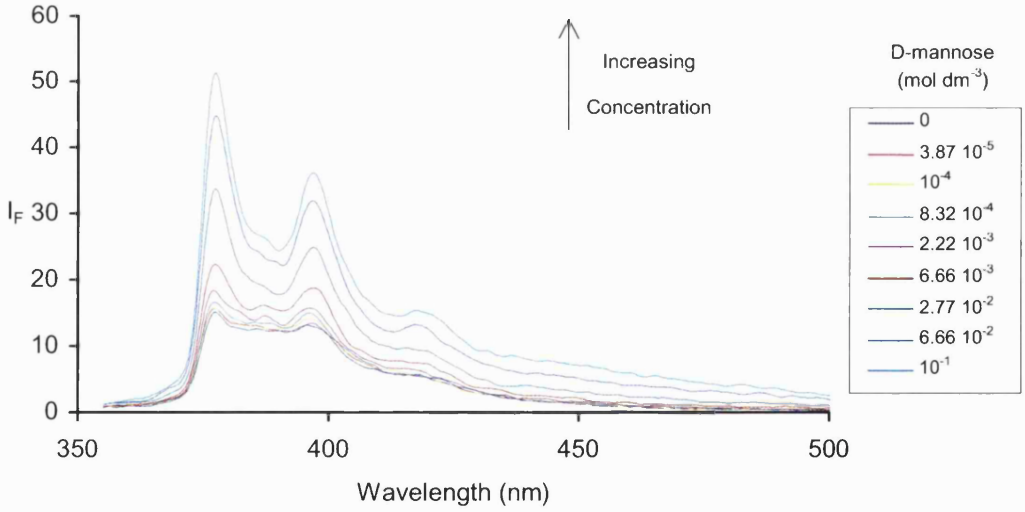

Appendix 31: Fluorescence Intensity (I_F) of Sensor **48** with increasing concentration of D-fructose at pH 8.21.

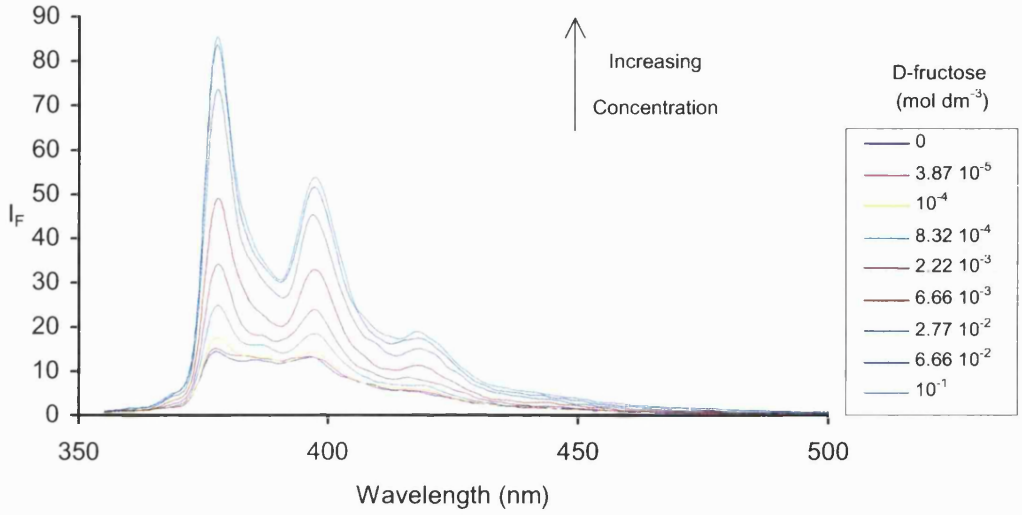

Appendix 32: CD Spectra of Sensor **48** in the presence of D-and L-glucose.